EFFECT OF SOLID COUPLANTS MADE OF HYDROPHILIC POLYMERS IN ULTRASONIC TESTING

A THESIS SUBMITTED TO
THE GRADUATE SCHOOL OF NATURAL AND APPLIED SCIENCES
OF
THE MIDDLE EAST TECHNICAL UNIVERSITY

BY

MUSTAFA İLKER ÇETİN

IN PARTIAL FULFILLMENT OF THE REQUIREMENTS FOR THE DEGREE OF

MASTER OF SCIENCE

IN

THE DEPARTMENT OF MECHANICAL ENGINEERING

DECEMBER 2003

Approval of the Graduate School of Natural and Applied Sciences.

Prof. Dr. Canan ÖZGEN
Director

I certify that this thesis satisfies all the requirements as a thesis for the degree of Master of Science.

Prof. Dr. Kemal İDER
Head of Department

This is to certify that we have read this thesis and that in our opinion it is fully adequate, in scope and quality, as a thesis for the degree of Master of Science.

Prof. Dr. Bülent DOYUM
Supervisor

Examining Committee Members

Prof. Dr. Ömer G. BİLİR

Prof. Dr. Bülent DOYUM

Prof. Dr. Suha ORAL

Assist. Prof. Dr. Serkan DAĞ

Assoc. Prof. Dr. Hakan GÜR (METE)

ABSTRACT

EFFECT OF SOLID COUPLANTS MADE OF HYDROPHILIC POLYMERS IN ULTRASONIC TESTING

Çetin, Mustafa İlker
M.S., Department of Mechanical Engineering
Supervisor: Prof. Dr. Bülent Doyum

December 2003, 134 pages

This thesis investigates the effect of hydrophilic polymers as novel solid couplants in ultrasonic inspection. These polymers can absorb large quantities of water, thus become soft and flexible, and also adapt themselves very well to applications.

In this study, experiments were carried out by preparing three different types of polymer membranes namely [Poly(HEMA), Poly(HEMA-co-GMA), Poly(HEMA-NN′-dH_2O)] with different thicknesses and monomer contents. Swelling ratios were determined in deionized water using 9mm diameter samples, cut from each polymer. Ultrasonic velocity and sound attenuation measurements were performed with pulse-echo and immersion techniques. These results were analyzed and compared with water, typical plastics and rubbers. In order to evaluate the coupling performance of hydrophilic polymers, weights of 50g, 200g, 500g and 1 kg were used as loading conditions to change the pressure applied to the transducer.

Results obtained with this study showed that hydrophilic polymers offer low attenuation at high frequencies and couple effectively while eliminating the risk of test piece contamination. The study also revealed that velocities of polymers decrease by increasing the water content. This research can be used as a guideline for an alternative choice of couplant while testing water sensitive materials in safety critical structures or where the test piece is avoided from contamination and also can be used for rough surfaces.

Keywords: Ultrasonic Testing, Hydrophilic Polymers, Couplant, Solid Couplant

ÖZ

HİDROFİLİK POLİMERLERDEN YAPILMIŞ TEMAS MADDELERİNİN ULTRASONİK TESTLERE ETKİSİ

Çetin, Mustafa İlker

Yüksek Lisans, Makina Mühendisliği Bölümü

Tez Yöneticisi: Prof. Dr. Bülent Doyum

Aralık 2003, 134 sayfa

Bu çalışma, temas maddesi olarak hidrofilik polimerlerin kullanımının ultrasonik muayenedeki etkisini araştırmaktadır. Bu polimerler yüksek miktarlarda su emebilmekte, bu suretle yumuşak ve esnek olmakta ve aynı zamanda kendilerini değişik uygulamalara iyi adapte edebilmektedirler.

Bu çalışmada, deneyler [Poly(HEMA), Poly(HEMA-co-GMA), Poly(HEMA-NN′-dH_2O)] olmak üzere değişik kalınlıkta ve monomer içerikli üç farklı polimer membranı hazırlanarak gerçekleştirilmiştir. Şişme oranları deionize suda, her polimerden kesilen 9mm çapında örneklerle tayin edilmiştir. Ultrasonik ses hızı ve ses zayıflaması ölçümleri, darbe-yankı ve daldırma teknikleri kullanılarak gerçekleştirilmiştir. Elde edilen sonuçlar analiz edilmiş; su, tipik plastikler ve kauçuklarla karşılaştırılmıştır. Hidrofilik polimerlerin temas performansını değerlendirmek için, 50g, 200g, 500g ve 1kg'lık ağırlıklar problara uygulanan basıncı değiştirmek için yükleme koşulları olarak kullanılmıştır.

Bu çalışmayla elde edilen sonuçlar, hidrofilik polimerlerin yüksek frekanslarda düşük sönümler sunduğunu ve test parçasının kirlenme riskini elimine ederek etkin olarak temas ettiğini göstermiştir. Çalışma aynı zamanda polimer hızlarının su içeriği arttıkça düştüğünü ortaya çıkarmıştır. Bu araştırma, kritik yapılardaki suya hassas malzemelerin testinde veya kirlenmeden kaçınılan test parçalarında, ve aynı zamanda pürüzlü yüzeylerde alternatif temas maddesi seçimi olarak bir rehber niteliğinde kullanılabilir.

Anahtar Kelimeler: Ultrasonik Test, Hidrofilik Polimerler, Temas Maddesi, Temas Ortamı, Katı Temas Maddesi, Katı Temas Ortamı

ACKNOWLEDGMENTS

I would like to express my sincere appreciation to my thesis supervisor Prof. Dr. A. Bülent DOYUM for his guidance, belief and continuous supervision throughout my study and also giving me a chance to work at the METU Non-Destructive Testing Center.

I wish to express my deepest gratefulness and special thanks to Prof. Dr. Adil DENİZLİ from Hacettepe University, Chemistry Department for sharing his knowledge, providing support in manufacturing the polymers and also encouraging me; Handan YAVUZ, for her friendship, helping me to relax and giving small tips during this study.

I'm also thankful to Mrs. Birnur DOYUM, for her support and valuable comments by sharing her knowledge and experience and helping me with the experimental setup; Orkun TUNCER, Ferhat SONAT and Orcan KOLANKAYA for their contributions throughout this study.

Finally, I'm grateful to my family and my girlfriend for their patience and continuous support and help to accomplish this study.

TABLE OF CONTENTS

CHAPTER

APPENDIX

LIST OF TABLES

TABLE

LIST OF FIGURES

FIGURE

CHAPTER I

INTRODUCTION

Ultrasonic Testing is one of the methods for the non-destructive testing of materials and structures which uses sound waves to detect small surface flaws and internal defects in material such as porosity, inclusions, cracks, laminations and disbonds in manufactured components. The principle of this method of inspection relies upon the reflection of ultrasound from interfaces between two different materials, two metals, a metal and a liquid or a metal and air. In other words; pulses of sound energy are sent into a material and if the pulses encounter a change in density or elasticity (interface) during travel through the specimen, they are reflected from the boundaries of the material and defects within it. The returning pulses are received, converted into an electrical signal, amplified, conditioned, and displayed on a screen.

Usually a piezoelectric transducer (probe) is applied to the surface to generate ultrasound and in the pulse-echo mode acts as both source and receiver [1, 2]. There are several types of transmitter probe in use but each type consists of crystal which is placed in contact with the material under test.

Transmission of ultrasound into the material to be tested can be limited by the roughness or curvature of the surface. In order to improve the transmittal of ultrasound a *couplant* is used between the ultrasonic transducer and the material to be tested. The most reliable couplant method is to use immersion [3], in which the test piece being fully immersed in a liquid, preferable a low viscosity silicone liquid (e.g. distilled water) which is called as the *immersion testing*. However this testing method is mostly not practical, particularly with large structures or for field inspection.

Presence of conventional couplants, such as oils, gels and water, is sometimes unsuitable for many materials mostly because of contamination. Open cell structures, porous materials, many metals and composites are typical examples. Alternative to liquid couplants, many attempts have been made in the form of non-contact techniques including air-coupled ultrasound, laser generation and detection systems and electromagnetic acoustic transducers (EMATS), also employment of solid coupling materials. These are summarized by Billson and Hutchinsm [4] and Drinkwater and Cawley [3, 5].

Solid coupled transducers have been available for many years [6] but they have been limited by the selection of material as natural rubber. It has been commonly used for solid coupling applications and although it has the ability to conform to an uneven test surface reasonably well, it imparts high attenuation to ultrasound, often forcing undesirable designs to be employed. Because natural rubbers are viscoelastic materials, their attenuation increases approximately linearly with frequency.

The main breakthrough here was the new solid coupling material. This enabled a shift in design philosophy away from that of low frequency, un-damped, through transmission devices which used a thin layer of highly attenuative solid couplant, towards higher frequency, highly damped, pulse echo devices where the solid couplant was used as a delay line.

Polymer materials give a novel and alternative choice as a solid coupling material. They have high specific strength; this is the reason for their increasing use in highly demanding technical applications where the potential failure of a component is critical.

The importance of these polymers in ultrasonic NDT area is that they demonstrate acoustic properties that lend themselves very well to implementation, in particular they have ability to transmit high frequencies by offering low attenuation and coupling efficiency to materials commonly encountered in NDT, especially steel [7].

Conventional hydrophilic polymers have been used extensively in medicine and pharmacy, also for soft contact lenses.

In this study, hydrophilic polymers were introduced as a new solid coupling material to the field of ultrasonic non-destructive testing. Their ultrasonic properties were discussed and employment of these polymers, their benefits and differences compared with the conventional couplants were observed.

Different from the earlier studies, different thicknesses were used in the experiments in order to observe distinctly the wave reflections taking place at the two interfaces (transducer-couplant, couplant-testpiece) at larger couplant thicknesses.

CHAPTER II

THEORETICAL BACKGROUND

Development of hydrophilic polymers to be used as solid couplants in ultrasonic inspection has become a shift in design philosophy. Presently there is no sufficient research published, because of its novelty; but a significant number of studies are underway for the improvement of conventional solid couplants in the name of hydrophilic polymers.

2.1 Non Destructive Testing

Defects of many types and sizes may be introduced to a material or component during manufacture and the exact nature and size of any defect will influence the subsequent performance of the component. It is therefore necessary to have non-destructive inspection for detecting the presence and rate of growth of defects which, if they remained undetected, could result in a catastrophic failure which could be very costly in terms of damage to materials or humans [9].

Simply, *Non Destructive Testing (NDT)* is the examination of an object or material with technology that does not affect its future usefulness. NDT can be used without destroying or damaging a product or material.

The first stage, simplest and oldest NDT technique is visual examination. Although it can be considered as a separate method, visual examination is actually a non-separable part of almost all other techniques. The basic principles and major features of the main NDT systems are given in Table 2.1.

Table 2.1 Types of Inspection Systems

Test Method	**Features & Applicability**
Liquid penetrant	Detection of defects which break the surface. Can be used on any metal, many plastics, glass and glazed ceramics
Magnetic particle	Detection of surface and sub-surface defects close to the surface. Can only be used on ferromagnetic materials (most steels and irons)
Electrical methods (Eddy currents)	Detection of surface defects and some sub-surface defects. Can also be used to measure the thickness of a non-conductive coating, such as paint, on a metal. Can be used for any metal
Ultrasonic testing	Detection of internal defects in addition to surface flaws. Can be used on most materials
Radiographic	Detection of internal defects, surface defects and the correctness of part assemblies. Can be used on many materials but there are limitations on the maximum material thickness

Among all test methods, ultrasonic testing gives a powerful and a wide usage because of its ability to detect internal flaws in materials and small surface cracks. But it does not necessarily mean that it is the best method for all inspection applications. Much will depend upon the type of flaw present and the shape and the size of the components to be examined.

2.2 Ultrasonic Testing

Ultrasonic techniques are regularly used for the in-service testing of parts and assemblies, also for the quality control inspection of part processed material, such as rolled slabs, as well as for the inspection of finished components.

In order to understand this testing method nature of sound propagation must be first considered.

2.2.1 Nature of Ultrasound

Sound waves are elastic waves which can be generated through both solid and liquid media. Ultrasound consists of a number of short pulses of inaudible sound, refers to sound which is too high pitched for the human ear to hear. Above about 20 kHz, the sound waves are referred to as “ultrasound” or “ultrasonics”.

Sound travels at one particular speed in any given material. Since sound travels in a material at a particular speed, the distance it has traveled can be determined by measuring the time taken [10].

2.2.2 Types of Ultrasonic Waves and Their Properties

Ultrasonic waves are mechanical or elastic waves and any mechanical wave is composed of discrete particles of material. Provided a material is not stressed by compression or tension beyond its elastic limit, its individual particles perform elastic oscillations. Due to induced particle vibration in the material and elastic properties of material, they have different wavelength in different materials.

An ultrasonic wave is characterized by its amplitude, frequency, wavelength, and attenuation coefficient.

Amplitude is the width of oscillations where frequency is number of oscillations per second (number of cycles per unit of time), normally stated as 1 cycle per second (f= [1/s]), called Hertz and abbreviated as Hz.

Wavelength is the distance, measured along the line of propagation, between two planes in which the particles are in the same state of motion. Numerically, if the particle vibration is sinusoidal the wavelength (λ) has a relation with the velocity of propagation and the wave frequency.

$$f = \frac{c}{\lambda} \tag{2.1}$$

c being the wave velocity and f is the frequency in Hz.

A pulse of ultrasonic energy can be considered as the synthesis of a series of purely sinusoidal waves of different frequencies and amplitudes [2].

Attenuation coefficient is a factor which is determined by the degree of weakening in sound wave energy per unit of distance traveled. It is composed of two parts, one (absorption) proportional to frequency, the other (scattering) dependent on the ratio of grain or particle size to wavelength. Since the attenuation is frequency dependent, a single attenuation coefficient only applies to a single frequency.

Ultrasonic waves are classified as shown in Table 2.2.

Table 2.2 Modes of Sound Waves

Wave Type In Solids	**Particle Vibrations**
Longitudinal (Compressional)	Parallel to wave direction
Transverse (Shear)	Perpendicular to wave direction
Surface (Rayleigh)	Elliptical orbit - symmetrical mode
Plate Wave - Lamb	Component perpendicular to surface (extensional wave)
Plate Wave - Love	Parallel to plane layer, perpendicular to wave direction
Stoneley (Leaky Rayleigh Waves)	Wave guided along interface
Sezawa	Antisymmetric mode

The wave described in Fig. 2.1 is called a *longitudinal wave* because the oscillations occur in the *longitudinal direction*, i.e. the direction of propagation. Since congressional and dilatational forces are active in it, it is also called a pressure or compression wave, and because its particle density fluctuates it has also been given the name density wave.

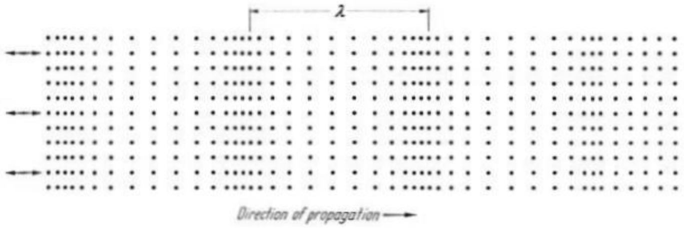

Figure 2.1 Longitudinal Wave

This is the real sound wave because it transmits the oscillations of a source of acoustic energy through the air to our ear. Research shows that the same wave also transmits sound through liquid or solid bodies [1].

However, in solid bodies also another kind of wave can occur, the *transverse wave* (also referred to as a *shear wave*) shown in Fig. 2.2 in the form of an instantaneous picture of the particle motion. It can be seen that in this case the particles no longer oscillate in the direction of propagation but at right angles to it, that is transverse.

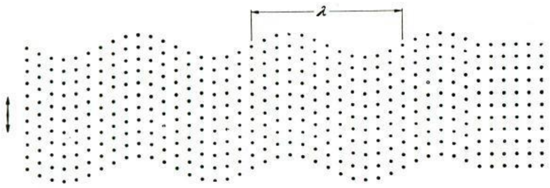

Figure 2.2 Transverse Wave

The excitations can be visualized as a motion in which the particles on the left interface of the body are moved sinusoidally up and down by a periodical shear force. In solid bodies such a shear force can be transmitted to the particles in the adjacent planes; their transverse oscillations will however show a lag in time, depending on their distance from the plane of exaction. This wave is also called a shear wave. Also in this case the wavelength is determined by the distance between two planes in which particles are in a similar state. In Fig. 2.2 the wavelength is indicated between two planes in which the particles at this moment pass through their position of rest in a direction from top to bottom [1].

Longitudinal and shear waves are the two most widely used modes of ultrasound in non-destructive testing.

Rayleigh waves or *surface waves* are the boundary waves which exist on the flat or curved boundary surface of large (infinite) solid substances. They are somewhat analogues to water waves in which the motion of particles is both transverse and longitudinal in a plane containing the direction of propagation and the normal to the surface. In Rayleigh waves the particle movement is elliptical and such waves exist only in the surface layer of large solids. At depths greater than two wavelengths below the surface, the particle motion is practically zero. Rayleigh waves on a solid surface are non-dispersive.

At an interface, either liquid/solid or solid/solid, there can also be an interface wave, which is undamped. The particle displacement is wave guided along interface. This is known as the *Stoneley wave*. At a solid liquid interface, where the density of liquid is low, *leaky Rayleigh waves*, where there is some transfer of ultrasonic energy back into the liquid, are possible [2].

In a thin film (solid / solid) when the particle oscillation is in a plane parallel to the interface, the waves are known as *Love waves*. Love waves are dispersive. In plate material where the thickness is the order of few wavelengths, various forms of plate waves are possible, the most important forms for NDT being *Lamb waves*. These are combination of compressional and shear waves, the proportion depending on the frequency.

Sometimes another two terms for the description of waves are used. *Creeping waves* are similar to Rayleigh waves and creeps along the surface. *Standing waves* are the superposition of two similar waves of identical frequency and amplitude but different directions of propagation.

Rayleigh, Plate and other waves are used for special applications in ultrasonic testing, but for industrial ultrasonic applications the most important types of wave are longitudinal and transverse waves.

2.2.3 Generation of Ultrasound

There are number of ways in which ultrasonic waves can be produced, but for non-destructive testing, most equipment uses the piezoelectric effect, or its inverse, for both transmitter and receiver probes.

Piezoelectric effect is a property of a certain natural crystal which, when subjected to mechanical strain, e.g. pressure, can develop electrical charges of the opposite sign on opposing faces. It is now possible to produce this effect in synthetic crystals (e.g., barium titanate) prepared from suitably processed mineral powders [11]. Conversely, the application of an electric potential will induce mechanical strain, e.g., compression or dilution, between opposing faces. This so-called inverse effect is utilized when a crystal is required to transmit ultrasonic waves and the direct effect when it is required to detect them.

Ultrasound is generated by an element in ultrasonic testing, identified as *transducer, crystal* or *probe*. Transducer is a device in which the application of an electric field across the active element produces mechanical deformation of the active element thereby generating ultrasonic vibrations and vice versa. The transducer forms the actual core in all non-destructive ultrasonic inspection procedures: The fact whether a workpiece can be inspected or not depends upon them. In numerous cases ultrasonic inspection becomes only feasible by use of transducers, which have appropriate acoustic properties. In any case the choice of the correct transducer is decisive for the quality and the reliability of inspection results.

Ultrasonic transducers may be classified as follows: Piezoelectric, electromagnetic, electrostatic, magnetostrictive, laser and other optical, miscellaneous [11]. Today, ultrasonic transducers work almost exclusively according to the piezoelectric effect.

Piezoelectric transducers (probes) convert electrical energy to mechanical energy or vice versa and each type consist of a crystal which is placed in contact, either directly or through a protective cover, with the material under test. There are several materials which may be used as transducers crystals and these include natural quartz, barium titanate, lead niobate and lithium sulphate.

Transducers may be of the normal type, or be angled. There are four fundamental transducer types [12]:

(1) Straight beam
(2) Angle beam
(3) Transmitter-Receiver (Twin crystal transducers)
(4) Delay line

In the *vertical* or *straight beam probe* (Fig. 2.3a), the piezoelectric element, which converts electrical energy into mechanical energy and vice versa, is mechanically attached to a backing material, most often called the damping block. The acoustic impedance of the damping block must be close to that of the piezoelectric material in order to suppress ringing resp. to enlarge the bandwidth. The second task of the damping block is to absorb that part of ultrasonic energy, generated by the piezoelectric element, which is going backward.

A protective and/or matching layer in front ensures that as much of the acoustic energy as possible is transmitted into the work piece. It also protects the probe against mechanical damage, while it is moved over a work piece, which may have a rough surface, or against chemical damage, when chemically aggressive fluids are used as couplants.

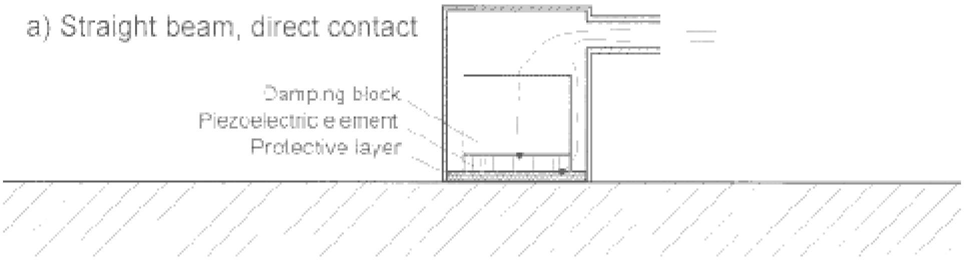

Figure 2.3a Basic construction of ultrasonic probe (Straight Beam Probe)

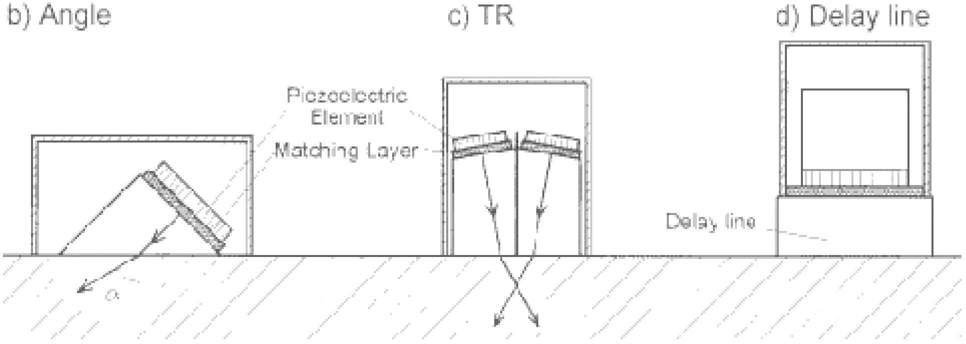

Figure 2.3b, c, d Basic construction of ultrasonic probe (Angle, TR, delay line)

With the *angle beam probe* (Fig. 2.3b), the ultrasound is transfered into the workpiece under at a specified angle. The *TR probe* (Fig. 2.3c) consists of one separate *transmitter* and *receiver* element each. Their sound field characteristics overlap in the workpiece. The piezo-elements are mounted on plastic wedges, which are generally made of plexiglass, polystyrene or other plastic materials of low acoustic absorption. Usually an acoustic matching layer is placed between the piezoelectric element and the plastic wedge. This ensures good energy transmission from the piezo element into the wedge. It also acts as a medium mechanical damping of the piezoelectric element.

These facts lead to a high sensitivity, rather short pulses and a high bandwidth. Therefore, angle beam probes build up like this do not need a separate backing material (damping block) on the rear face of the piezoelectric element, as far as not the extremely short pulses of thickness probes are expected from the probe.

The construction of the *"Delay line" probe* (Fig. 2.3d) complies basically with that of the vertical beam probe. However here, the sound is transmitted into the workpiece via an additional delay-line made of plastics with low ultrasonic absorption. The delay line can be either rigidly fixed to the front face of the vertical probe or can be interchangeable. The time delay until the ultrasonic signal enters the workpiece avoids, that echoes from flaws close to the surface appear within the dead zones of the ultrasonic flaw detector, which are caused by the high voltage excitation pulses. Use of delay-line probes is a simple measure to have an excellent near field resolution.

Depending on the application, transducers also differ with respect to the size of the active piezoelectric elements, their frequency, bandwidth and the basic design. The sound field characteristics of a transducer, which are expected under normal inspection conditions, are generally derived from the diameter and the frequency of the piezoelectric element.

A normal probe (SBP, TR, Delay Line) transmits a longitudinal (compressional) wave where oscillations occur in the direction of propagation, i.e. longitudinal direction, and angle probes (ABP) transmit shear (transverse) waves where oscillations occur at right angles to the direction of propagation or transmit Rayleigh waves which are the boundary or surface waves. Most normal ultrasonic tests use ultrasound in the form of longitudinal waves.

Ultrasound is generated by the help of one of these probes. An ultrasonic wave incident on a crystal causes it to vibrate, producing an alternative current across the crystal faces. Ultrasound is transmitted as a series of pulses of extremely short duration and during the time interval between transmissions, the crystal can detect reflected signals.

2.2.4 Characteristics of an Ultrasonic Beam

The ultrasonic waves generated by a disc-shaped crystal will emerge initially as a parallel-sided beam which later diverges, as shown in figure 2.4. The spread of the beam, α, is related to the frequency and the disc dimensions by the relationship

$$\sin\frac{\alpha}{2} = \frac{1.12\lambda}{d} \qquad (2.2)$$

where λ is the wavelength and *d* is the diameter of the disc (both in mm).

An ultrasonic beam can be divided into three zones: the dead zone, the near zone and the far zone.

The dead zone is the distance below the surface of a material in which a defect cannot be detected. A crystal is stimulated into vibration by an exciting voltage for a very short time to produce a short duration pulse of ultrasound. The crystal, even though heavily damped, does not stop vibrating immediately on cessation of the exciting voltage but 'rings' for a short time. It is not possible to detect a flaw during this ringing time (see figure 2.4b).

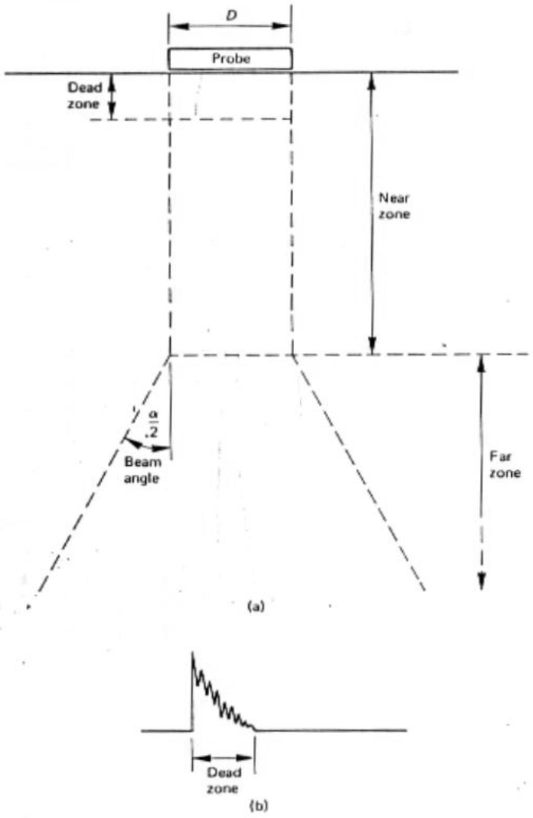

Figure 2.4 (a) Ultrasonic beam shape, (b) Appearance of dead zone on screen display

The near zone or *Fresnel zone* is the zone in which the beam is almost parallel sided. The length N, of the near zone is given by the approximate relationship

$$N = \frac{D^2}{4\lambda} \tag{2.3}$$

where *D* is the crystal diameter. The detection sensitivity is not constant throughout the near zone and is greatest towards the far end of this zone.

The far zone or *Fraunhofer zone* is the region beyond the near zone where beam spread occurs, and within this zone the sensitivity decreases with the square of the distance from the crystal. The ultrasonic beam is more uniform in the far field.

As the diameter of a crystal is reduced then, for a constant frequency, the beam spread angle increases, the length of the near zone decreases and a lower intensity beam is generated.

2.2.5 Waves at Boundaries

2.2.5.1 Reflection and Transmission of Ultrasonic Waves Incident on a Plane between Two Media

When a beam of ultrasonic wave reaches a boundary between two media, a proportion of the incident waves are reflected at the interface and a proportion are transmitted across the interface. For normal incidence waves, perpendicular to the surface, the transmission across the interface will be of the compression (longitudinal) wave type. The percentages of energy transmitted and reflected depend on acoustic impedance, Z, defined for each material as the product of material density and ultrasonic velocity.

$$Z = \rho V \tag{2.4}$$

For comp. waves

$$V = V_c = \left(\frac{E(1-\upsilon)}{(1+\upsilon)(1-2\upsilon)\rho} \right)^{1/2} \tag{2.5}$$

For shear waves $$V = V_s = \left(\frac{E}{2(1+\upsilon)\rho} \right)^{1/2} \qquad (2.6)$$

where

ρ : Density of the material (kg/m^3),

V : Velocity of the wave (m/s),

E : Modulus of elasticity (Young’s Mod.) (N/m^2),

ν : Poisson’s ratio,

For two materials of different acoustic impedances, Z_1 and Z_2, the percentages of energy transmitted (E_T) and energy reflected (E_R) are defined as:

$$E_T = \frac{4Z_1Z_2}{(Z_1+Z_2)^2} x100 \qquad (2.7)$$

$$E_R = 100 - E_T = \left(\frac{Z_1 - Z_2}{Z_1 + Z_2} \right)^2 x100 \qquad (2.8)$$

Equations 2.7 and 2.8 are for transmitted and reflected energies; for amplitude values, the square root is taken. Also these formulae are valid for both compressional and transverse waves, but as a transverse wave cannot be sustained in a liquid, it is always completely reflected at a solid/liquid or solid/gas interface.

2.2.5.2 Reflection and Refraction of Ultrasonic Waves Incident on a Plane between Two Media

When the incident beam is at some angle other than normal, that portion of the beam which is transmitted across the interface will be refracted. However, there may be two refracted beams transmitted into the metal, because part of the transmitted energy is converted into the shear wave mode. One refracted beam will be of the compression type while the other will be a shear wave, as shown in figure 2.5. It should be noted that at a solid/solid interface there will also be a reflected shear wave.

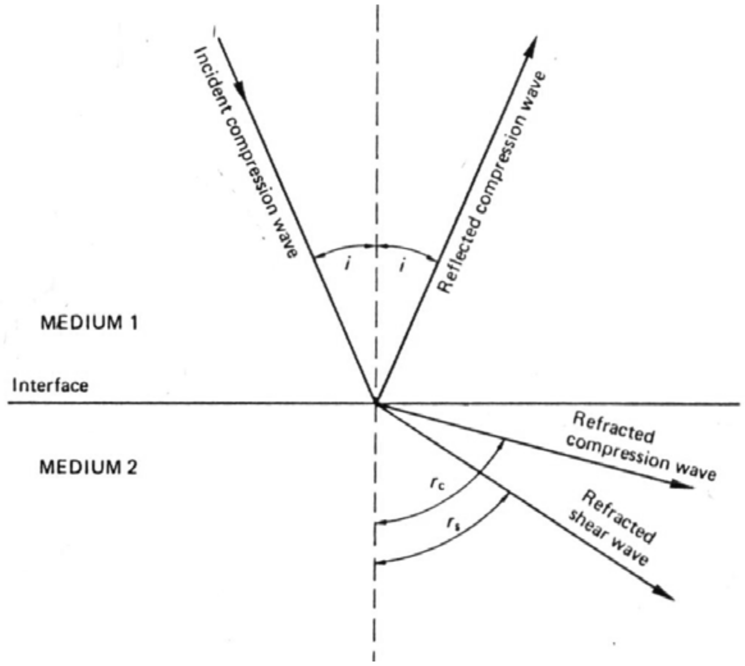

Figure 2.5 Reflection and refraction at an interface

The directions of propagation of the refracted compression and shear wave components at the interface between two media may be determined using Snell's refraction law:

Compression wave component $$\frac{\sin i}{\sin r_c} = \frac{V_{c1}}{V_{c2}} \tag{2.9}$$

Shear wave component $$\frac{\sin i}{\sin r_s} = \frac{V_{c1}}{V_{s2}} \tag{2.10}$$

At an interface it is possible to have mode conversion. Sound waves can change their mode of propagation when hitting the surface of a solid medium at an oblique angle. If the reflected part is perpendicular to the incident, then the direction of vibration of the particles remains the same after passing the point where the direction of propagation goes through a 90° change, i.e. a longitudinal wave is completely converted to a transverse wave. This conversion can also occur reciprocally, i.e. it is immaterial whether a longitudinal or a transverse wave was first generated, after conversion the other type will be present. If the sum of the angles of incidence and reflection for that portion is other than 90° then only a partial mode conversion occurs. This means that after reflection both transverse and longitudinal waves propagate in different directions.

Figures 2.6 and 2.7 shows the general cases of an incident compressional and shear wave respectively.

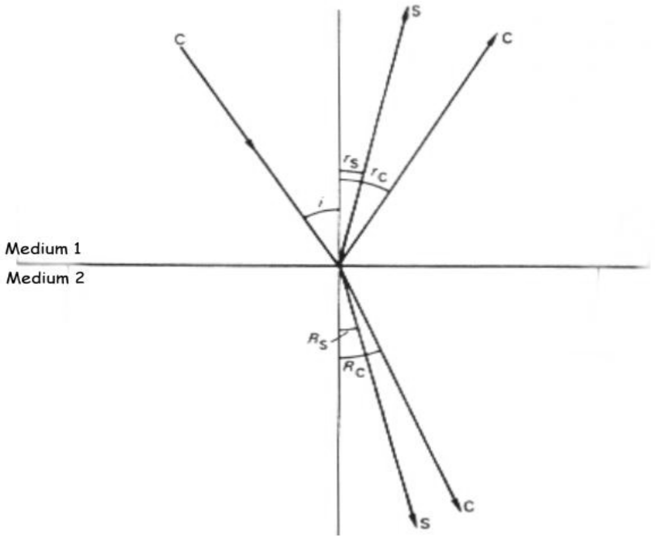

Figure 2.6 Compressional wave at an angle on to an interface between two materials, showing mode conversions. C denotes compressional waves and S shear waves, $r_c = i$ (the angle of incidence), and $V_1 > V_2$

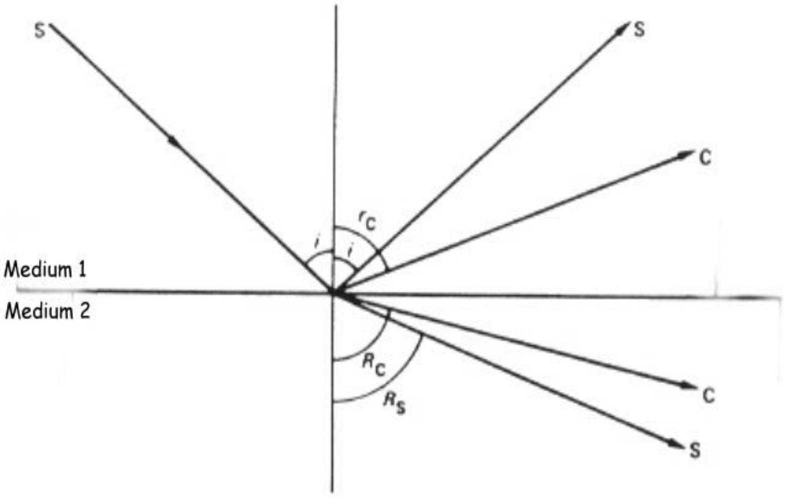

Figure 2.7 Shear wave at an angle on to an interface between two materials, showing mode conversions. C denotes compressional waves and S shear waves, and $V_1 > V_2$.

In Figure 2.6 $$\frac{\sin i}{V_{C1}} = \frac{\sin r_s}{V_{S1}} = \frac{\sin r_c}{V_{C1}} = \frac{\sin R_s}{V_{S2}} = \frac{\sin R_c}{V_{C2}} \tag{2.11}$$

In Figure 2.7 $$\frac{\sin i}{V_{S1}} = \frac{\sin r_c}{V_{C1}} = \frac{\sin R_s}{V_{S2}} = \frac{\sin R_c}{V_{C2}} \tag{2.12}$$

2.2.6 Attenuation

Attenuation is the energy loss or decrease in ultrasonic intensity as the wave travels through the medium and such loss occurs along the whole travel path of the sound beam. Attenuation is expressed in decibel (dB). In idealized materials, sound pressure (signal amplitude) is only reduced by the spreading of the wave. Natural materials, however, all produce an effect which further weakens the sound. This further weakening result from two basic causes, which are *scattering* and *absorption* [13].

In scattering, sound is scattered at microscopic interfaces (grain boundaries, second phase particles and inclusions constitute microscopic interfaces in metals and alloy) in directions other than its original direction of propagation where conversion of sound to other forms of energy is absorption. The combined affect of scattering and absorption is *attenuation*.

The sound attenuation increases with an increase in the frequency and generally proportional to the square of sound frequency.

Absolute measurements of attenuation are very difficult to obtain because the echo amplitude depends on factors. The actual value of the attenuation coefficient for a given material is highly dependent on the way in which the material was manufactured in addition to amplitude. Thus, quoted values of attenuation only give a rough indication of the attenuation and should not be automatically trusted. Generally, a reliable value of attenuation can only be obtained by determining the attenuation experimentally for the particular material being used.

Formally ultrasonic attenuation is described in terms of an *attenuation coefficient* (α)

$$I = I_0 \exp(-\alpha t) \tag{2.13}$$

where I is the intensity at a distance t from an initial intensity I_0. Generally, α is taken as the sum of the true attenuation coefficient α_T and the scattered coefficient α_S.

Attenuation coefficient, in general, is obtained by the ratio of the amplitudes of the first backwall echo to that of the second backwall echo seen in a typical A-scan display like the one shown in Figure 2.8.

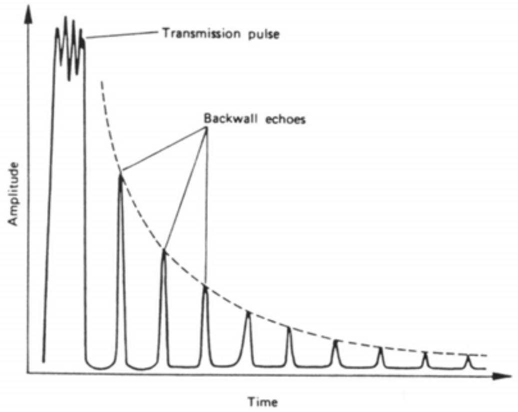

Figure 2.8 Measurement of attenuation: multiple backwall echo method

A convenient way of measuring changes in intensity, or amplification, is in terms of decibels (dB). A decibel is one-tenth of a bel, which is a unit based on logarithms to base 10, so that if the two powers are P_1 and P_2 they are said to differ by n bels if

$$\frac{P_1}{P_2} = 10^n \tag{2.14}$$

or $n = \log_{10}\left(P_1 / P_2\right)$ bels

$$n = 10 \cdot \log_{10}\left(P_1 / P_2\right) \text{ decibels (dB)} \tag{2.15}$$

Acoustic power (or intensity) is proportional to the square of the amplitude, so for comparison of amplitudes A_1 and A_2 the equation can be rewritten

$$n = 10 \cdot \log_{10}\left(\frac{A_1^{\,2}}{A_2^{\,2}}\right) = 20 \cdot \log_{10}\left(\frac{A_1}{A_2}\right) \tag{2.16}$$

Frequently, ultrasonic attenuation coefficients are given in dB/mm and for many engineering materials such as mild steel are very low (e.g. $5\text{x}10^{-3}$ dB/mm at 2 MHz) [2].

2.2.6.1 Measuring Attenuation Coefficient (α) Using Immersion Testing

The velocity of sound in water varies as a function of temperature. The equation relating the ultrasonic velocity of fresh water to its temperature is:

$$V_{fw} = 1410 + 4.21T - 0.037T^2 \tag{2.17}$$

Where:

V_{fw} = ultrasonic velocity of fresh water (m/s)

T = water temperature (degrees Celcius, ^{0}C)

The amplitude of the signals reflected from and transmitted by the liquid/solid (coupling liquid to test object) interface can be calculated from the acoustic impedances of the liquid and test object by the equations [21]:

$$R = \frac{Z_w - Z_s}{Z_w + Z_s} \tag{2.18}$$

and

$$T = \frac{2Z_w}{Z_w + Z_s} \tag{2.19}$$

where

Z_w = acoustic impedance of the material on the incident side of the interface,

Z_s = acoustic impedance of the material on the exit side of the interface,

R = reflected amplitude divided by the incident amplitude,

T = transmitted amplitude divided by the incident amplitude.

Z_w and Z_s values can be calculated from Equation 2.4 defined for each material.

The ratio of the signal reflected from the front surface to the signal reflected from the back surface of a plate of thickness "*t*" is:

$$\frac{F}{B} = (1 - R^2) \cdot e^{2\alpha t} \qquad (2.20)$$

from which the attenuation coefficient "α" can be calculated.

$$\alpha = \frac{1}{2t} \ln \left[\frac{F/B}{\left(1 - R^2\right)} \right] \qquad (2.21)$$

2.2.7 Ultrasonic Testing Techniques

Conventional ultrasonic testing may be conducted in one of two ways[8]:

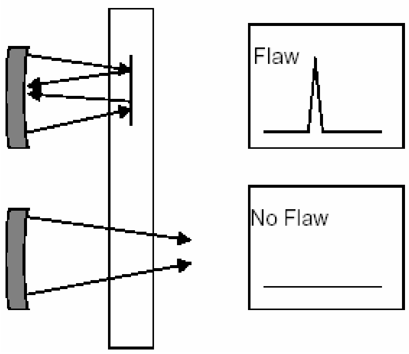

Figure 2.9 Pulse-echo technique

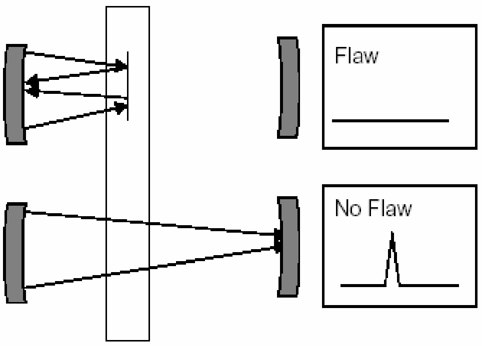

Figure 2.10 Through-transmission technique

The *pulse-echo (reflection) technique* (Figure 2.9) uses a single transducer. A flaw is indicated by the presence of a reflected signal. If this flaw is smaller than the cross section of the sound beam, part of the beam bypasses the flaw and strikes the backwall. The flaw in turn transmits an echo wave, depending on its form and size, and it reaches to the receiver. The echo wave coming from the flaw is indicated according to its transit time. Later the wave reflected from the bottom of the material to be tested arrives a correspondingly longer delay. Both echoes are indicated according to their intensity, namely echo height. The time interval between the transmitted and reflected pulses is a measure of the distance of the discontinuity from the surface, and the size of the return pulse can be a measure of the size of the flaw. If a backwall echo appears in addition to the echo from the flaw, its transit time corresponds to the thickness of the specimen.

In most applications, this time interval is a few microseconds or less. The two-way transit time measured is divided by two to account for the down-and-back travel path and multiplied by the velocity of sound in the test material. The result is expressed in the well-known relationship

$$d = vt/2 \qquad \text{or} \qquad v = 2d/t \tag{2.22}$$

where ‘d’ is the distance from the surface to the discontinuity in the test piece, ‘v’ is the velocity of sound waves in the material and ‘t’ is the measured round-trip transit time.

The *through-transmission technique* (Figure 2.10) uses separate transmit and receive transducers on opposite sides of the component under test. A flaw is indicated by the absence of a transmitted signal. This technique is particularly suitable for detecting disbonds in multilayer or complex structures where the reflected signal might be difficult to analyze. It also gives very good sensitivity but is limited by the need to access both sides of the component and to co-ordinate the movement of two transducers.

The pulse-echo method has certain advantages over the transmission method. These are:

(a) The specimen may be of any shape.
(b) Access to only one side of the testpiece is required.

(c) Only one coupling point exists, thus minimizing error.
(d) The distance of the defects from the probe can be measured.

2.2.7.1 Immersion Testing

All the techniques of inspection which have been discussed so far are of the type known as 'contact scanning' in which the inspection probe or probes are held in contact with the surface of the material, through a thin film of liquid *couplant*.

Immersion testing occurs by submerging the test piece and probe(s) in a tank of water and is ideally suited for the examination of part processed or finished parts in a production plant and the test equipment is usually fully automated. Examples of its use are for the inspection of slabs before these are machined into aircraft structural components, for the inspection of gas turbine discs, and for the inspection of aircraft wheels. In the case of the last mentioned item, a large airline may use immersion testing for the routine maintenance inspections [9].

The screen display obtained during an immersion test shows a blip corresponding to the water/metal interface, a backwall echo from the material and, between these two, a blip corresponding to any defect which may be present (Figure 2.11). The distance between the probe and test material must be set so that repeat echoes from the water/metal interface do not appear within the length of the time base corresponding to the thickness of metal. A time-base delay is usually incorporated into the display so that the first peak visible at the left-hand edge of the screen corresponds to the metal/water interface.

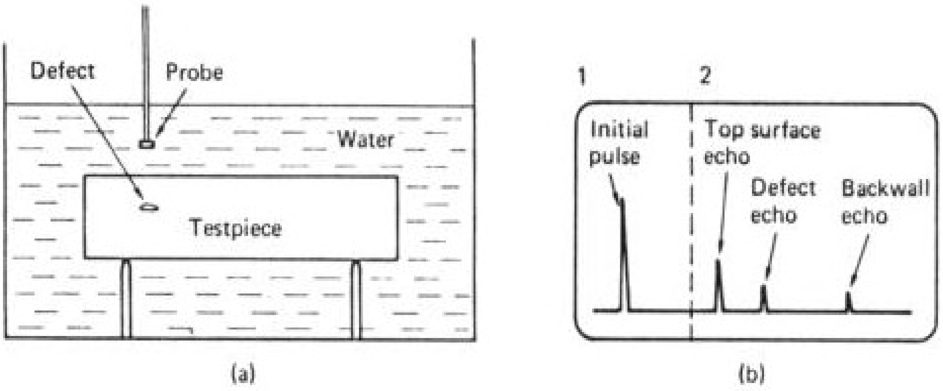

Figure 2.11 Immersion Testing: (a) testpiece arrangement; (b) screen display

2.2.8 The Role of Couplants

The *couplant* is used to transmit the ultrasonic energy through the interface between the probe and the material to be tested, and has an effect on the amplitude of the signal [14]. In another words, its purpose is to compensate for imperfect contact between both of the probe and the test piece, caused by curvature and/or surface roughness.

Couplants typically consist of water, glycerin, or a variety of oil and water based gels. All liquid couplants have much lower acoustic impedance than the materials of most test pieces. Of all suitable liquids glycerin has the highest acoustic impedance and is an excellent couplant, but expensive.

Grease and petroleum jelly can be used on vertical surfaces; they are also expensive and unpleasant to handle. The most commonly used couplant is medium-viscosity oil among liquid couplants.

The couplant to be used is appropriately selected according to the testing or environmental conditions, for example, water is not appropriate to the inspection of carbon steel due to corrosion, and viscous couplants may be required to inspect the inclined place.

All couplant layers reduce the sensitivity of testing and broaden the width of the reflected pulses. In theory, if the couplant thickness is one-quarter of the wavelength the multiple reflections in the couplant layer interfere, canceling one another out, and cause a loss of energy back to the piezoelectric crystal when it is in the receiving mode. If the couplant thickness is half of the wavelength, there is no interference canceling, but some additional pulse broadening due to the extra time-delay of the multiple reflected pulse in reaching the receiver.

In practice, with a typical surface, the couplant layer does not have a constant thickness over the width of the probe element, and the main effect is to add another unquantifiable variable to the height of the reflected pulse echoes. If a piece of metal foil is placed in the couplant layer, with couplant liquid on each face, there is a considerable reduction in the multiple reflections and so in the signal broadening, but more gain has to be used to maintain reflected signal height.

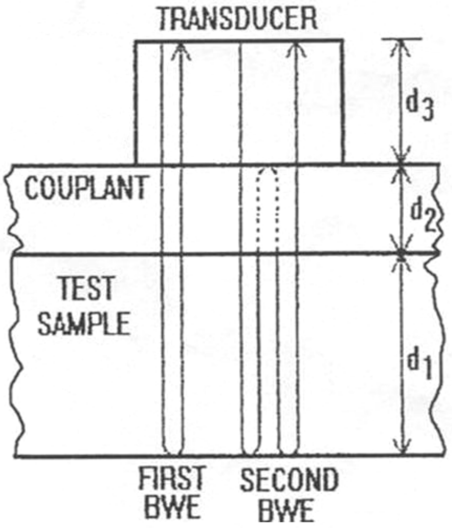

Figure 2.12 Transducer–Couplant–Test Sample Relation

The presence of the couplant is important for the sensitivity of the inspection in two ways;

- The attenuation of ultrasound in a couplant is much less than in an air,
- The couplant counters the acoustic impedance mismatch between the two materials (transducer-test piece).

Attenuation and acoustic velocity are two main properties that dictate the performance of a couplant [15]. Attenuation affects the amplitude of the signal and acoustic velocity determines both transit time and refracted angles.

Uniform coupling at all points of a given specimen is very important for quick and reliable evaluation of the readings.

Although the employment of liquid couplants has clear advantages, they have also some limitations:

- The application and removal of the couplant is time consuming and therefore costly part of the testing procedure.

- Danger of contaminating the component might be unacceptable. Ultrasonic inspection is often required in circumstances where the test piece material must not become wet or saturated with water. Typical examples include open cell structures, aerospace materials, porous components such as a part-finished honeycomb structures with porous skins. Other materials such as foam, wood or paper based products may be damaged by contact with water, or be incapable of withstanding the application of heat to dry them afterwards. Indeed, with the increasing use of composites in aerospace and other safety critical structures, the issue of couplant caused contamination is of growing importance.

- Another common problem is loss of couplant from the probe face, which causes the signal amplitude to vary making interpretation difficult. This problem is most pronounced when the test piece surface is rough and scanning speed is high.

To eliminate these limitations and to develop alternative techniques, many attempts have been made in the form of non-contact techniques including air-coupled ultrasound, laser generation and detection systems and electromagnetic acoustic transducers (EMATS) [7]. The air-coupled ultrasonic technique has in addition shown to be very efficient and fast for the testing of large areas, but air causes an impedance mismatch and the sound attenuation is increasing in air by increasing the frequency. Nowadays air-coupled ultrasound problems are being minimized. Use of laser systems can cause scorching of the test piece surface due to the high levels of energy involved. Such systems are also very expensive, making practical use unlikely at this time. EMAT probes can only operate on electrically conducting test pieces, which eliminates use on composites and other non-metallic structures and have much lower sensitivity than piezoelectric transducers.

Another way to overcome the need for a liquid couplant is the employment of solid coupling media. Transducers of this type commonly use a soft solid, typically a rubber between the transducer and test piece, which conforms around surface undulations of the test surface when in pressed contact. There are two common designs for such a transducer; a static probe whereby a rubber tip is attached to the face of a conventional contact transducer, and a wheel probe typically consisting of a transducer crystal at the hub of the wheel which is free to roll over the test piece, coupling being provided by a rubber tire [5].

2.2.8.1 Reflection and Transmission of Ultrasonic Waves Incident on a Plane between Two Media Including Couplant Factor

Since a thin layer is formed by using the couplant between the transducer and the test material, percentages of energy transmitted and energy reflected become different from Eqs. (2.7) and (2.8) in real contact testing. In this case, percentage of energy transmitted, is represented as follows [14]:

$$E_T = \frac{4}{2+\left(\frac{Z_3}{Z_1}+\frac{Z_1}{Z_3}\right)\cos^2 k_2 d+\left(\frac{Z_3{}^2}{Z_1 Z_3}+\frac{Z_1 Z_3}{Z_2}\right)\sin^2 k_2 d} x100 \qquad (2.23)$$

If the layer thickness is very small compared with the wavelength, i.e $k_2d \ll 1$ and $Z_2 < Z_1, Z_3$

then $\cos k_2 d \approx 1$ and $\sin k_2 d \approx k_2 d$

where

k_2: wave number in the layer and $k_2 = 2\pi/\lambda_2$,

λ_2: wavelength of the layer,

d: layer thickness,

Z_1, Z_2, Z_3 : acoustic impedances of transducer, layer(couplant) and the test piece, respectively.

The couplant having higher value of transmission coefficient is more effective for flaw detection, and the reflection coefficient should be known to measure the attenuation coefficient of the test material.

As seen from the equation (2.23) since the acoustic impedances of the transducer and test material are fixed, the intensity of the transmitted wave is influenced by the wavelength of transducer, the thickness and the characteristic acoustic impedance of the couplant being used and equation (2.23) shows that the smaller thickness of a layer, the stronger intensity of a transmitted wave.

2.2.8.2 Couplant Correction (Thickness) Factor

Couplant correction factor, K, is used for correction of transit time (velocity) measurements [16].

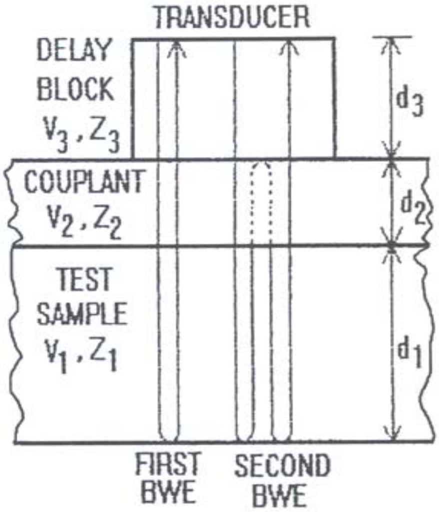

Figure 2.13 Basic configuration used in ultrasonic thickness measurements

Referring to Figure 2.13, transit time between the initial pulse and first backwall echo (BWE) of the test sample when a delay block is used is:

$$2\left(\frac{d_1}{V_1}+\frac{d_2}{V_2}+\frac{d_3}{V_3}\right) \tag{2.24}$$

where V_1, V_2 and V_3 are the ultrasonic longitudinal velocities in the test sample, couplant and transducer delay block, respectively. The transit time between the initial pulse and second BWE is:

$$2\left(\frac{2d_1}{V_1}+\frac{d_2}{V_2}+\frac{d_3}{V_3}\right)+K \tag{2.25}$$

where *K* is the correction factor due to couplant. Subtraction of equation (2.24) from equation (2.25) gives the transit time between first backwall echo (BWE) and second BWE is:

$$t_2 - t_1 = \frac{2d_1}{V_1} + K \tag{2.26}$$

Correction factor, *K*, can be calculated from:

$$K = \frac{1}{2\pi f} \tan^{-1}\left[\frac{(n_2 d_1 - n_1 d_2)\sin\theta\cos\theta}{n_1 d_1 \cos^2\theta + n_2 d_2 \sin^2\theta}\right] \tag{2.27}$$

where

f = frequency,

$n_1 = Z_2 (Z_3 - Z_1)$,

$d_1 = Z_2 (Z_3 - Z_1)$,

$n_2 = Z_2^2 - Z_1 Z_3$,

$d_2 = Z_2^2 + Z_1 Z_3$,

$\theta = 2\pi L f / V_2$,

L = thickness of couplant,

$V = 2L / t_2 - t_1$ (phase velocity for couplant thickness),

Z_1, Z_2, Z_3 are the acoustic impedances.

If the ultrasonic velocities and densities are known in the material of the transducer's face, couplant and the sample, the correction factor *K* can be evaluated from this equation for various frequencies and couplant thickness.

2.2.8.3 Couplant Effect on the Backwall Echoes and Attenuation Coefficient

Backwall echoes and also attenuation are influenced by the thin couplant layer. To measure the attenuation coefficient of a material, the amplitude of the backwall echoes reflected from the bottom surface of a specimen is compared.

Total attenuation can be calculated from (2.16) and attenuation coefficient is generally obtained by the ratio of the amplitudes of the first backwall echo to that of the second backwall echo. It is called the apparent attenuation coefficient. Including the couplant effect it can be calculated as follows [14]:

$$\alpha^{\prime} = 20\frac{1}{2h}\log\frac{\sqrt{R_1}V_1}{V_2} - \frac{5}{h}\log R_I \quad (dB/m) \tag{2.28}$$

where,

$R_1 = E_R / 100$,

V_1, V_2 = Amplitude of the echoes, and h = specimen thickness.

2.3 Polymers

Polymers can be defined as molecules of very high molecular weight, formed by joining together a number of molecules (monomers) of low molecular weight. These molecular units can all be identical, called homopolymer, or they can consist of two or more types, called copolymers.

Polymers are classified in several ways: by how the molecules are synthesized, by their molecular structure, or by their chemical family. However the most commonly used method to describe polymers is in terms of their mechanical and thermal behavior [17]. They are classified as thermoplastic, thermosetting polymers and elastomers. Table 2.3 compares the three major polymer categories.

Table 2.3 Classification of Polymers

Behavior	General Structure	Diagram
Thermoplastic	Flexible linear chains	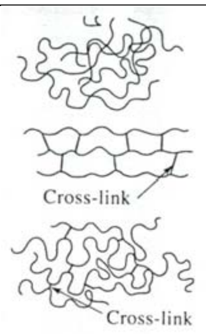
Thermosetting	Rigid three-dimensional network	
Elastomers	Linear cross-linked chains	

Thermoplastic polymers are composed of long chains produced by joining small molecules, or monomers; they behave in a plastic, ductile manner and soften when heated to elevated temperatures. Thermosetting polymers are composed of long chains of molecules that are strongly cross-linked each other to form three-dimensional network structure. These polymers are stronger, but brittle than thermoplastics. And elastomers, including rubbers, have an intermediate structure in which some cross-linking of the chains is allowed to occur.

All of the polymers have a complex three-dimensional structure that is difficult to describe pictorially. Figure 2.14 shows three way representation a segment of polyethylene, the simplest of the thermoplastic polymers.

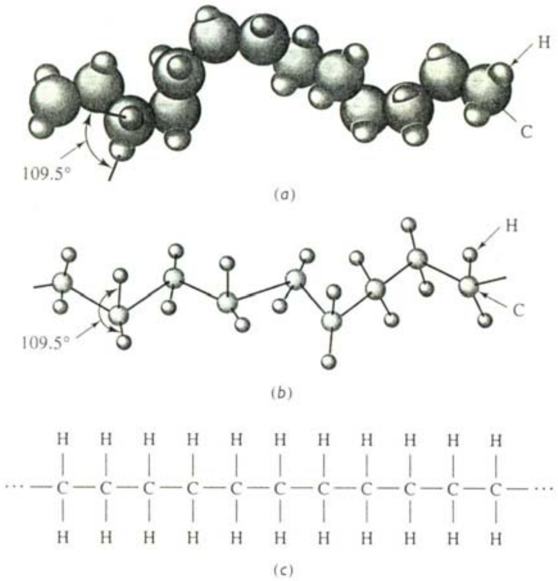

Figure 2.14 Three ways to represent the structure of polyethylene: (a) a solid 3D model, (b) 3D space model, (c) a simple 2D model

The polymer chain consists of a backbone of carbon atoms; two hydrogen atoms are bonded to each carbon atom in the chain. The chain twists and turns throughout space. The simple two-dimensional model in Figure 2.14(c) includes the essential elements of the polymer structure and is used to describe the various polymers. The single lines (-----) between the carbon atoms and between the carbon and hydrogen atoms represent a single covalent bond. Two parallel lines (==) represent a double covalent bond between atoms.

There is a relatively small but important group of polymers that are water soluble; these materials are often referred to “water-soluble gums” or “water-soluble resins”. As with polymers in general, it is convenient to divide these into three groups according to their origin, i.e., natural, modified natural (semisynthetic), and synthetic.

Synthetic polymers have the advantage that they are generally much simpler in their chain structure than most natural or modified natural polymers, while with synthetic copolymers a variety of degrees of complexity can be introduced in a controlled fashion. This makes these water-soluble synthetic polymers almost ideal model substances for developing techniques for studying aqueous solutions of polymers, and for testing theories of the behavior of such systems.

2.3.1 Hydrophilic Polymers

Hydrophilic polymers are synthetic polymers and capable of absorbing large quantities of water and water acts as a plasticizer causing the polymer to expand and become flexible. If the hydrophilic polymer is cross-linked, it swells but does not dissolve in water. The cross-links also guarantee a predictable expansion ratio. When dehydrated the polymers are hard with machining properties and placing them in water allows them to hydrate. Complete hydration is reached after a period of time depending on the final water uptake capacity of the polymer together with the thickness of the polymer, until they reach equilibrium [18].

Hydrophilic polymers are available in both homopolymer and copolymer forms. Hydrophilic copolymers are essentially made up of two monomer constituents; hydrophilic and hydrophobic. The hydrophobic part provides the long-term structure of the final material whereas the hydrophilic part provides hydration sites (e.g. OH or N) [19, 20]. It is to these sites that water bonds ionically. In addition, a small amount of free water enters some tiny voids opened upon expansion of the polymer. The amount of water absorbed by a hydrophilic copolymer is dictated by the ratio of hydrophilic to hydrophobic components.

An asset to hydrophilic polymer technology is the associated chemical flexibility. As the quantity of the hydrophilic component of a copolymer may be easily controlled, the ultimate water content on full hydration may be accurately defined. Similarly, the hydrophobic (or backbone) component can comprise of a number of different polymers providing alternative mechanical properties for the final hydrated material. Conventional hydrophilic polymers have low notch-tear strength. Suitable choice of monomer system and polymer fabrication method can dramatically improve tear strength.

Conventional hydrophilic polymers have been used extensively in medicine and pharmaceutics owing the body’s readiness to accept them as a result of their high water contents. Indeed, such materials may be more commonly recognized as those used for soft contact lenses [19].

2.4 Previous Studies

Many attempts have been made in the practical application of solid coupled ultrasonic transducers. Billson and Hutchins [4] described the use of a static, solid coupled longitudinal wave probe operating at a centre frequency of 5 MHz using a new low loss, synthetic rubber coupling medium as a delay line and found that it gave good results when used in the pulse-echo mode on various samples of industrial interest.

Drinkwater and Cawley [5] reported a similar static, solid coupled longitudinal wave probe operating at a centre frequency of 7 MHz using another low loss rubber (Figure 2.16). Both devices worked in pulse echo mode. Such new coupling materials gave scope for higher frequency wheel probes such as the one described by Drinkwater and Cawley [3, 5] which operated at a centre frequency of 3.8 MHz (Figure 2.15). This device was capable of operating in pulse echo mode and showed great promise for use in generating C-scan data without risk of test piece contamination.

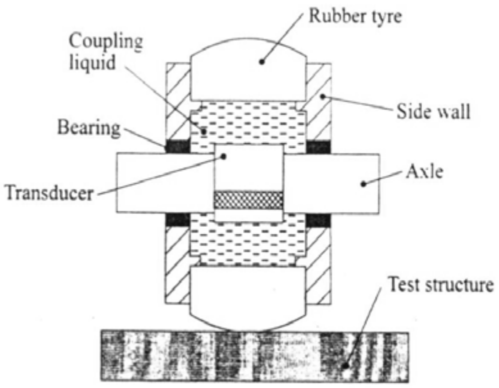

Figure 2.15 Wheel probe

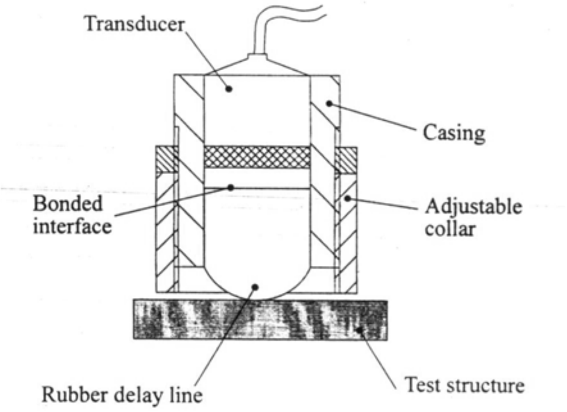

Figure 2.16 Static Probe

Another and most recent study for today in the development of new couplants used as solid couplants is the construction of another wheel probe by Bourne, Newborough and Highgate [19]. In this work the feasibility of employing hydrophilic polymers as novel, solid contact ultrasonic couplants for this application had been investigated and this work culminated in a prototype dry coupled wheel probe capable of working at > 5 MHz in pulse echo mode and providing excellent resolution while eliminating the risk of testpiece contamination.

For that study a prototype wheel probe had been produced to demonstrate the performance and scope of the hydrophilic material for use in NDT. This is a water filled wheel with a 13mm thick tire consisting of hydrophilic material. As the acoustic properties of the hydrophilic polymer tire are very similar to those of water, there is very little ultrasound reflected from the boundary between the water and the inside surface of the tire.

In practice this wheel probe is used manually to monitor thickness and to search for defects or as a part of a scanning system as shown in Figure 2.17.

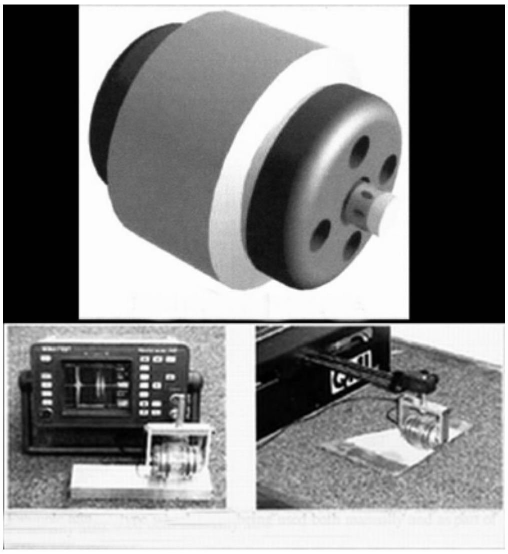

Figure 2.17 Model of prototype wheel probe and an example of this probe being used both manually and as part of a scanning system [19]

CHAPTER III

EXPERIMENTAL PROCEDURE

3.1 Experimental Set-up

In our experiments involving hydrophilic polymers, the following materials and devices were used:

- 2.25 MHz, 3.5 MHz, 5 MHz, 10 MHz (.5” Diameter each) and 20 MHz Logitudinal Transducers (Panametrics), obtained from NDT Center of Middle East Technical University (METU)
- 150 MHz Gould DataSYS 740 Digital Oscilloscope (CRT), obtained from METU
- Solid Couplants (Hydrophilic monomers are purchased to produce hydrophilic polymers):

  2-Hydroxyethyl methacrylate(HEMA) : Purchased from Sigma Chemical Co. and stored at 4 ^{o}C until use.
  Glycidyl methacrylate (GMA): Obtained from Aldrich and stored at 4 ^{o}C until use.
  EGDMA – ethylenglycoldimethacrylate: Crosslinker
  N,N’-methylenbisacrylamide (BIS;Fluka): Crosslinker

Benzoyl Peroxide : Initiator. Purchased from Merck AG (Darmstadt, Germany) and stored at room temperature until use.

- *Deionized Water:* Obtained from Hacettepe University and stored at room temperature until use.
- *Petri Dishes (Glass Mould)*: Purchased from BIOSTAR
- Liquid couplant (Water)
- Steel Test Piece [82x72x34 (mm)], obtained from METU
- Weights (50g, 200g, 500g, 1kg)

In this study, three different hydrophilic polymers [Poly(HEMA), Poly(HEMA-co-GMA), Poly(HEMA-NN′-dH_2O)] with different thicknesses and monomer contents were used as couplants and compared with water, medium-viscosity oil, typical plastics and rubbers.

3.1.1 P(HEMA)

P(HEMA) is a synthetic water-soluble polymer (hydrophilic) or defined as hydrogel and generally used in contact lenses, drug delivery systems, biomedical applications, chromatographic columns and flocculating agents.

P(HEMA) is clear and chemically stable. Another property is its hydrophilicity, also good swelling in water and electrolytic solutions. Physical properties of p(HEMA) gels such as porosity, water content and solute permeability, may be modified by varying polymerization conditions, and thus optimum conditions can be selected. Its chemical structure is given in Figure 3.1.

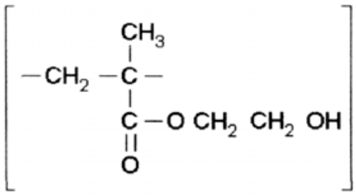

Figure 3.1 Chemical Structure of poly(HEMA)

3.1.2 Glycidyl methacrylate (GMA)

Glycidyl methacrylate (GMA) is a high purity, dual functionality monomer ideally suited for coating (Automotive Coatings, Powder Coatings, Radiation Curable Coatings, Waterborne Coatings Resins, etc) and resin applications. The most important feature of GMA monomer is its versatility. GMA monomer can react with an extremely wide range of monomers and functionalized molecules, providing greater flexibility and freedom in polymer design. These reactions provide polymers with a long list of performance benefits, including; excellent weathering and acid resistance, improved impact resistance, adhesive strength, water resistance, heat resistance, thermoplastic polymer blend compatibility.

3.1.3 Deionized Water

All water used in the experiments was purified using a Barnstead (Dubuque, IA) ROpure LP® reverse osmosis unit. Deionization is the process of removing the dissolved ionized solids from water by ion exchange. The difference between the soft water and deionizing systems is that soft water exchanges Calcium and Magnesium minerals for Sodium minerals (or salt), while deionized water removes ALL minerals and leaves no excess minerals behind.

3.2 Preparation of Polymer Membranes

Preparation of the p(HEMA) membrane was carried out according to the following procedure.

A 5 ml mixture consisting of 2 ml vacuum distilled monomer 2-hydroxyethyl methacrylate and 5 mg of benzoyl peroxide as a polymerization initiator and phosphate buffer (3ml, 0.1 M, pH 7) was placed in a test tube, and mixed by vortexing. The mixture was then poured into a round glass mould (9 cm in diameter) and exposed to ultraviolet radiation (UV), (360 nm), (12 W lamp, P.W. Allen and Co.) for 10 min under nitrogen atmosphere. Oxygen was removed from the mixture by bubbling nitrogen gas through the mixture. In order to remove oxygen impurity present in the nitrogen gas, nitrogen was bubbled through a solution contained in a washing bottle (60 % pyrogallic acid 100 ml and 40 % KOH 50 ml).

After completion of the photopolymerization, the membrane obtained was washed several times with distilled water and ethyl alcohol, and cut into circular pieces with a perforator. Membrane was stored in deionized water at 4^0C until use.

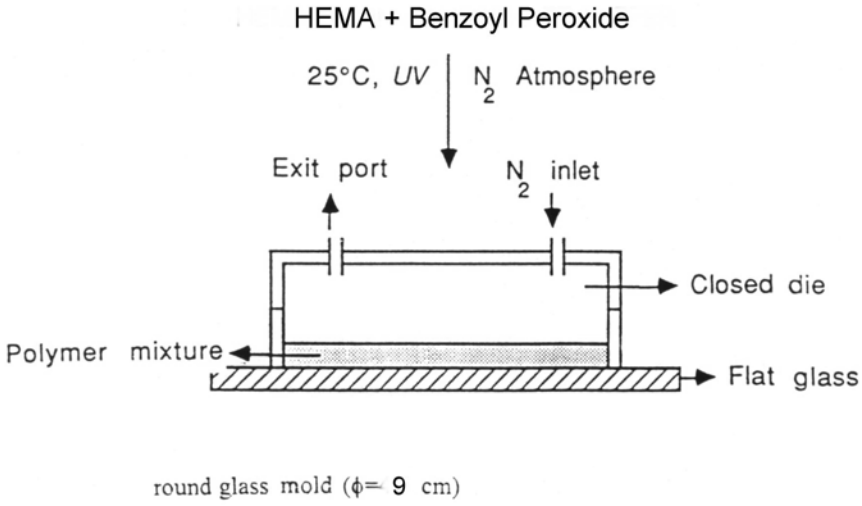

Figure 3.2 Membrane Preparation System

Preparation of other hydrophilic polymer membranes was carried out as the same procedure above. These polymers include different ratios and types of monomers (E.g. GMA). For example; 6 ml, 9 ml and 12 ml mixtures with the contents of 50, 100 and 150 μl GMA are prepared as a new type of polymer, becoming a copolymer namely poly (HEMA-co-GMA), with different thicknesses in the same way.

3.2.1 Swelling Ratio and Thickness Measurements of Membranes

Swelling ratios were determined in deionized water. The experiment was conducted as follows: produced membranes were taken from round glass mould (∅=9cm) and from each polymer, a few circular pieces of membrane with 9mm diameter were cut. Initially dry membranes (∅=9mm, dried 12h at 45^0C in a vacuum oven) were carefully weighed before being placed in deionized water. Then dry membrane pieces were placed in water and kept at a constant temperature of 25 °C. The swollen membrane was taken out from the water periodically, wiped using a filter paper, and weighed by an electronic balance (Scaltec SBA 31, Germany). The swelling ratio of the membranes was calculated by using the following expression:

$$Swelling\ Ratio(\%) = \left(\frac{W_H - W_D}{W_D} \right) \times 100$$

where

W_H : hydrated weight of the polymer and,

W_D : dehydrated weight of the polymer.

Since the membranes are characterized by thin film geometry, a one-dimensional water sorption process is assumed. Results were shown in tables in terms of weight versus time.

Thicknesses were measured by a Nikon Alphaphot YS microscope, which is shown in Figure 3.3.

This microscope has the advantage of zooming with its 4x, 10x, 40x and 100x objectives. The main eyepiece also has 10x objective with scales in µm. Also with an optional camera equipment attached to the microscope, structure of the membranes can be photographed.

In this study, cross section views of 9mm membranes were taken by a camera attached to the microscope.

Figure 3.3 Nikon Alphaphot

3.2.2 Transit Time and Ultrasonic Velocity Measurements

Ultrasonic velocity measurements were performed at pulse-echo mode using immersion technique (Figure 3.4).

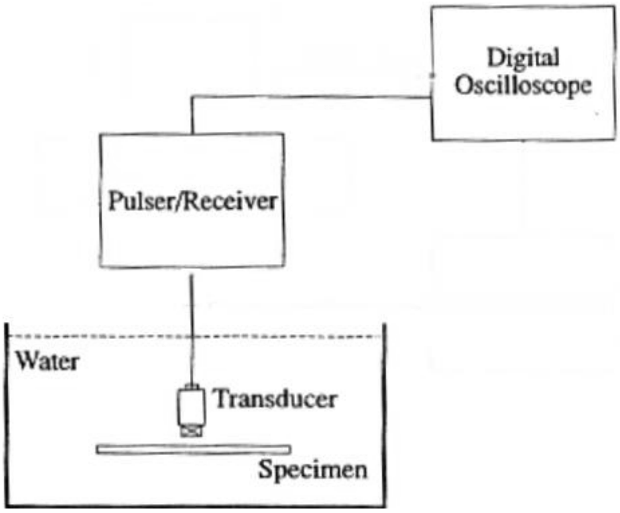

Figure 3.4 Schematic representation of the apparatus for immersion technique

Hydrophilic polymers were immersed in deionized water as shown in Figure 3.5.

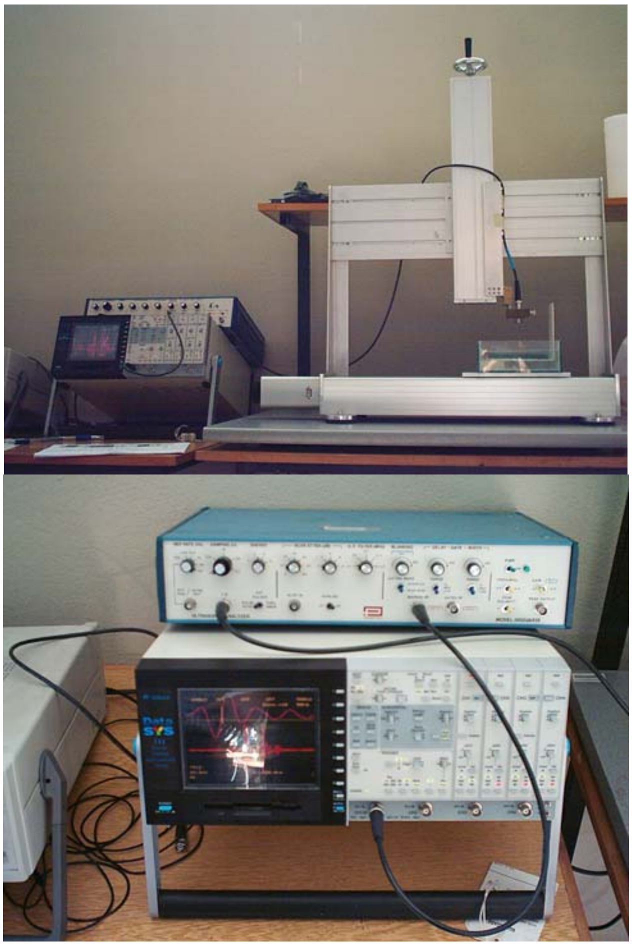

Figure 3.5 The apparatus used to measure velocity and attenuation

Different from the conventional immersion testing, in our study, a new approach was put into practice. Since hydrophilic membranes could not stay stable in the water, a glass with dimensions 12x12cm and 10mm thickness with a 2 cm hole at the center was manufactured. Polymer membranes were placed between this glass and a metal plate with a slightly greater hole at the center. This setup was wholly immersed in water (Figure 3.6). 10 MHz longitudinal immersion probe was placed through the hole and echoes were observed. For the consecutive backwall echoes to be observed, an air bubble was formed. Air bubble produced an acoustic impedance mismatch between the polymer and the water, so that the consecutive backwall echoes could be clearly seen.

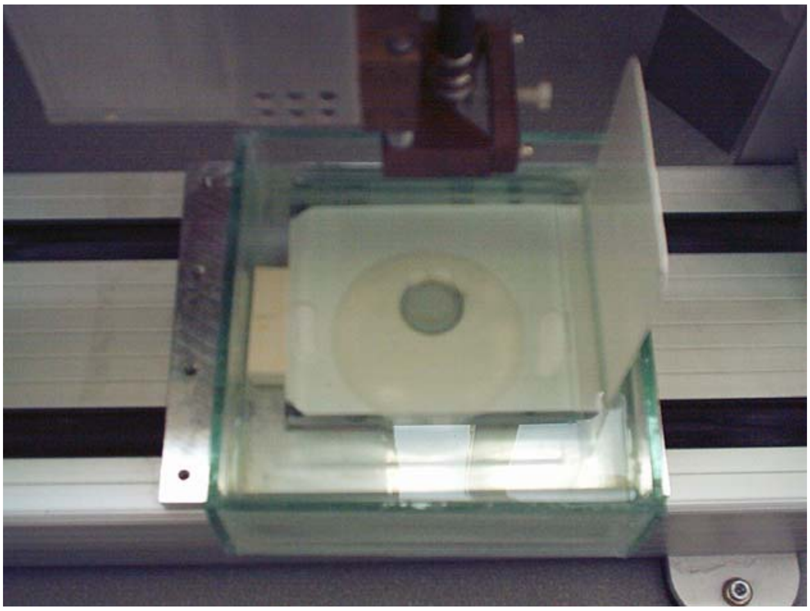

Figure 3.6 Experimental Setup

Before travel time (transit time) and velocity measurement of hydrophilic polymers, which were stored at 4^0C in the refrigerator, they were taken outside and waited to come to the desired temperature, which is the room temperature. Experiments were performed at a room temperature of 26±1 ^{0}C and water temperature 25±1^{0}C.

Velocities were found from equation (2.22) and related to velocities, acoustic impedances were found from equation (2.4) given in Chapter 2. Echo views for each polymer could be saved to the 3½ Floppy Diskette by 150 MHz Gould DataSYS 740 Digital Oscilloscope.

For each velocity measurement depending on the transit time, three different points on the polymer were selected and 20 separate measurements were taken for each point by pressing the hold button on the digital oscilloscope. Transit times were calculated by measuring the distance between backwall echoes (10 measurements for the distance between maximum points of the 1st peaks of the 1st and 2nd backwall echoes (BWE), 10 measurements for the distance between zero crossing of the 2nd peaks of the 1st and 2nd backwall echoes (BWE)). After completing all of these measurements, an average value is calculated.

3.2.3 Attenuation Measurements

Ultrasonic attenuation of solid couplants was measured by Panametrics longitudinal wave transducers connected with an oscilloscope. These measurements were performed at frequencies of 2.25MHz, 3.5MHz, 5MHz, 10 MHz and 20MHz using pulse-echo and immersion techniques. The same procedure and setup was used as in the velocity measurements. Polymer membranes were placed between a glass and a metal plate. Transducers at various frequencies were immersed in water and positioned over membranes at a definite distance. For the attenuation measurements front surface and backwall echoes were observed.

Amplitude values of the front surface and backwall echoes were found in terms of dB (decibel) by adjusting both echoes to 80% screen height one by one. Also, the amounts of ultrasound transmitted and reflected were determined using equations (2.18) and (2.19) given in Chapter 2 and obtained values were used to determine the attenuation coefficient.

Attenuation coefficient with respect to frequency values were plotted using equation (2.21). The results were interpreted and compared with the conventional couplants, oil and water, in addition to typical plastics and rubbers.

3.3 Coupling Efficiency

For these experiments, a steel test block was selected and solid couplants (hydrophilic polymers) with various thicknesses and water contents were placed between the transducer and the test block. It was assumed that there is perfect contact at the interface.

The ability of a solid couplant to make a good surface contact with the test piece is of vital importance for efficient transfer of ultrasonic energy. In order to evaluate the coupling performance of hydrophilic polymers, a test procedure was used as shown in Figure 3.7.

The pressure applied to the transducer was varied while the amplitude and frequency of the testpiece backwall echo was monitored. For the loading conditions weights of 50g, 200g, 500g and 1 kg were used as loads.

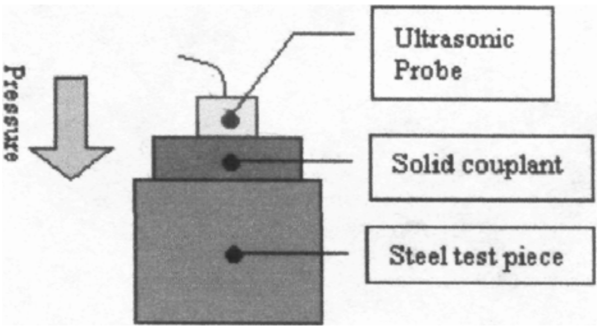

Figure 3.7 Test Procedure for Observation of Coupling Efficiency

Before placing the polymers over the testpiece, excess water on the polymers was wiped using filter paper. The interfaces between the probe-hydrophilic polymer and polymer-testpiece were coupled with a drop of water to ensure perfect contact. This guarantees that good surface contact is reached.

Tests were implemented firstly by selecting unloading condition (no load applied to the transducer). Secondly, weights were applied to the transducers for the loading conditions. Values were obtained in terms of dB (decibel).

The procedures were repeated many times for each polymer to monitor reproducibility.

CHAPTER 4

RESULTS AND DISCUSSION

4.1 Swelling Ratio and Thickness Measurements of Membranes

Although hydrophilic polymer samples were produced in the same way, some showed inconsistent trends in swelling ratio measurements. This is due to the amount and type of crosslinker used in polymers, inhomogeneous polymerization or the type of the polymer.

Results were shown in tables in terms of weight versus time. The number “10x” indicates that the polymer specimen thickness was measured with a 10x lens of the Nikon Alphaphot microscope. Thicknesses more than 1000 μm could be seen with a 4x lens of the microscope.

All hydrophilic polymers absorbed water until they reach to the equilibrium, which is the point where polymers cannot absorb more water. Table 4.1 through Table 4.6 shows the swelling ratio results of Poly(HEMA) membranes. The subscript (6ml, 9ml, 12ml) indicates the amount of mixture of the produced polymer. For this type of polymers different ratios of EGDMA(ethylene glycol dimethacrylate - crosslinker) was used to vary the water content of polymer.

Table 4.1 Swelling Ratio and Thickness of Poly(HEMA)$_1$

M_{HEMA} (dry) = 0.0257 g

Time (Min)	Weight (g)	Time (Min)	Weight (g)	Thickness (t)	Swelling Ratio
5	0,0328	60	0,0420	450µm (10x)	%64,98
10	0,0352	65	0,0422		
15	0,0363	70	0,0423		
20	0,0381	75	0,0424		
25	0,0389	80	0,0424		
30	0,0398				
35	0,0404				
40	0,0409				
45	0,0413				
50	0,0415				
55	0,0419				

Table 4.2 Swelling Ratio and Thickness of Poly(HEMA)$_2$

M_{HEMA} (dry) = 0.0342 g

Time (Min)	Weight (g)	Time (Min)	Weight (g)	Thickness (t)	Swelling Ratio
5	0,0416	55	0,0543	570µm (10x)	%62,57
10	0,0442	60	0,0547		
15	0,0468	65	0,0556		
20	0,0475	70	0,0557		
25	0,0492	75	0,0556		
30	0,0501				
35	0,0511				
40	0,0518				
45	0,0530				
50	0,0540				

Table 4.3 Swelling Ratio and Thickness of Poly(HEMA)$_3$

M_{HEMA} (dry) = 0.0235 g

Time (Min)	Weight (g)	Time (Min)	Weight (g)	Time (Min)	Weight (g)	Thickness (t)	Swelling Ratio
5	0,0301	50	0,0414	95	0,0457	550μm (10x)	%126,8
10	0,0330	55	0,0420	100	0,0459		
15	0,0344	60	0,0429	115	0,0459		
20	0,0357	65	0,0432	120	0,0461		
25	0,0372	70	0,0436	130	0,0469		
30	0,0383	75	0,0442	140	0,0475		
35	0,0395	80	0,0446	150	0,0480		
40	0,0404	85	0,0450	175	0,0487		
45	0,0409	90	0,0456	Saturated	0,0533		

Poly (HEMA)$_1$ and Poly(HEMA)$_2$ reached to the equilibrium nearly at 65 minutes where Poly(HEMA)$_3$ reached more than 3 hours due to the reasons mentioned above. This variation can also be clearly observed visually from the structure of polymer. Poly(HEMA)$_3$ was more opaque than other two polymers. Poly(HEMA)$_3$ had a swelling ratio %126.8, also more time was needed for equilibrium.

Table 4.4 Swelling Ratio and Thickness of Poly(HEMA)$_{6ml}$

M_{HEMA} (dry) = 0.0221 g

Time (Min)	Weight (g)	Time (Min)	Weight (g)	Time (Min)	Weight (g)	Thickness (t)	Swelling Ratio
5	0,0281	55	0,0402	115	0,0453	680μm (10x)	%119,5
10	0,0309	60	0,0411	120	0,0459		
15	0,0324	65	0,0415	130	0,0467		
20	0,0337	70	0,0419	140	0,0472		
25	0,0352	75	0,0426	150	0,0477		

Table 4.4 Continued

Time (Min)	Weight (g)	Time (Min)	Weight (g)	Time (Min)	Weight (g)	Thickness (t)	Swelling Ratio
30	0,0363	80	0,0431	175	0,0485		
35	0,0375	85	0,0435	190	0,0484		
40	0,0384	90	0,0441	195	0,0485		
45	0,0390	95	0,0443				
50	0,0395	100	0,0448				

Table 4.5 Swelling Ratio and Thickness of Poly(HEMA)$_{9ml}$

M_{HEMA} (dry) = 0.0300 g

Time (Min)	Weight (g)	Time (Min)	Weight (g)	Time (Min)	Weight (g)	Thickness (t)	Swelling Ratio
5	0,0366	50	0,0474	95	0,0535	1125μm (4x)	% 109,67
10	0,0386	55	0,0489	100	0,0541		
15	0,0404	60	0,0497	105	0,0543		
20	0,0415	65	0,0503	110	0,0548		
25	0,0432	70	0,0508	190	0,0604		
30	0,0444	75	0,0514	220	0,0613		
35	0,0453	80	0,0523	280	0,0630		
40	0,0462	85	0,0533	290	0,0629		
45	0,0474	90	0,0532	295	0,0629		

Table 4.6 Swelling Ratio and Thickness of Poly(HEMA)$_{12ml}$

M_{HEMA} (dry) = 0.0407 g

Time (Min)	Weight (g)	Time (Min)	Weight (g)	Time (Min)	Weight (g)	Thickness (t)	Swelling Ratio
5	0,0486	50	0,0722	95	0,0906	1750μm (4x)	% 153,56
10	0,0539	55	0,0746	100	0,0924		
15	0,0562	60	0,0760	105	0,0943		

Table 4.6 Continued

Time (Min)	Weight (g)	Time (Min)	Weight (g)	Time (Min)	Weight (g)	Thickness (t)	Swelling Ratio
20	0,0584	65	0,0785	110	0,0962		
25	0,0611	70	0,0806	190	0,1026		
30	0,0632	75	0,0824	200	0,1026		
35	0,0651	80	0,0486	280	0,1031		
40	0,0681	85	0,0873	295	0,1032		
45	0,0701	90	0,0886	300	0,1032		

Swelling ratios of Poly(HEMA)$_{6ml}$, Poly(HEMA)$_{9ml}$ and Poly(HEMA)$_{12ml}$ were resulted in high values. Besides the amount of crosslinker, increasing monomer content per unit area affects UV polymerization behavior and tends to increase polymer molecules. This results in swelling ratio to increase.

Tables 4.7 through 4.15 show the swelling ratio results of Poly(HEMA-co-GMA) type membranes. Calculated values are very close to each other. Glycidyl methacrylate (GMA) has a property of water resistance, thus behaved like a crosslinker. Increasing GMA content decreased swelling ratio as seen from the results.

Table 4.7 Swelling Ratio and Thickness of Poly(HEMA-co-GMA), VT=6ml, 50µl GMA, $M_{Poly(HEMA-co-GMA)}$ (dry) = 0.0256 g

Time (Min)	Weight (g)	Time (Min)	Weight (g)	Thickness (t)	Swelling Ratio
5	0,0291	55	0,0378	580µm (10x)	% 62,1
10	0,0305	60	0,0378		

Table 4.7 Continued

Time (Min)	Weight (g)	Time (Min)	Weight (g)	Thickness (t)	Swelling Ratio
15	0,0316	65	0,0383		
20	0,0325	70	0,0384		
25	0,0335	80	0,0387		
30	0,0347	90	0,0394		
35	0,0352	95	0,0397		
40	0,0361	100	0,0398		
45	0,0366	105	0,0401		
50	0,0369	Saturated	0,0415		

Table 4.8 Swelling Ratio and Thickness of Poly(HEMA-co-GMA), VT=6ml, 100µl GMA, $M_{Poly(HEMA\text{-}co\text{-}GMA)}$ (dry) = 0.0139 g

Time (Min)	Weight (g)	Thickness (t)	Swelling Ratio
5	0,0172	350µm (10x)	% 58,27
10	0,0188		
15	0,0198		
20	0,0207		
25	0,0214		
30	0,0214		
35	0,0217		
40	0,0220		
45	0,0222		
50	0,0220		
55	0,0221		
60	0,0221		
65	0,0220		
70	0,0220		

Table 4.9 Swelling Ratio and Thickness of Poly(HEMA-co-GMA), VT=6ml, 150µl GMA, $M_{Poly(HEMA\text{-}co\text{-}GMA)}$ (dry) = 0.0119 g

Time (Min)	Weight (g)	Time (Min)	Weight (g)	Thickness (t)	Swelling Ratio
5	0,0143	60	0,0184	330µm (10x)	% 55,46
10	0,0155	65	0,0185		
15	0,0166	70	0,0184		
20	0,0174	75	0.0185		
25	0,0178				
30	0,0178				
35	0,0179				
40	0,0184				
45	0,0184				
50	0,0183				
55	0,0182				

Table 4.10 Swelling Ratio and Thickness of Poly(HEMA-co-GMA), VT=8ml, 50µl GMA, $M_{Poly(HEMA\text{-}co\text{-}GMA)}$ (dry) = 0.0281 g

Time (Min)	Weight (g)	Time (Min)	Weight (g)	Thickness (t)	Swelling Ratio
5	0,0326	65	0,0424	600µm (10x)	% 61,56
10	0,0344	70	0,0428		
15	0,0357	75	0.0427		
20	0,0368	80	0,0432		
25	0,0375	90	0,0434		
30	0,0390	100	0,0438		
35	0,0397	110	0,0440		
40	0,0404	150	0,0444		
45	0,0407	170	0,0446		
50	0,0411				
55	0,0417	Saturated	0,0454		
60	0,0422				

Table 4.11 Swelling Ratio and Thickness of Poly(HEMA-co-GMA), VT=8ml, 100µl GMA, $M_{Poly(HEMA\text{-}co\text{-}GMA)}$ (dry) = 0.0321 g

Time (Min)	Weight (g)	Time (Min)	Weight (g)	Thickness (t)	Swelling Ratio
5	0,0370	65	0,0467	750µm (10x)	% 59,2
10	0,0384	70	0,0471		
15	0,0398	75	0.0472		
20	0,0406	80	0,0475		
25	0,0415	90	0,0482		
30	0,0423	100	0,0484		
35	0,0433	110	0,0489		
40	0,0439				
45	0,0447	150	0,0497		
50	0,0452	170	0,0496		
55	0,0459				
60	0,0462	Saturated	0,0511		

Table 4.12 Swelling Ratio and Thickness of Poly(HEMA-co-GMA), VT=8ml, 150µl GMA, $M_{Poly(HEMA\text{-}co\text{-}GMA)}$ (dry) = 0.0211 g

Time (Min)	Weight (g)	Time (Min)	Weight (g)	Thickness (t)	Swelling Ratio
5	0,0244	65	0,0323	460µm (10x)	% 55,45
10	0,0259	70	0,0323		
15	0,0268	75	0.0324		
20	0,0279	80	0,0325		
25	0,0283	85	0,0327		
30	0,0294	90	0,0326		
35	0,0300	100	0,0327		
40	0,0305	105	0,0328		
45	0,0310	110	0,0327		
50	0,0311	120	0,0328		
55	0,0318				
60	0,0318	Saturated	0,0328		

Table 4.13 Swelling Ratio and Thickness of Poly(HEMA-co-GMA)$_1$, VT=12ml, 50µl GMA, M$_{Poly(HEMA-co-GMA)}$ (dry) = 0.0492 g

Time (Min)	Weight (g)	Time (Min)	Weight (g)	Time (Min)	Weight (g)	Thickness (t)	Swelling Ratio
5	0,0532	65	0,0635	135	0,0706	1175µm (4x)	% 61,38
10	0,0552	70	0,0641	140	0,0708		
15	0,0565	75	0.0649				
20	0,0577	80	0,0651	Saturated	0.0794		
25	0,0589	85	0,0654				
30	0,0593	90	0,0662				
35	0,0601	95	0,0663				
40	0,0607	100	0,0668				
45	0,0614	105	0,0668				
50	0,0614	110	0,0676				
55	0,0625	115	0,0680				
60	0,0634	120	0,0684				

Table 4.14 Swelling Ratio and Thickness of Poly(HEMA-co-GMA)$_2$, VT=12ml, 100µl GMA, M$_{Poly(HEMA-co-GMA)}$ (dry) = 0.0542 g

Time (Min)	Weight (g)	Time (Min)	Weight (g)	Thickness (t)	Swelling Ratio
5	0,0583	70	0,0687	1250µm (4x)	% 60,33
10	0,0598	75	0.0693		
15	0,0612	80	0,0697		
20	0,0624	85	0,0702		
25	0,0629	90	0,0706		
30	0,0639	95	0,0711		
35	0,0648	100	0,0716		
40	0,0654	105	0,0717		
45	0,0662	110	0,0721		
50	0,0668	120	0,0728		
55	0,0673	135	0,0756		
60	0,0676	140	0,0759		
65	0,0683	Saturated	0.0869		

Table 4.15 Swelling Ratio and Thickness of Poly(HEMA-co-GMA)$_3$, VT=12ml, 150µl GMA, $M_{Poly(HEMA-co-GMA)}$ (dry) = 0.0526 g

Time (Min)	Weight (g)	Time (Min)	Weight (g)	Thickness (t)	Swelling Ratio
5	0,0564	70	0,0654	1750µm (4x)	% 53,8
10	0,0580	75	0.0657		
15	0,0590	80	0,0661		
20	0,0597	90	0,0667		
25	0,0606	95	0,0674		
30	0,0613	100	0,0677		
35	0,0619	105	0,0679		
40	0,0624	110	0,0680		
45	0,0632	120	0,0688		
50	0,0635	135	0,0711		
55	0,0638				
60	0,0649	Saturated	0.0809		
65	0,0651				

Table 4.16 through 4.18 shows the swelling ratios of new type of polymer Poly(HEMA-NN′). High amount of crosslinker (NN′-methylen bisacrylamide) present in the polymer makes it monomer; therefore these polymers turn into a copolymer.

Tables 4.17 and 4.18 shows the swelling ratios of Poly(HEMA-NN′-dH_2O). In this polymer, crosslink agent (NN′) and dH_2O contents were varied. Deionized water (dH_2O) was used as dilution media to observe the effect of water in polymerization system. Water did not participate to polymerization. It only affected photopolymerization, thus swelling ratios.

Table 4.16 Swelling Ratio and Thickness of Poly(HEMA-NN′), VT=6ml (3ml HEMA, 3ml NN′), $M_{Poly(HEMA-NN')}$ (dry) = 0.0219 g

Time (Min)	Weight (g)	Time (Min)	Weight (g)	Thickness (t)	Swelling Ratio
5	0,0270	70	0,0352	480μm (10x)	% 67,58
10	0,0285	75	0.0354		
15	0,0300	80	0,0357		
20	0,0308	85	0,0355		
25	0,0332	90	0,0355		
30	0,0331	100	0,0360		
35	0,0339	105	0,0362		
40	0,0342	110	0,0364		
45	0,0343				
50	0,0348	Saturated	0,0367		
55	0,0352				
60	0,0353				
65	0,0353				

Table 4.17 Swelling Ratio and Thickness of Poly(HEMA-NN′-dH_2O), VT=6ml(3ml HEMA, 1ml NN′, 2ml dH_2O),$M_{Poly(HEMA-NN-dH2O')}$(dry)=0.0166 g

Time (Min)	Weight (g)	Time (Min)	Weight (g)	Thickness (t)	Swelling Ratio
5	0,0213	50	0,0267	440μm (10x)	% 63,85
10	0,0230	55	0,0267		
15	0,0244	60	0,0268		
20	0,0251	65	0,0268		
25	0,0258	70	0,0267		
30	0,0261	75	0.0268		
35	0,0263	80	0,0268		
40	0,0263				
45	0,0264	Saturated	0,0272		

Table 4.18 Swelling Ratio and Thickness of Poly(HEMA-NN′-dH_2O), VT=6ml(3ml HEMA, 2ml NN′, 1ml dH_2O),$M_{Poly(HEMA\text{-}NN'\text{-}dH2O)}$(dry)=0.0480 g

Time (Min)	Weight (g)	Time (Min)	Weight (g)	Thickness (t)	Swelling Ratio
5	0,0545	65	0,0654	1125μm (4x)	% 74,8
10	0,0565	70	0,0664		
15	0,0567	75	0.0669		
20	0,0581	80	0,0674		
25	0,0593	90	0,0682		
30	0,0604	100	0.0696		
35	0,0613	110	0,0703		
40	0,0620	150	0,0727		
45	0,0628	170	0,0737		
50	0,0634				
55	0,0641	Saturated	0,0839		
60	0,0649				

Figure 4.1 Cross-section views of polymers (∅=9mm membrane pieces)

4.2 Transit Time and Ultrasonic Velocity Measurements

All transit time and velocity measurements were obtained at 200 mV and 5μs range. Results were shown in tables and figures. From the figures below, you can also find the results of transit time measurements approximately by counting the units between consecutive backwall echoes (same phase of echoes). Since the range is 5μs, each division on the screen corresponds to 0.5μs and because each division has 5 units, the distance between units corresponds to 0.1μs(100ns).

Calculated polymer velocities were compared between each other and results showed that the higher the water content of the polymer, the closer the values are to those of pure water. It is also noteworthy that the acoustic impedance of all of the polymers evaluated in this study demonstrated acoustic impedances very close to that of water (V_w = 1480 m/s, Z_w=1.48(Nsm^{-3})x10^6 at 20^0C) [21].

Table 4.19 Poly(HEMA)$_1$ (t=450 µm, % 64,98 swelling ratio, M_{HEMA}dry=0,0257g)

Measurement	**Δt (ns)**	**Velocity (m/s)**
1	564	1595,7
2	562	1601,4
3	561	1604,3
4	560	1607,1
5	568	1584,5
6	569	1581,7
7	561	1604,3
8	569	1581,7
9	569	1581,7
10	560	1607,1
Average	564,3	**1595,0**

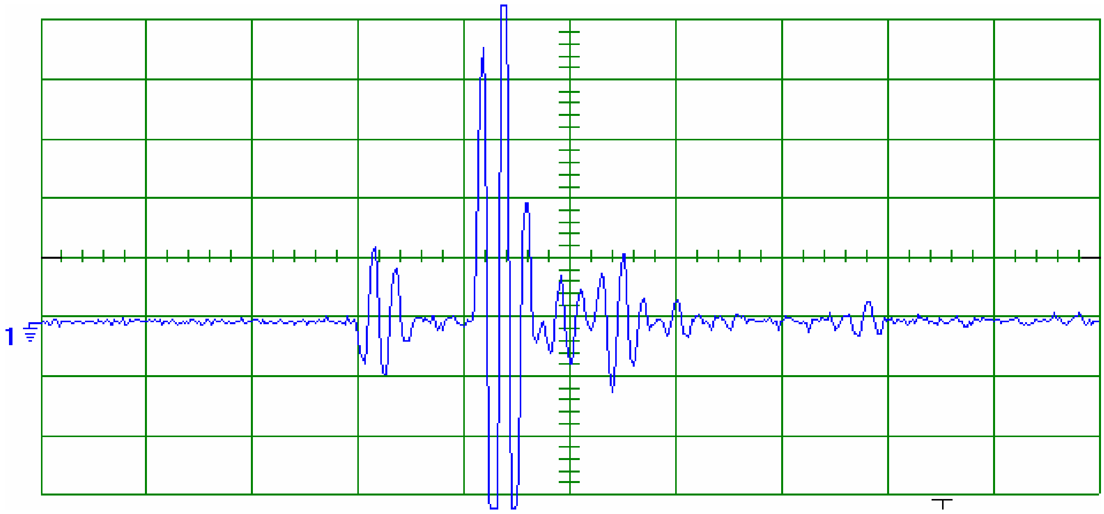

Figure 4.2 Screen Display of Poly(HEMA)$_1$

Table 4.20 Poly(HEMA)$_2$ (t=570 µm, % 62,57 swelling ratio, M_{HEMA}dry=0,0342g)

Measurement	**Δt (ns)**	**Velocity (m/s)**
1	626	1821,1
2	627	1818,2
3	628	1815,3
4	628	1815,3
5	630	1809,5
6	630	1809,5
7	629	1812,4
8	631	1806,7
9	630	1809,5
10	629	1812,4
Average	628,8	**1813,0**

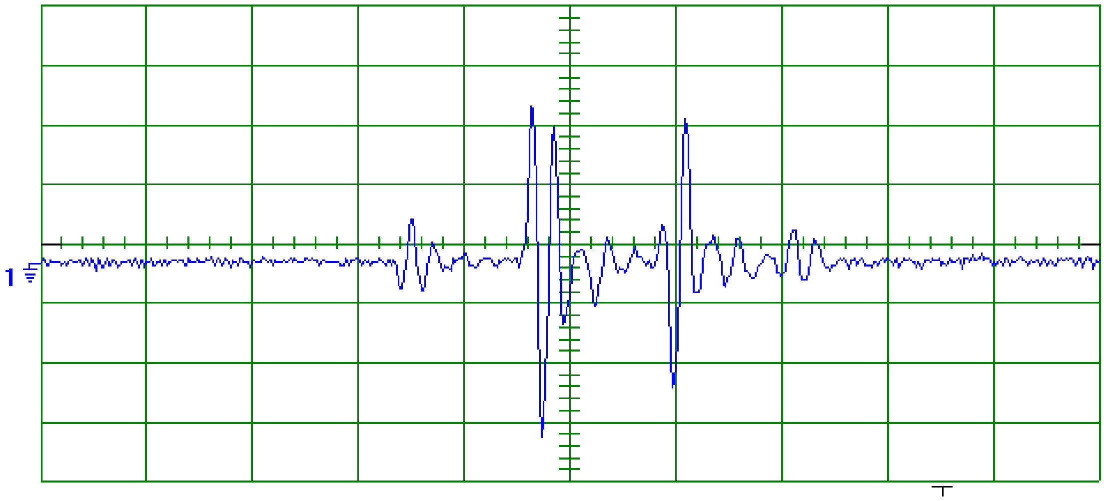

Figure 4.3 Screen Display of Poly(HEMA)$_2$

Table 4.21 Poly(HEMA)$_3$ (t=550 µm, % 126,8 swelling ratio, M_{HEMA}dry=0,0235g)

Measurement	**Δt (ns)**	**Velocity (m/s)**
1	613	1794,5
2	613	1794,5
3	614	1791,5
4	615	1788,6
5	615	1788,6
6	614	1791,5
7	615	1788,6
8	614	1791,5
9	614	1791,5
10	615	1788,6
Average	614,2	**1791,0**

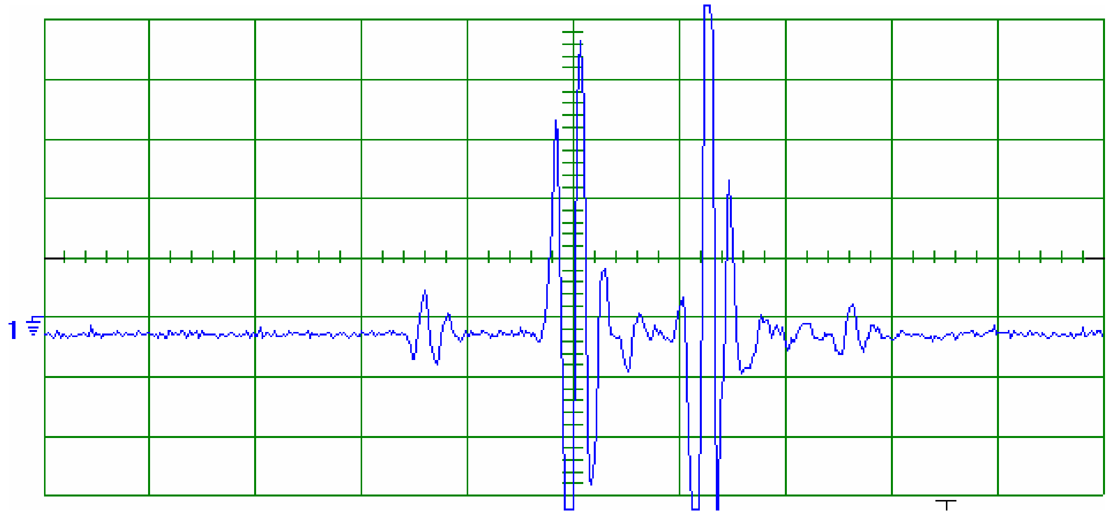

Figure 4.4 Screen Display of Poly(HEMA)$_3$

Table 4.22 Poly(HEMA)$_{6ml}$ (t=680 µm, % 119,5 swelling ratio, M$_{HEMA}$dry=0,0221g)

Measurement	**Δt (ns)**	**Velocity (m/s)**
1	662	2054,4
2	663	2051,3
3	661	2057,5
4	664	2048,2
5	662	2054,4
6	662	2054,4
7	662	2054,4
8	660	2060,6
9	661	2057,5
10	662	2054,4
Average	661,9	**2054,7**

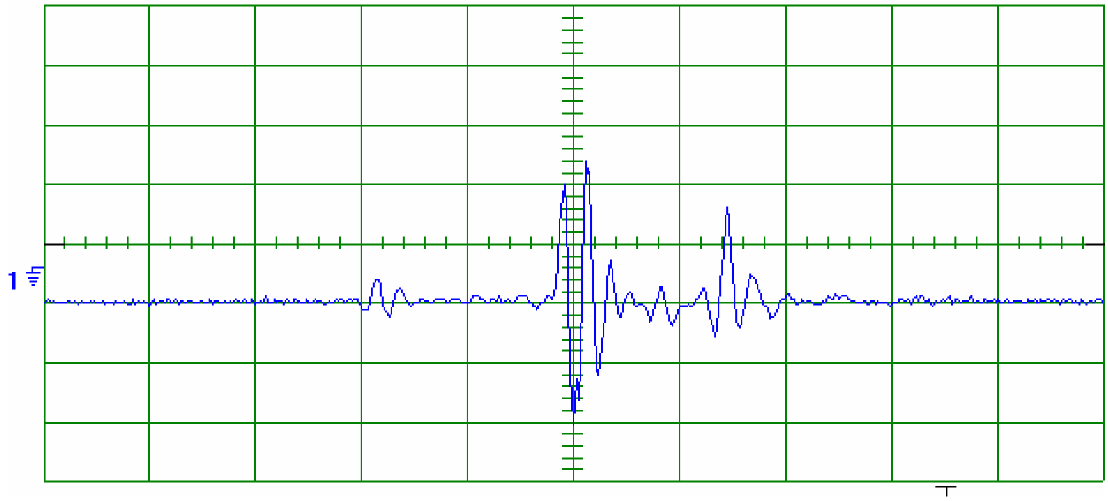

Figure 4.5 Screen Display of Poly(HEMA)$_{6ml}$

Table 4.23 Poly(HEMA)$_{9ml}$ (t=1125 µm, % 109,67 swelling ratio, M$_{HEMA}$dry=0,0300g)

Measurement	**Δt (µs)**	**Velocity (m/s)**
1	1,332	1689,2
2	1,339	1680,4
3	1,338	1681,6
4	1,340	1679,1
5	1,336	1684,1
6	1,339	1680,4
7	1,334	1686,7
8	1,341	1677,9
9	1,338	1681,6
10	1,341	1677,9
Average	1,338	**1681,9**

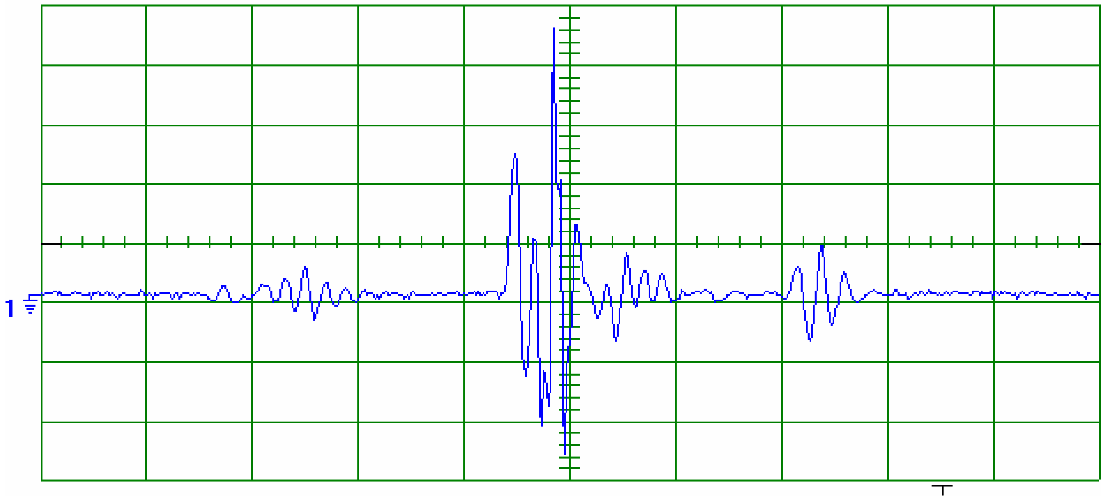

Figure 4.6 Screen Display of Poly(HEMA)$_{9ml}$

Table 4.24 Poly(HEMA)$_{12ml}$ (t=1750 µm, % 153,56 swelling ratio, M$_{HEMA}$dry=0,0407g)

Measurement	**Δt (µs)**	**Velocity (m/s)**
1	1,939	1805,1
2	1,940	1804,1
3	1,931	1812,5
4	1,937	1806,9
5	1,936	1807,9
6	1,940	1804,1
7	1,941	1803,2
8	1,939	1805,1
9	1,935	1808,8
10	1,938	1806,0
Average	1,938	**1806,4**

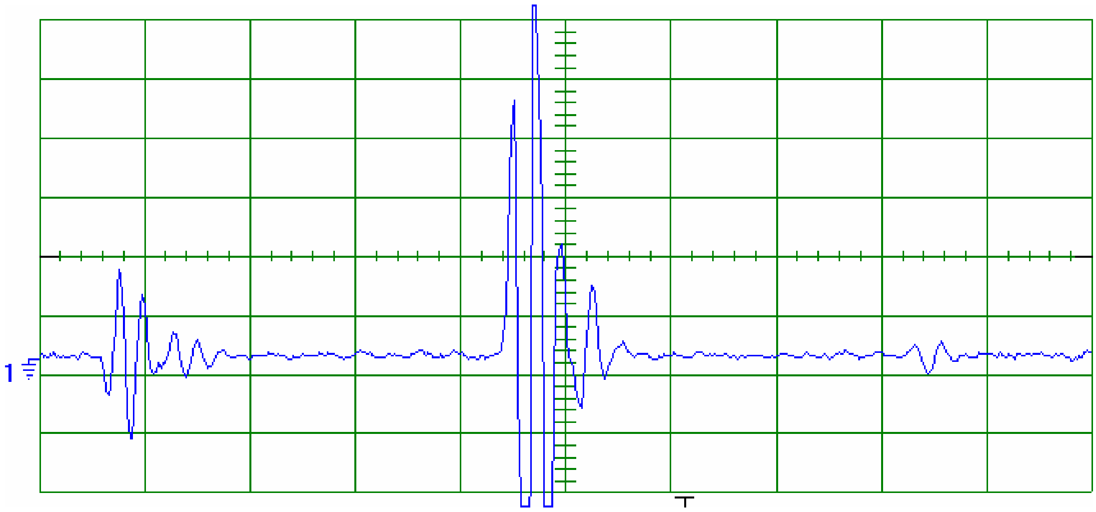

Figure 4.7 Screen Display of Poly(HEMA)$_{12ml}$

Table 4.25 Poly(HEMA-co-GMA), VT=6ml, 50µl GMA (t=580 µm, % 62,1 swelling ratio, $M_{Poly(HEMA-co-GMA)}$ (dry) = 0.0256 g)

Measurement	**Δt (ns)**	**Velocity (m/s)**
1	634	1829,7
2	631	1838,4
3	633	1832,5
4	634	1829,7
5	632	1835,4
6	633	1832,5
7	633	1832,5
8	631	1838,4
9	634	1829,7
10	633	1832,5
Average	632,8	**1833,1**

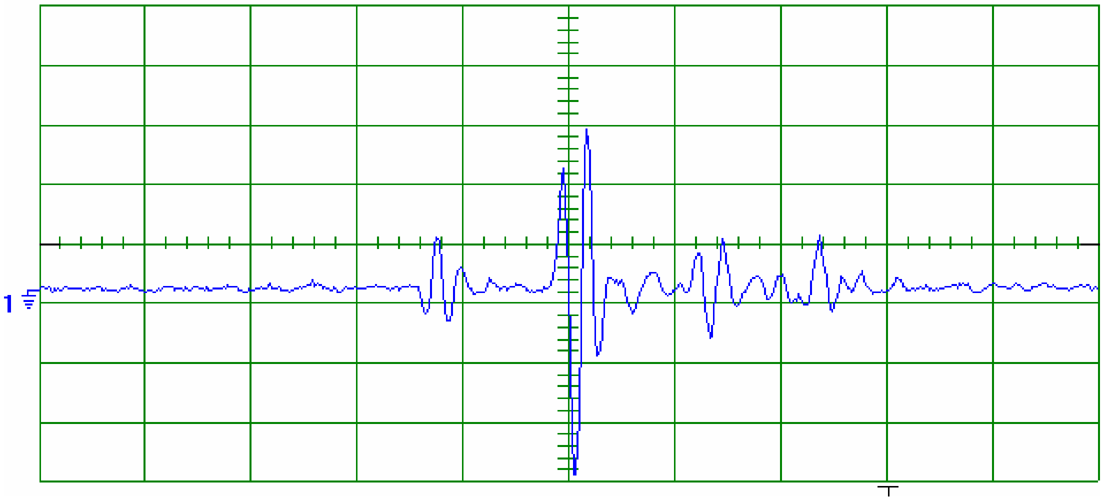

Figure 4.8 Screen Display of Poly(HEMA-co-GMA), VT=6ml, 50µl GMA

Table 4.26 Poly(HEMA-co-GMA), VT=6ml,100µl GMA (t=350 µm,% 58,27 swelling ratio, $M_{Poly(HEMA\text{-}co\text{-}GMA)}$ (dry) = 0.0139 g)

Measurement	**Δt (ns)**	**Velocity (m/s)**
1	456	1535,1
2	457	1531,7
3	458	1528,4
4	457	1531,7
5	458	1528,4
6	457	1531,7
7	457	1531,7
8	458	1528,4
9	457	1531,7
10	458	1528,4
Average	457,3	**1530,7**

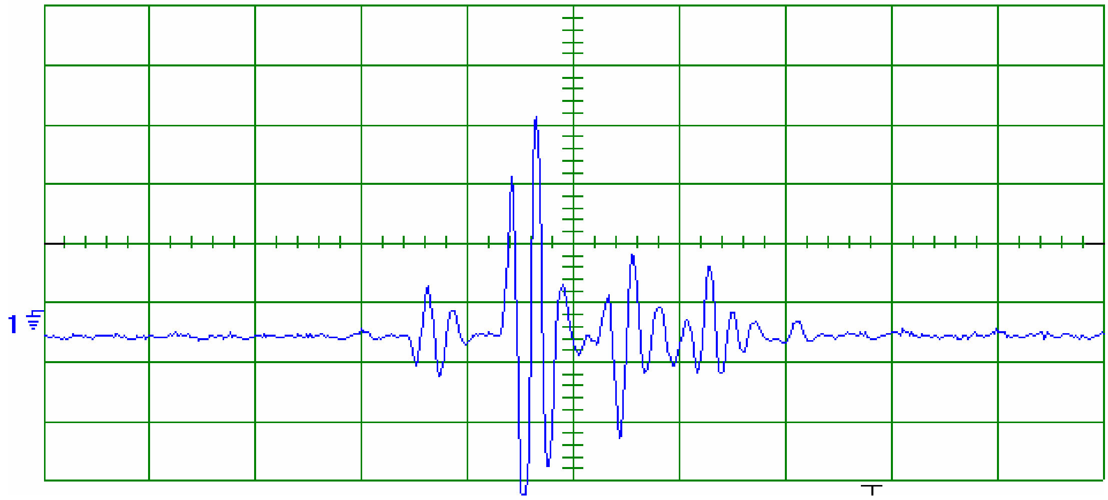

Figure 4.9 Screen Display of Poly(HEMA-co-GMA), VT=6ml, 100µl GMA

Table 4.27 Poly(HEMA-co-GMA), VT=6ml,150µl GMA (t=330 µm,% 55,46 swelling ratio, $M_{Poly(HEMA-co-GMA)}$ (dry) = 0.0119 g)

Measurement	**Δt (ns)**	**Velocity (m/s)**
1	550	1200,0
2	549	1202,2
3	549	1202,2
4	551	1197,8
5	550	1200,0
6	550	1200,0
7	551	1197,8
8	551	1197,8
9	550	1200,0
10	550	1200,0
Average	550,1	**1199,8**

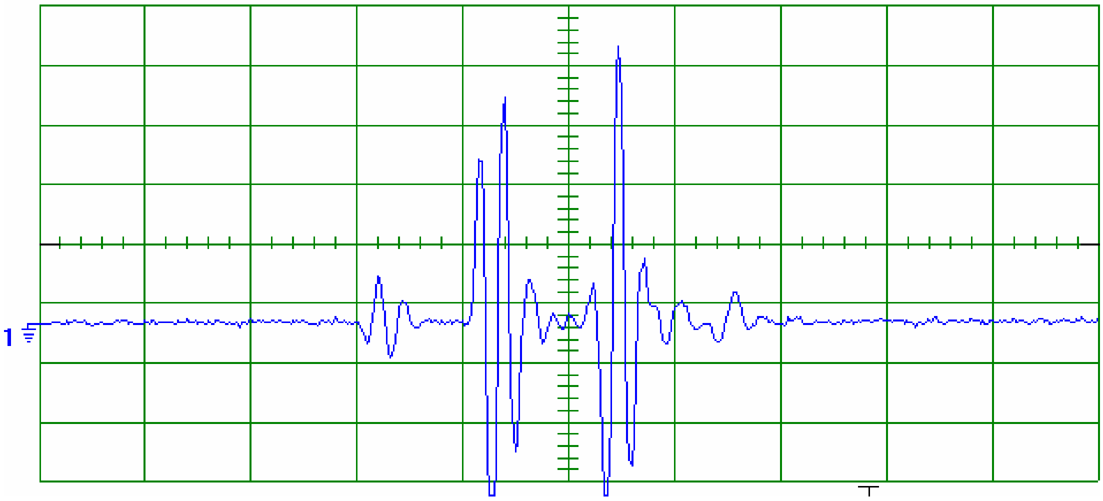

Figure 4.10 Screen Display of Poly(HEMA-co-GMA), VT=6ml, 150µl GMA

Table 4.28 Poly(HEMA-co-GMA), VT=8ml, 50µl GMA (t=600 µm,% 61,56 swelling ratio, $M_{Poly(HEMA\text{-}co\text{-}GMA)}$ (dry) = 0.0281 g)

Measurement	**Δt (ns)**	**Velocity (m/s)**
1	668	1796,4
2	665	1804,5
3	666	1801,8
4	666	1801,8
5	667	1799,1
6	668	1796,4
7	668	1796,4
8	664	1807,2
9	669	1793,7
10	670	1791,0
Average	667,1	**1798,8**

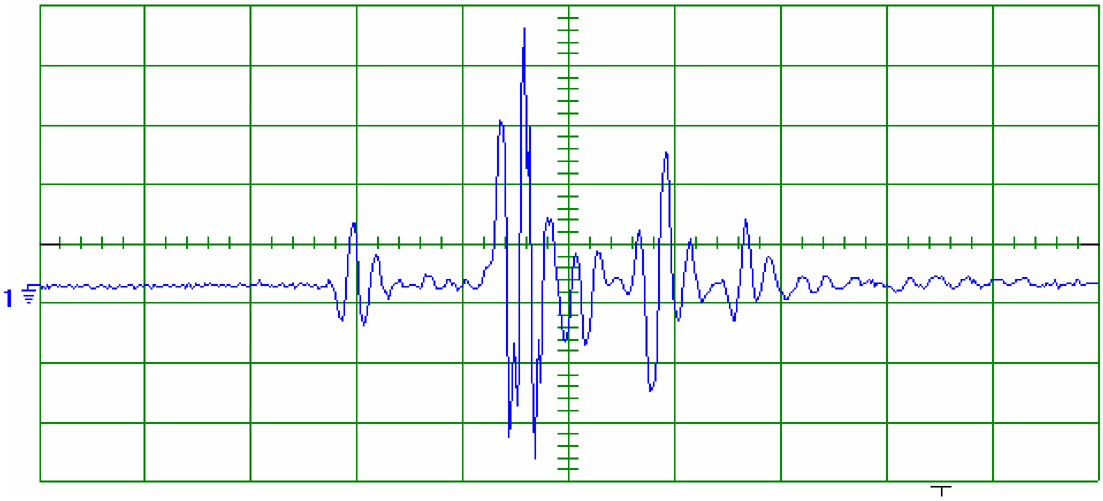

Figure 4.11 Screen Display of Poly(HEMA-co-GMA), VT=8ml, 50µl GMA

Table 4.29 Poly(HEMA-co-GMA), VT=8ml, 100µl GMA (t=750 µm,% 59,2 swelling ratio, $M_{Poly(HEMA-co-GMA)}$ (dry) = 0.0321g)

Measurement	**Δt (ns)**	**Velocity (m/s)**
1	717	2092,1
2	715	2097,9
3	717	2092,1
4	716	2095,0
5	717	2092,1
6	717	2092,1
7	715	2097,9
8	715	2097,9
9	716	2095,0
10	716	2095,0
Average	716,1	**2094,7**

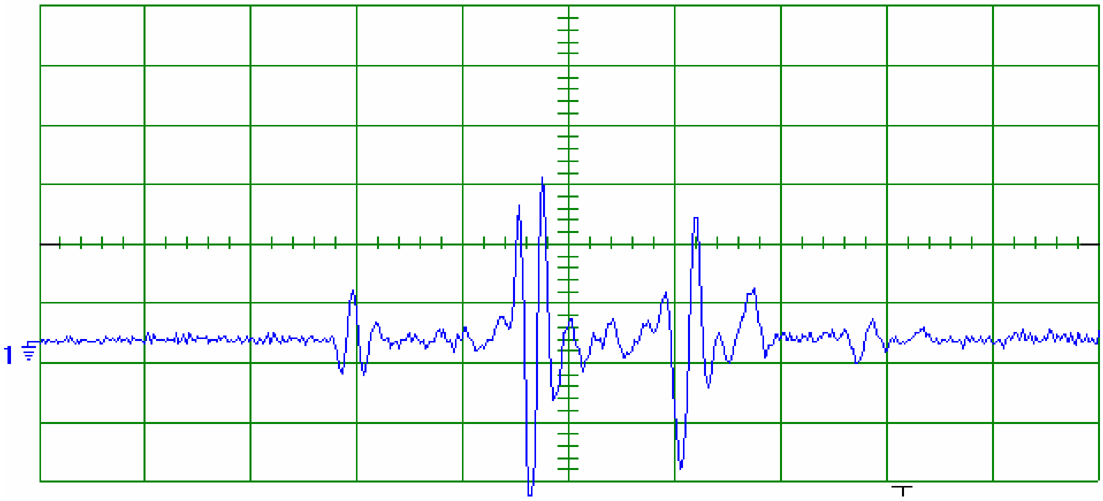

Figure 4.12 Screen Display of Poly(HEMA-co-GMA), VT=8ml, 100µl GMA

Table 4.30 Poly(HEMA-co-GMA), VT=8ml,150µl GMA (t=460 µm,% 55,45 swelling ratio, $M_{Poly(HEMA-co-GMA)}$ (dry) = 0.0211g)

Measurement	**Δt (ns)**	**Velocity (m/s)**
1	562	1637,0
2	564	1631,2
3	562	1637,0
4	565	1628,3
5	562	1637,0
6	564	1631,2
7	562	1637,0
8	564	1631,2
9	563	1634,1
10	564	1631,2
Average	563,2	**1633,5**

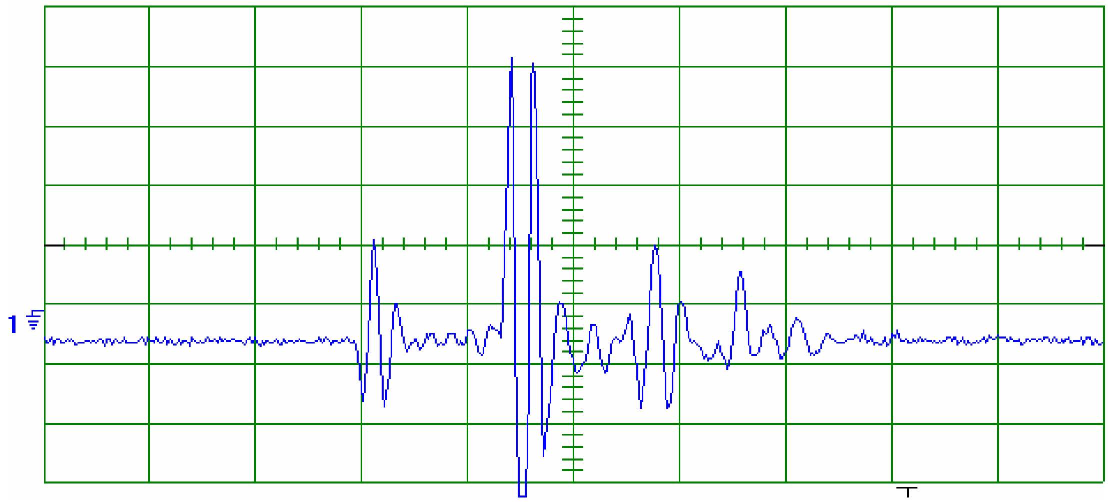

Figure 4.13 Screen Display of Poly(HEMA-co-GMA), VT=8ml, 150µl GMA

Table 4.31 Poly(HEMA-co-GMA)$_1$, VT=12ml, 50µl GMA, (t=1175 µm, % 61,38 swelling ratio, $M_{Poly(HEMA\text{-}co\text{-}GMA)}$ (dry) = 0.0492 g)

Measurement	**Δt (µs)**	**Velocity (m/s)**
1	1,330	1766,9
2	1,331	1765,6
3	1,330	1766,9
4	1,330	1766,9
5	1,332	1764,3
6	1,330	1766,9
7	1,329	1768,2
8	1,330	1766,9
9	1,329	1768,2
10	1,330	1766,9
Average	1,330	**1766,8**

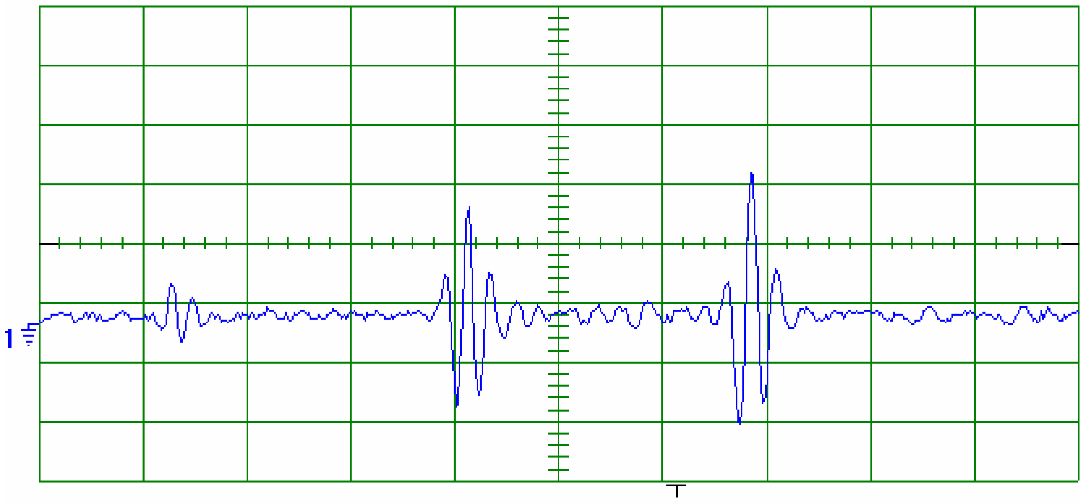

Figure 4.14 Screen Display of Poly(HEMA-co-GMA)$_1$,VT=12ml,50µl GMA

Table 4.32 Poly(HEMA-co-GMA)$_2$, VT=12ml, 100µl GMA, (t=1250 µm, % 60,33 swelling ratio, $M_{Poly(HEMA\text{-}co\text{-}GMA)}$ (dry) = 0.0542g)

Measurement	**Δt (µs)**	**Velocity (m/s)**
1	1,530	1634,0
2	1,529	1635,1
3	1,534	1629,7
4	1,531	1632,9
5	1,527	1637,2
6	1,529	1635,1
7	1,529	1635,1
8	1,531	1632,9
9	1,530	1634,0
10	1,531	1632,9
Average	1,530	**1633,9**

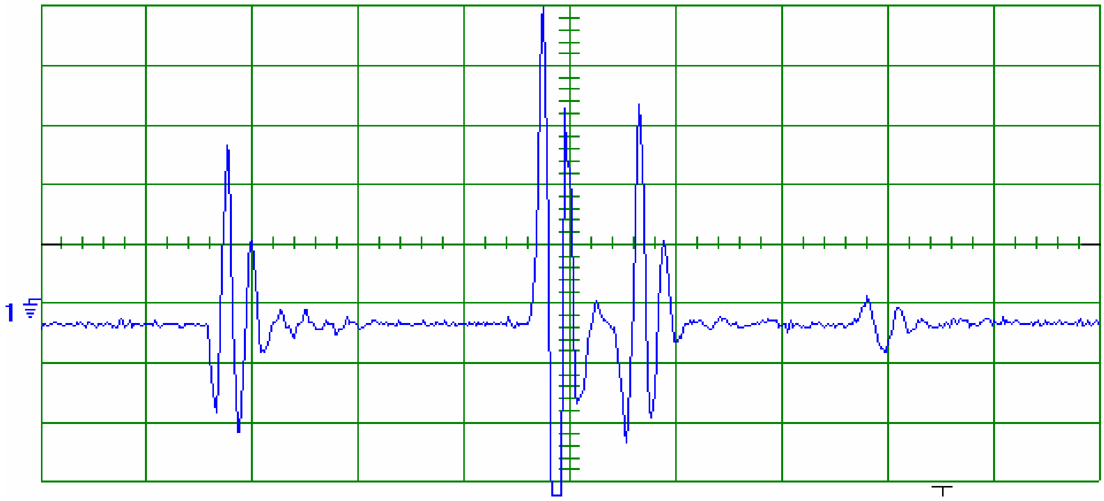

Figure 4.16 Screen Display of Poly(HEMA-co-GMA)$_2$,VT=12ml,100µlGMA

Table 4.33 Poly(HEMA-co-GMA)$_3$, VT=12ml, 150µl GMA, (t=1750 µm, % 53,8 swelling ratio, $M_{Poly(HEMA-co-GMA)}$ (dry) = 0.0526g)

Measurement	**Δt (µs)**	**Velocity (m/s)**
1	1,470	2381,0
2	1,474	2374,5
3	1,470	2381,0
4	1,469	2382,6
5	1,475	2372,9
6	1,471	2379,3
7	1,470	2381,0
8	1,466	2387,4
9	1,473	2376,1
10	1,477	2369,7
Average	1,472	**2378,5**

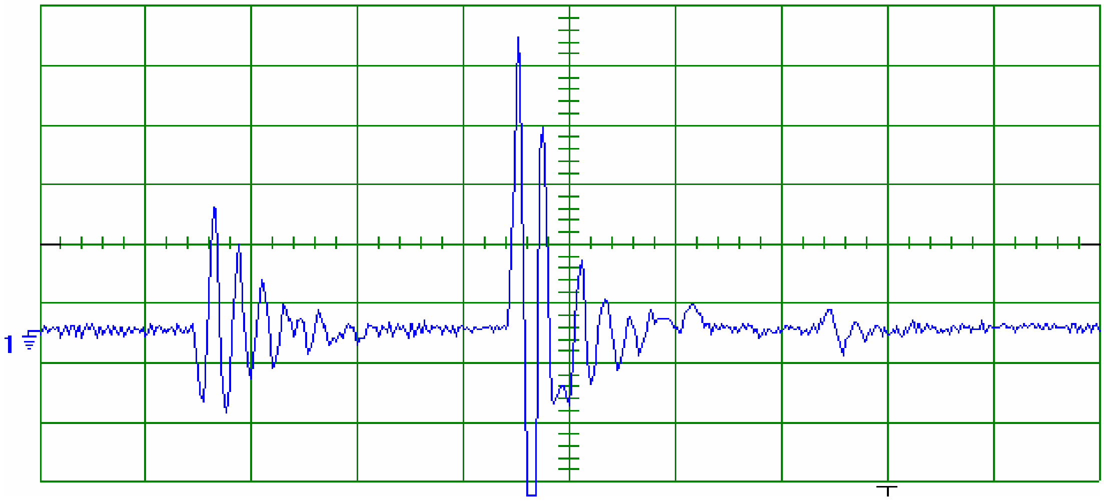

Figure 4.15 Screen Display of Poly(HEMA-co-GMA)$_3$,VT=12ml,150µlGMA

Table 4.34 Poly(HEMA-NN′), VT=6ml (3ml HEMA, 3ml NN′) (t=480µm, %67,58 swelling ratio, $M_{Poly(HEMA-NN')}$ (dry) = 0.0219 g)

Measurement	**Δt (ns)**	**Velocity (m/s)**
1	556	1726,6
2	554	1732,9
3	554	1732,9
4	556	1726,6
5	556	1726,6
6	554	1732,9
7	555	1729,7
8	553	1736,0
9	554	1732,9
10	556	1726,6
Average	554,8	**1730,4**

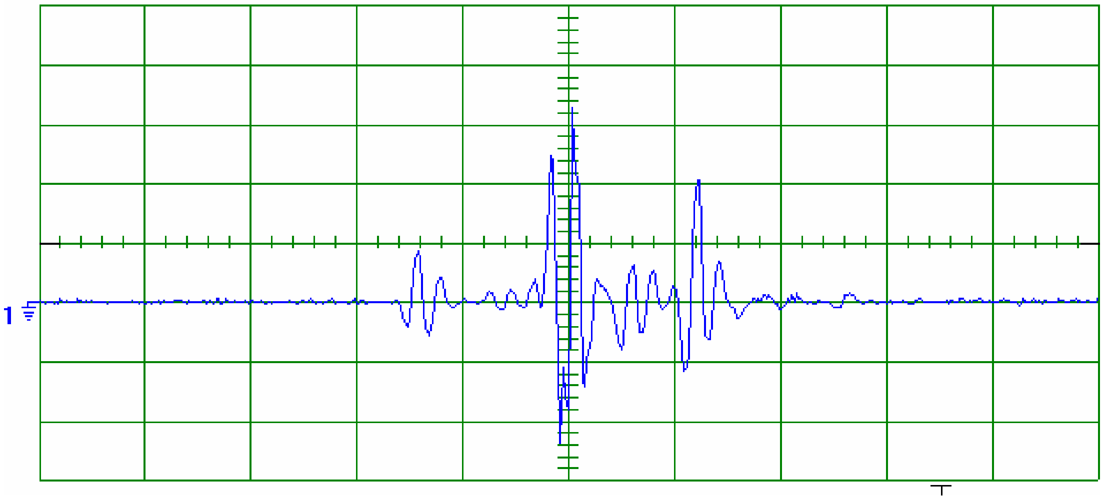

Figure 4.17 Screen Display of Poly(HEMA-NN′), (3ml HEMA, 3ml NN′)

Table 4.35 Poly(HEMA-NN′-dH_2O), VT=6ml (3ml HEMA, 2ml NN′, 1ml dH_2O) (t=1125µm, %74,8 swelling ratio, $M_{Poly(HEMA-NN'-dH2O)}$ (dry)=0.0480g)

Measurement	**Δt (µs)**	**Velocity (m/s)**
1	1,072	2098,9
2	1,060	2122,6
3	1,075	2093,0
4	1,062	2118,6
5	1,070	2102,8
6	1,068	2106,7
7	1,067	2108,7
8	1,070	2102,8
9	1,074	2095,0
10	1,064	2114,7
Average	1,068	**2106,4**

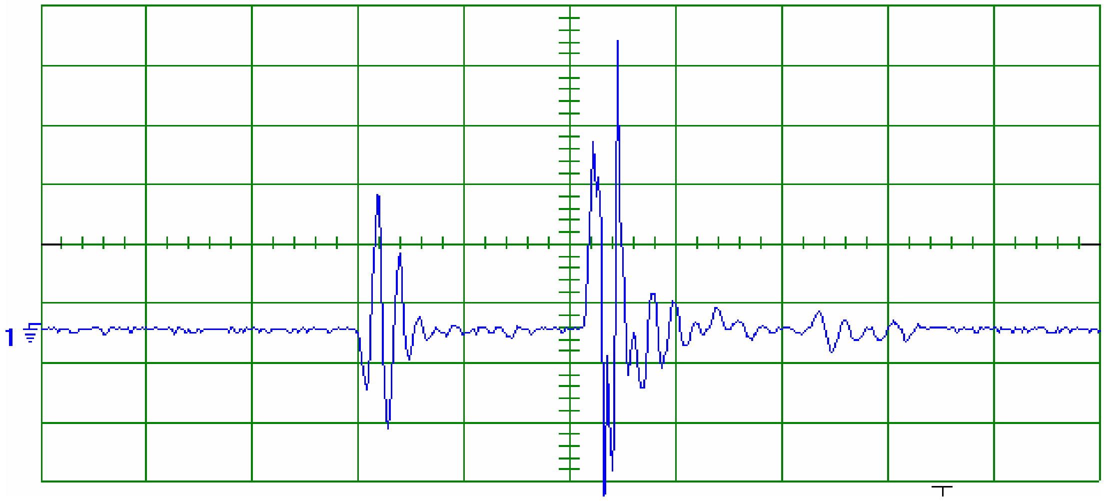

Figure 4.18 Screen Display of Poly(HEMA-NN′-dH_2O), VT=6ml (3ml HEMA, 2ml NN′, 1ml dH_2O)

Table 4.36 Poly(HEMA-NN′-dH$_2$O), VT=6ml (3ml HEMA, 1ml NN′, 2ml dH$_2$O) (t=440μm, %63,85 swelling ratio, $M_{Poly(HEMA-NN'-dH2O)}$ (dry)=0.0166g)

Measurement	**Δt (ns)**	**Velocity (m/s)**
1	547	1608,8
2	547	1608,8
3	549	1602,9
4	548	1605,8
5	548	1605,8
6	549	1602,9
7	547	1608,8
8	546	1611,7
9	549	1602,9
10	550	1600,0
Average	548	**1605,8**

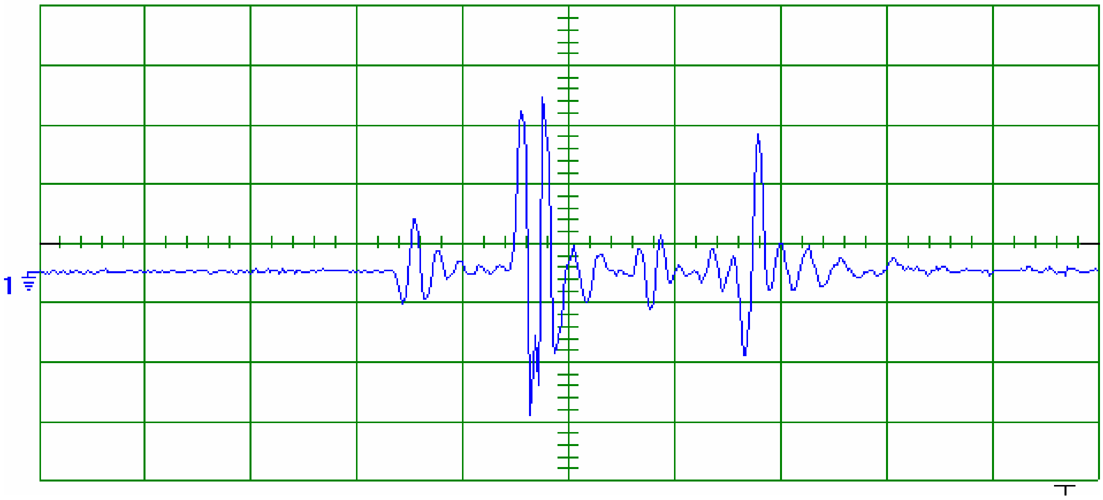

Figure 4.19 Screen Display of Poly(HEMA-NN′-dH$_2$O), VT=6ml (3ml HEMA, 1ml NN′, 2ml dH$_2$O)

Table 4.37 Acoustic Impedances of Hydrated Hydrophilic Polymer Samples

Sample	**Density (kg/m^3)**	**Ultrasonic Velocity (m/s)**	**Acoustic Impedance (Ns/m^3)x10^6**
Poly(HEMA)$_1$	991,467	1595	1,581
Poly(HEMA)$_2$	1026,419	1813	1,861
Poly(HEMA)$_3$	1019,740	1791	1,826
Poly(HEMA)$_{6ml}$	1121,135	2054,7	2,304
Poly(HEMA)$_{9ml}$	878,867	1681,9	1,478
Poly(HEMA)$_{12ml}$	926,972	1806,4	1,674
Poly(HEMA-co-GMA) VT=6ml, 50µl GMA	1124,722	1833,1	2,062
Poly(HEMA-co-GMA) VT=6ml, 100µl GMA	988,052	1530,7	1,512
Poly(HEMA-co-GMA) VT=6ml, 150µl GMA	881,217	1199,8	1,057
Poly(HEMA-co-GMA) VT=8ml, 50µl GMA	1189,405	1798,8	2,140
Poly(HEMA-co-GMA) VT=8ml, 100µl GMA	1070,988	2094,7	2,243
Poly(HEMA-co-GMA) VT=8ml, 150µl GMA	1120,834	1633,5	1,831
Poly(HEMA-NN′), VT=6ml (3ml HEMA, 3ml NN′)	1201,849	1730,4	2,080
Poly(HEMA-NN′-dH2O), VT=6ml (3ml HEMA,1ml NN′,2ml dH2O)	971,720	1605,8	1,560
Poly(HEMA-NN′-dH2O), VT=6ml (3ml HEMA,2ml NN′,1ml dH2O)	1172,289	2106,4	2,469
Poly(HEMA-co-GMA)$_1$ VT=12ml, 50µl GMA	1062,204	1766,8	1,877
Poly(HEMA-co-GMA)$_2$ VT=12ml, 100µl GMA	1092,785	1633,9	1,786
Poly(HEMA-co-GMA)$_3$ VT=12ml, 150µl GMA	726,667	2378,5	1,728

Table 4.37 lists the ultrasonic velocity and acoustic impedance of a range of hydrated hydrophilic polymers. If almost the same thicknesses were taken into account, it could be easily seen that increasing water content results in decrease in the velocity as seen in Tables 4.38, 4.39 and 4.40.

Table 4.38 Ultrasonic Velocities and Acoustic Impedances of Poly(HEMA)$_1$, Poly(HEMA-NN′-dH2O) [VT=6ml (3ml HEMA, 1ml NN′,2ml dH2O)] and Poly(HEMA-co-GMA) [VT=8ml, 150µl GMA]

Sample	**Ultrasonic Velocity (m/s)**	**Acoustic Impedance (Ns/m^3)x10^6**
Poly(HEMA-co-GMA), V$_T$=8ml, 150µl GMA, **t=460µm**, % 55,45 SR*	1633,5	1,831
Poly(HEMA-NN′-dH2O), V$_T$=6ml (3ml HEMA, 1ml NN′,2ml dH2O), **t=440µm**, % 63,85 SR	1605,8	1,560
Poly(HEMA)$_1$, **t=450µm**, % 64,98 SR	1595	1,581

* SR: Swelling Ratio

Table 4.39 Ultrasonic Velocities and Acoustic Impedances of Poly(HEMA)$_2$, Poly(HEMA)$_3$ and Poly(HEMA-co-GMA), VT=6ml, 50µl GMA.

Sample	**Ultrasonic Velocity (m/s)**	**Acoustic Impedance (Ns/m^3)x10^6**
Poly(HEMA-co-GMA), V$_T$=6ml, 50µl GMA, **t=580µm,** % 62,1 SR	1833,1	2,062
Poly(HEMA)$_2$, **t=570µm,** % 62,57 SR	1813	1,861
Poly(HEMA)$_3$, **t=550µm,** % 126,8 SR	1791	1,826

Table 4.40 Ultrasonic Velocities and Acoustic Impedances of Poly(HEMA)$_{9ml}$ and Poly(HEMA-NN′-dH2O) [VT=6ml (3ml HEMA,2ml NN′,1ml dH2O)]

Sample	**Ultrasonic Velocity (m/s)**	**Acoustic Impedance (Ns/m^3)x10^6**
Poly(HEMA-NN′-dH2O), V$_T$=6ml (3ml HEMA,2ml NN′,1ml dH2O), **t=1125µm,** % 74,8 SR	2106,4	2,469
Poly(HEMA)$_{9ml}$, **t=1125µm,** % 109,67 SR	1681,9	1,478

Although the results seem to be fine, unusual circumstances might occur. For instance; 6ml, 100 µl GMA included Poly(HEMA-co-GMA) with thickness 350 µm and swelling ratio % 58,27 resulted in velocity of 1530,7m/s where 6ml, 150 µl GMA included Poly(HEMA-co-GMA) with thickness 330 µm and swelling ratio % 55,46 resulted in velocity of 1199,8m/s (Table 4.41). It is believed that this condition was due to the reason of polymer deformation (microorganisms are formed and they change the structure of the polymer) or inhomogeneous polymerization.

Table 4.41 Ultrasonic Velocities and Acoustic Impedances of Poly(HEMA-co-GMA) [VT=6ml, 100µl GMA] and Poly(HEMA-co-GMA) [VT=6ml, 150µl GMA]

Sample	**Ultrasonic Velocity (m/s)**	**Acoustic Impedance (Ns/m^3)x10^6**
Poly(HEMA-co-GMA), V$_T$=6ml, 100µl GMA, **t=350µm,** % 58,27 SR	1530,7	1,512
Poly(HEMA-co-GMA), V$_T$=6ml, 150µl GMA, **t=330µm,** % 55,46 SR	1199,8	1,057

4.3 Attenuation Measurements

Table 4.42 Amplitudes of the Front Surface and Backwall Echoes at various frequencies (dB)

		Frequency									
		2.25 MHz		**3.5 MHz**		**5MHz**		**10Mhz**		**20Mhz**	
Sample	**Acoustic Impedance (Ns/m^3)x10^6**	**F (dB)**	**B_1 (dB)**	**F (dB)**	**B_1 (dB)**	**F (dB)**	**B_1 (dB)**	**F (dB)**	**B_1 (dB)**	**F (dB)**	**B_1 (dB)**
Poly(HEMA)$_1$	1,581	60	60,5	69	70	59,5	61	60	64	92,5	99,5
Poly(HEMA)$_2$	1,861	59	59,5	70,5	72	59,5	62	56	61	79	87,5
Poly(HEMA)$_3$	1,826	55	56	59,5	62,5	54	58,5	50,5	58	68,5	77
Poly(HEMA)$_{6ml}$	2,304	59,5	62,5	67	71,5	58	63,5	54,5	62,5	73	87,5
Poly(HEMA)$_{9ml}$	1,478	56,5	57,5	62	66,5	52	58	55,5	64,5	75,5	85,5
Poly(HEMA)$_{12ml}$	1,674	58	58,5	69,5	72	59	63	59	66	71,5	85
Poly(HEMA-co-GMA) VT=6ml, 50µl GMA	2,062	68,5	69,5	82,5	85	78,5	82	48	52	70	75
Poly(HEMA-co-GMA) VT=6ml, 100µl GMA	1,512	54,5	55,5	72,5	74	66	71	68	74	74	81
Poly(HEMA-co-GMA) VT=6ml, 150µl GMA	1,057	67,5	68	73,5	75,5	62	64,5	65,5	70,5	78,5	87
Poly(HEMA-co-GMA) VT=8ml, 50µl GMA	2,140	59,5	61,5	68,5	72,5	61	65,5	62,5	67,5	79,5	88

Table 4.42 Continued

		Frequency									
		2.25 MHz		**3.5 MHz**		**5MHz**		**10Mhz**		**20Mhz**	
Sample	**Acoustic Impedance (Ns/m^3)x10^6**	**F (dB)**	**B_1 (dB)**	**F (dB)**	**B_1 (dB)**	**F (dB)**	**B_1 (dB)**	**F (dB)**	**B_1 (dB)**	**F (dB)**	**B_1 (dB)**
Poly(HEMA-co-GMA) VT=8ml, 100µl GMA	2,243	63,5	65	74	75,5	62,5	65	62,5	67,5	74,5	80,5
Poly(HEMA-co-GMA) VT=8ml, 150µl GMA	1,831	69	69,5	74,5	76	67	69	68,5	73	92,5	98,5
Poly(HEMA-NN′), VT=6ml (3ml HEMA, 3ml NN′)	2,080	52,5	53	67,5	69,5	54	56,5	54	59,5	69	76
Poly(HEMA-NN′-dH2O), VT=6ml (3ml HEMA,1ml NN′,2ml dH2O)	1,560	62	63,5	68,5	73	58,5	63,5	53,5	65	70,5	86
Poly(HEMA-NN′-dH2O), VT=6ml (3ml HEMA,2ml NN′,1ml dH2O)	2,469	57,5	58	66	67	56,5	58,5	54	59,5	71,5	77,5
Poly(HEMA-co-GMA)$_1$ VT=12ml, 50µl GMA	1,877	72,5	74,5	76,5	80	66,5	70,5	67	74	80,5	95
Poly(HEMA-co-GMA)$_2$ VT=12ml, 100µl GMA	1,786	52	57	58	64	46,5	57,5	54,5	70,5	69	88,5
Poly(HEMA-co-GMA)$_3$ VT=12ml, 150µl GMA	1,728	61	67,5	66	74	55,5	65	53,5	66,5	65	85,5

Table 4.43 Attenuation Coefficient at Various Frequencies

Sample	**ATTENUATION COEFFICIENT [α (dB/mm)]**				
	2.25 MHz	**3.5 MHz**	**5MHz**	**10MHz**	**20Mhz**
Poly(HEMA)$_1$	0,0650	0,1289	0,1929	0,5127	0,8965
Poly(HEMA)$_2$	0,0615	0,1624	0,2634	0,5159	0,8694
Poly(HEMA)$_3$	0,1142	0,3235	0,4805	0,7945	0,8992
Poly(HEMA)$_{6ml}$	0,2888	0,4158	0,5005	0,7121	1,2624
Poly(HEMA)$_{9ml}$	0,0512	0,2303	0,3070	0,4605	0,5117
Poly(HEMA)$_{12ml}$	0,0174	0,0832	0,1326	0,2313	0,4451
Poly(HEMA-co-GMA) VT=6ml, 50µl GMA	0,1221	0,2710	0,3702	0,4199	0,5191
Poly(HEMA-co-GMA) VT=6ml, 100µl GMA	0,1646	0,2468	0,8224	0,9869	1,1514
Poly(HEMA-co-GMA) VT=6ml, 150µl GMA	0,1313	0,3929	0,4802	0,9162	1,5268
Poly(HEMA-co-GMA) VT=8ml, 50µl GMA	0,2193	0,4111	0,4591	0,5071	0,8429
Poly(HEMA-co-GMA) VT=8ml, 100µl GMA	0,1430	0,1430	0,2198	0,4117	0,4884
Poly(HEMA-co-GMA) VT=8ml, 150µl GMA	0,0743	0,1994	0,2620	0,5748	0,7625
Poly(HEMA-NN′), VT=6ml (3ml HEMA, 3ml NN′)	0,0891	0,2690	0,3289	0,6887	0,8686
Poly(HEMA-NN′-dH2O), VT=6ml (3ml HEMA,1ml NN′,2ml dH2O)	0,1969	0,5894	0,6548	1,5052	2,0285
Poly(HEMA-NN′-dH2O), VT=6ml (3ml HEMA,2ml NN′,1ml dH2O)	0,0538	0,0794	0,1305	0,3096	0,3352
Poly(HEMA-co-GMA)$_1$ VT=12ml, 50µl GMA	0,1037	0,1772	0,2017	0,3487	0,7161
Poly(HEMA-co-GMA)$_2$ VT=12ml, 100µl GMA	0,2336	0,2796	0,5099	0,7402	0,9013
Poly(HEMA-co-GMA)$_3$ VT=12ml, 150µl GMA	0,2154	0,2648	0,3141	0,4292	0,6759

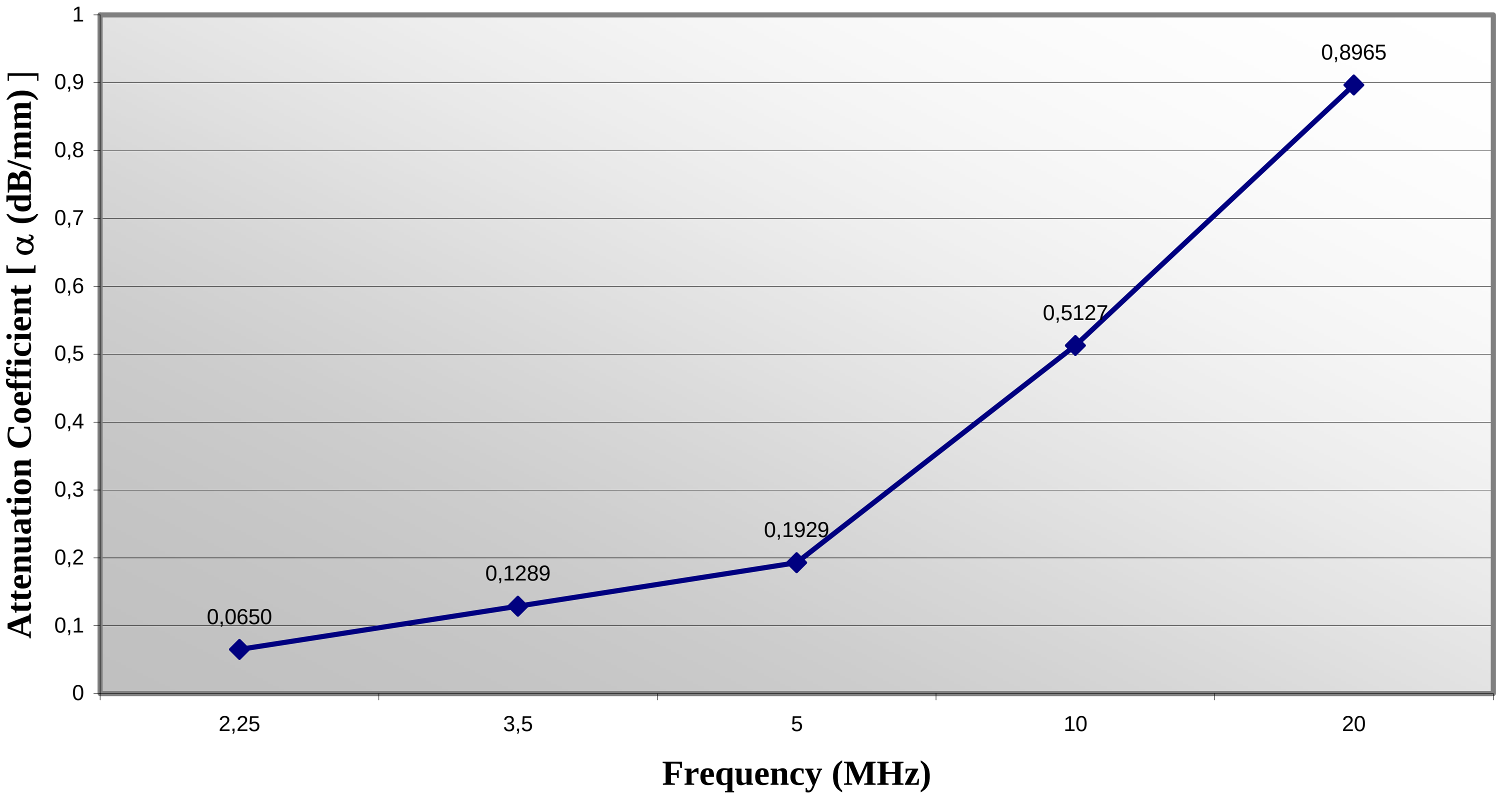

Figure 4.20 Attenuation Coefficient of Poly (HEMA)$_1$

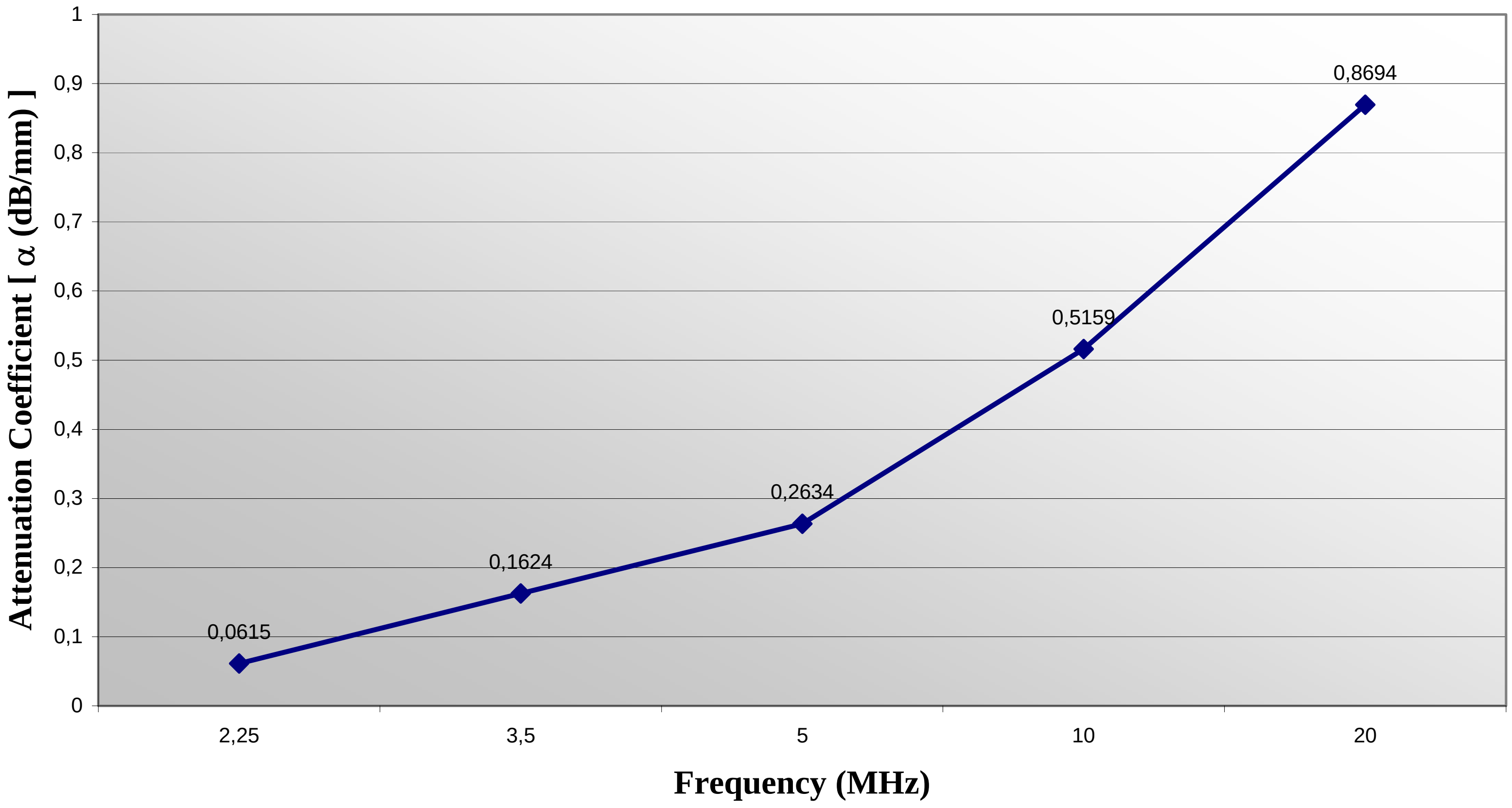

Figure 4.21 Attenuation Coefficient of Poly $(HEMA)_2$

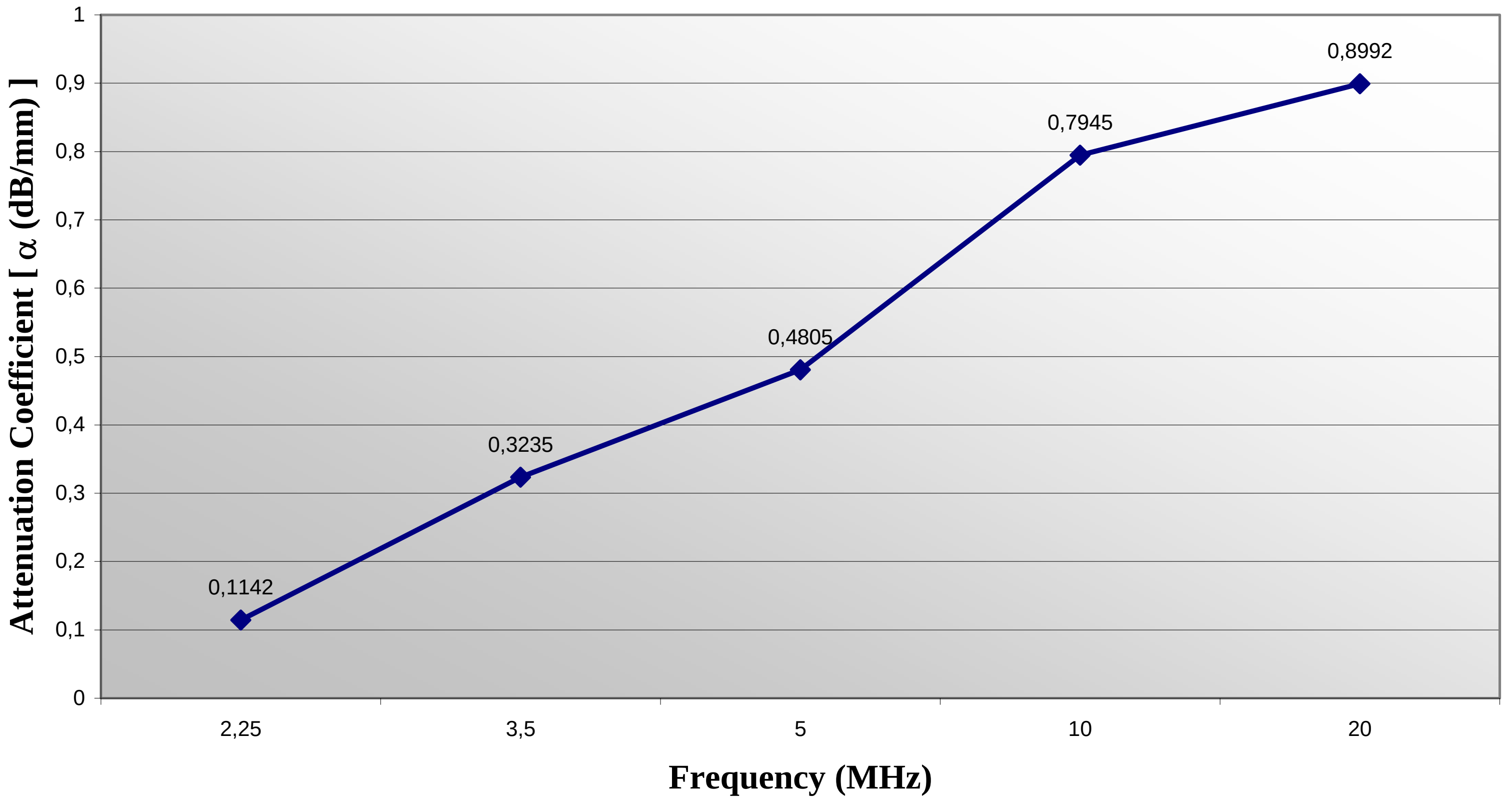

Figure 4.22 Attenuation Coefficient of Poly (HEMA)$_3$

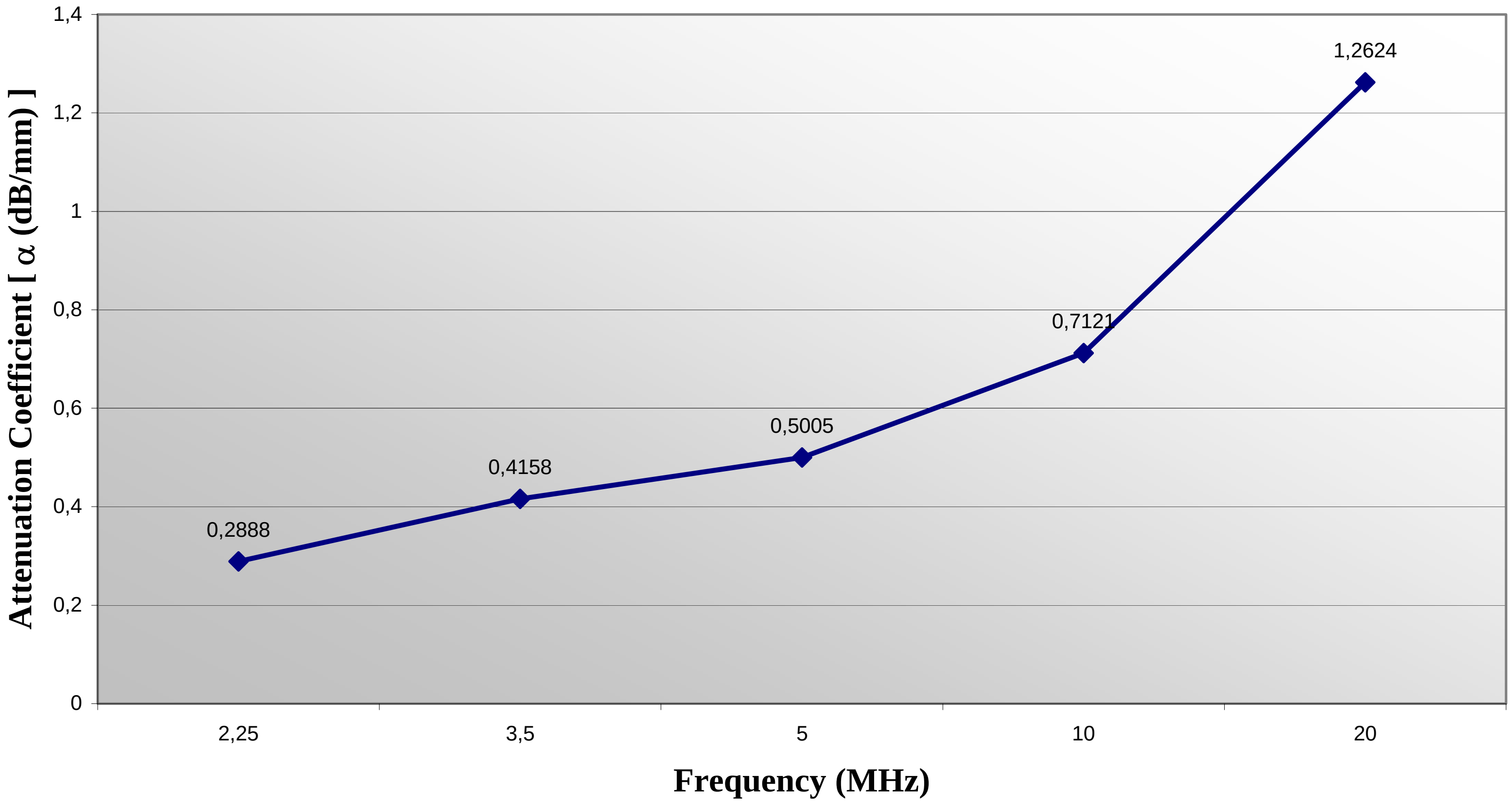

Figure 4.23 Attenuation Coefficient of Poly $(HEMA)_{6ml}$

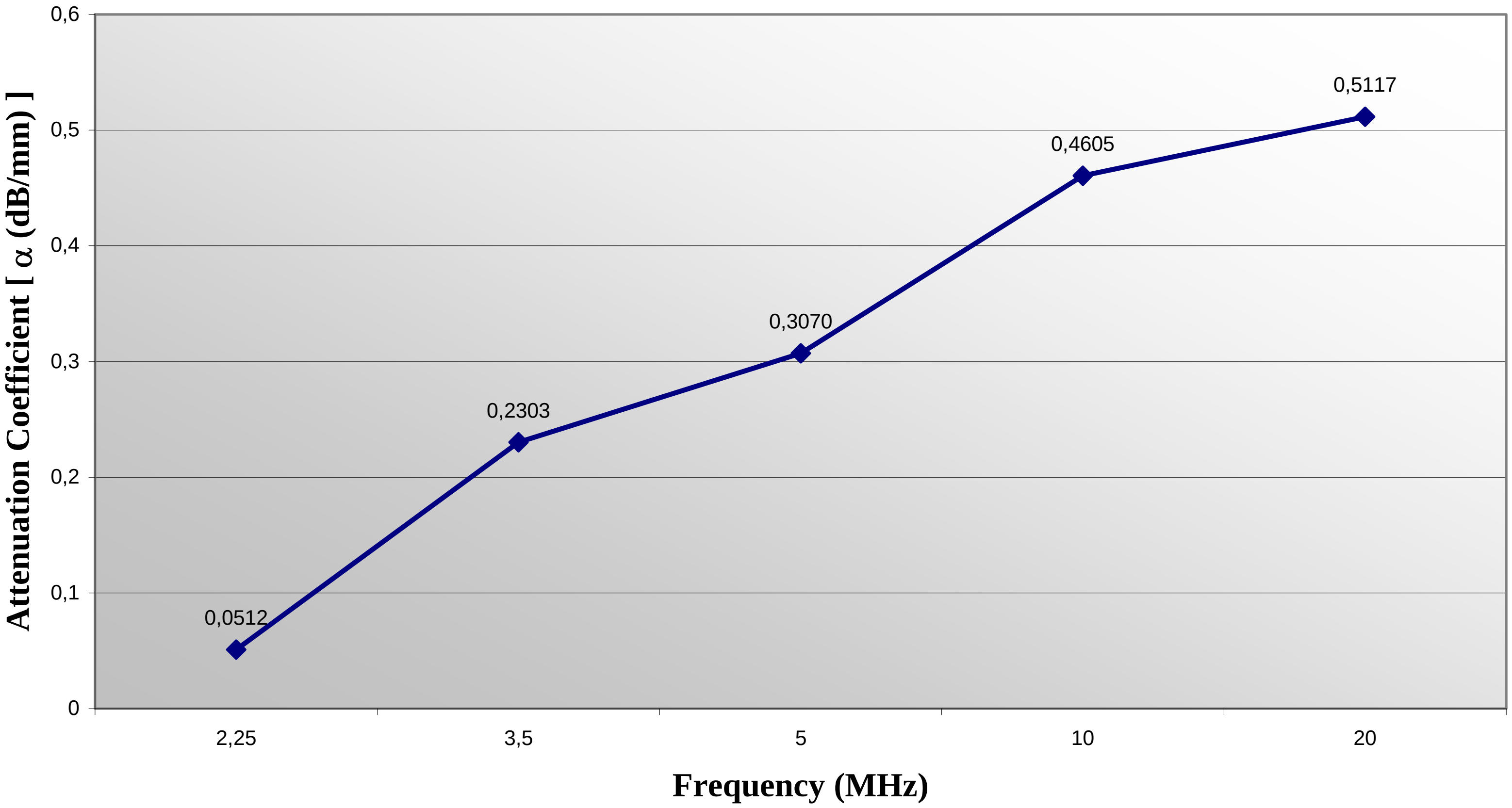

Figure 4.24 Attenuation Coefficient of Poly (HEMA)$_{9ml}$

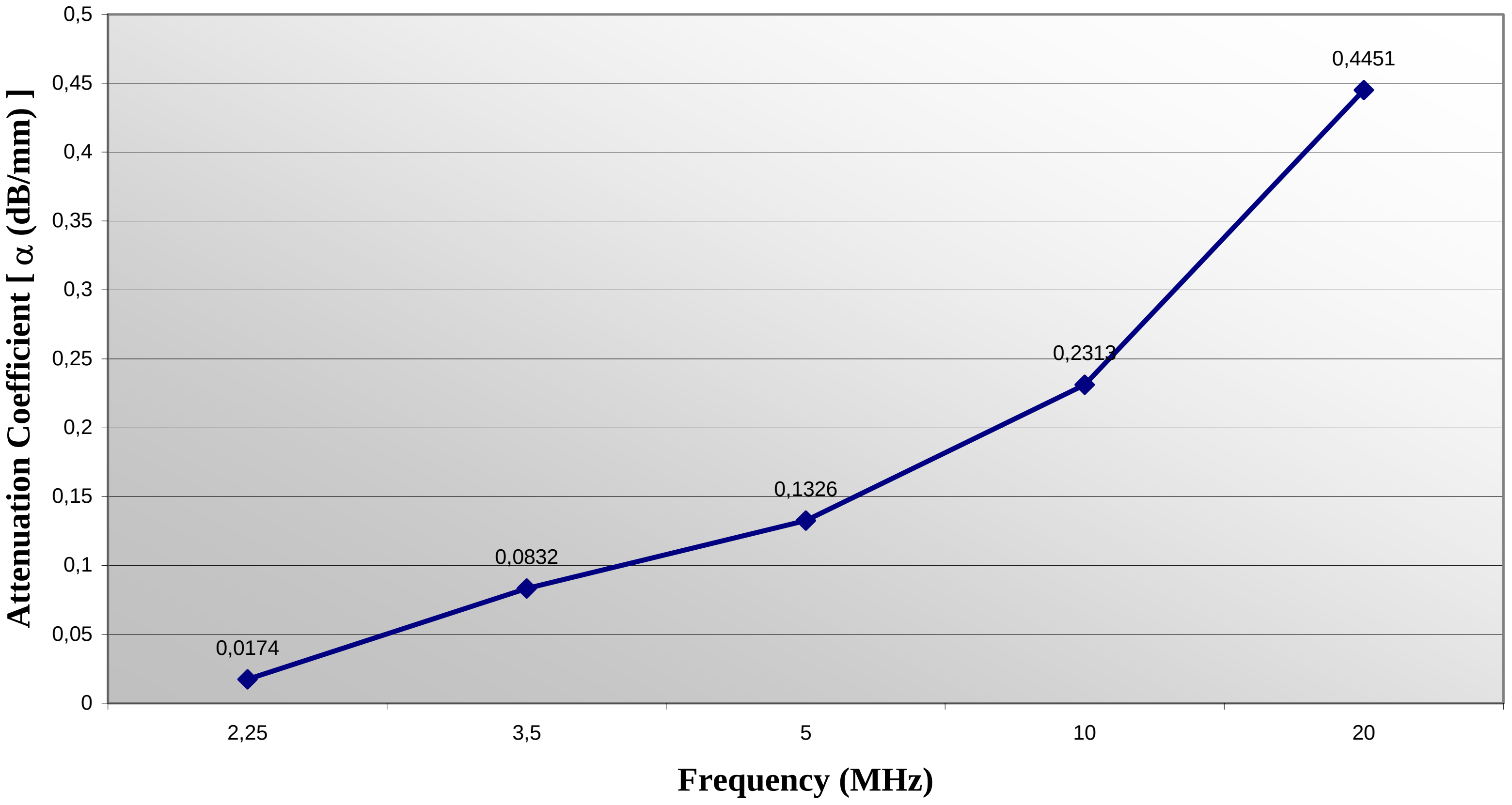

Figure 4.25 Attenuation Coefficient of Poly (HEMA)$_{12ml}$

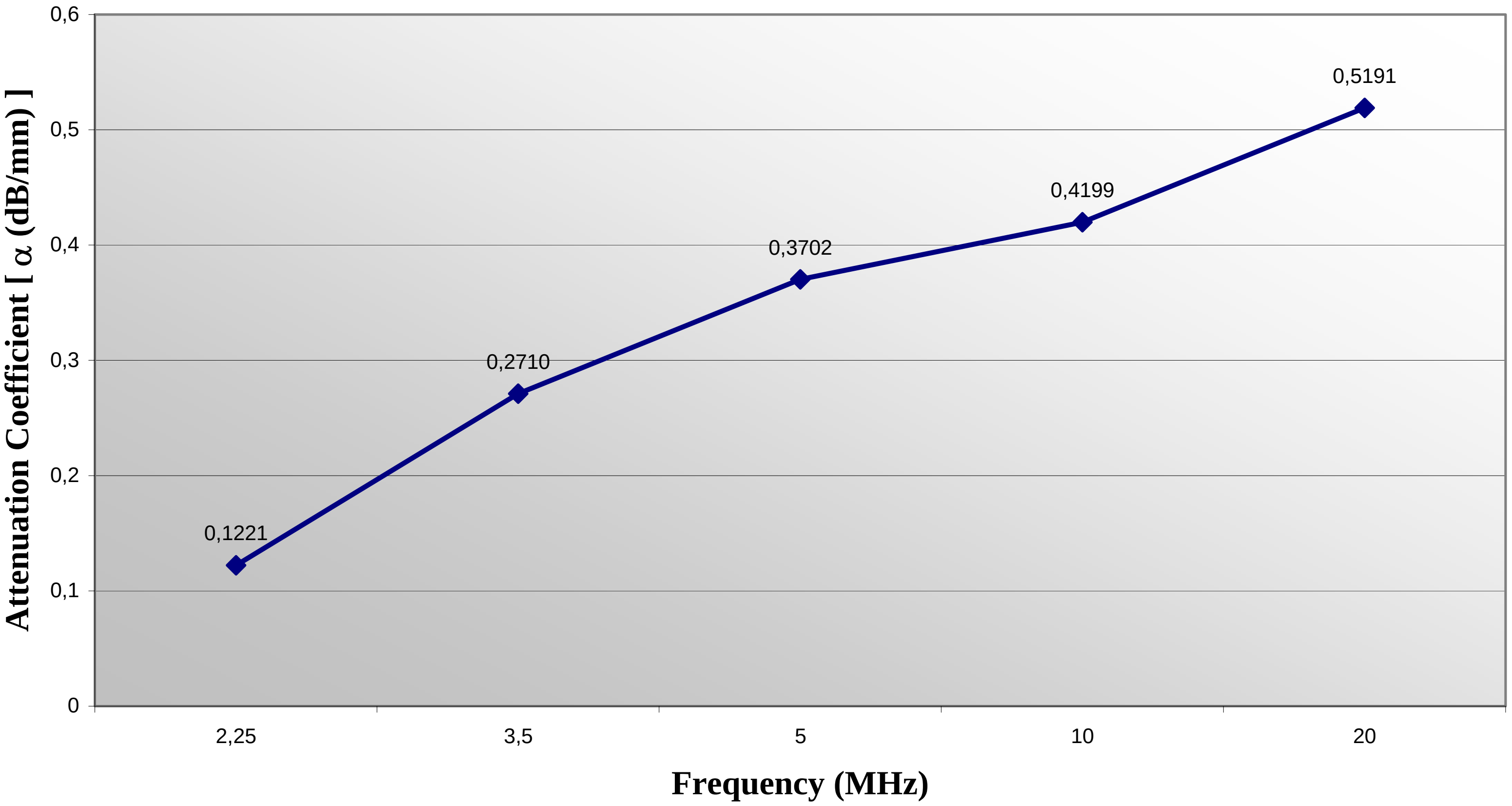

Figure 4.26 Attenuation Coefficient of Poly(HEMA-co-GMA) VT=6ml, 50µl GMA

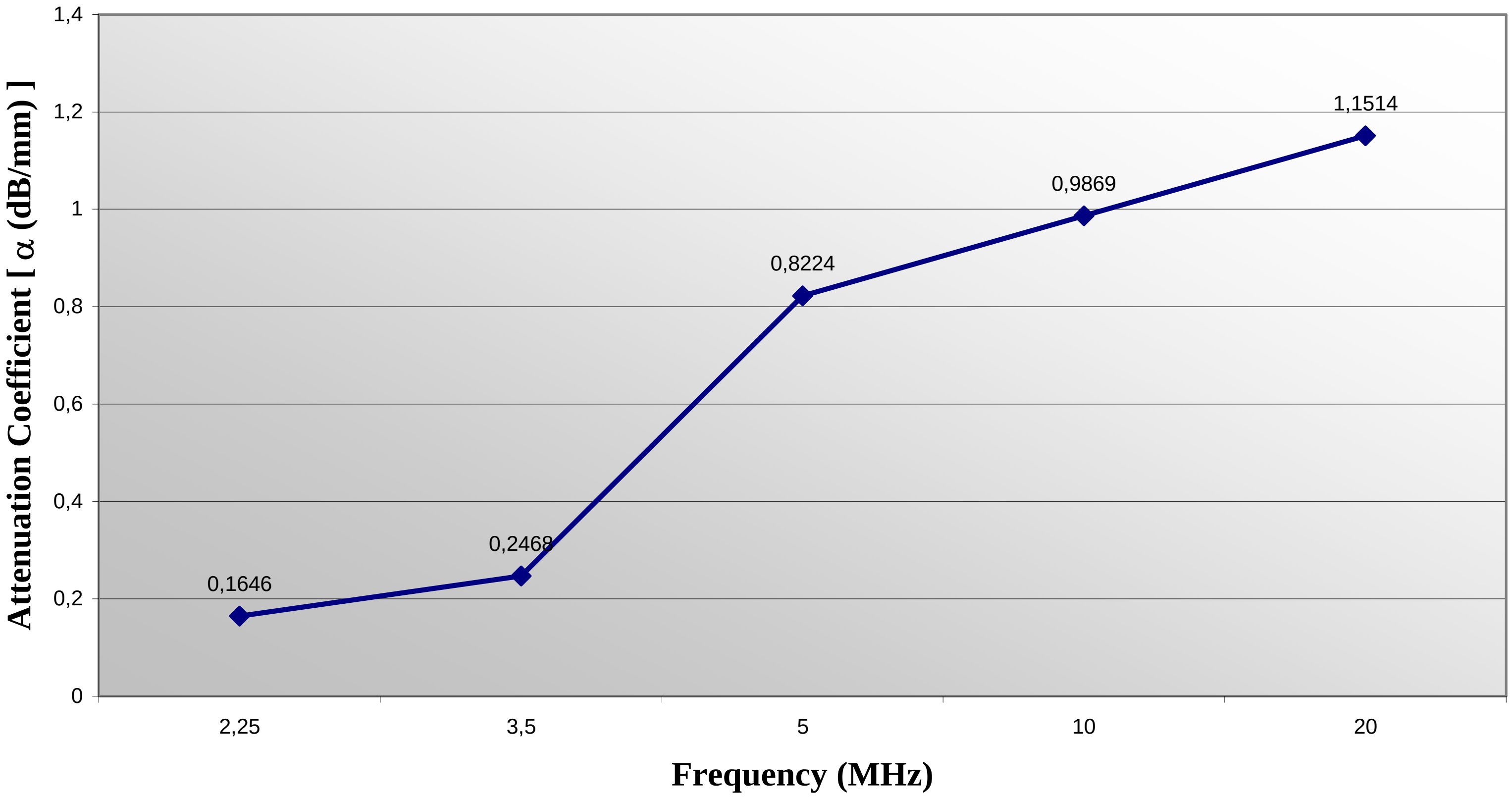

Figure 4.27 Attenuation Coefficient of Poly(HEMA-co-GMA) VT=6ml, 100µl GMA

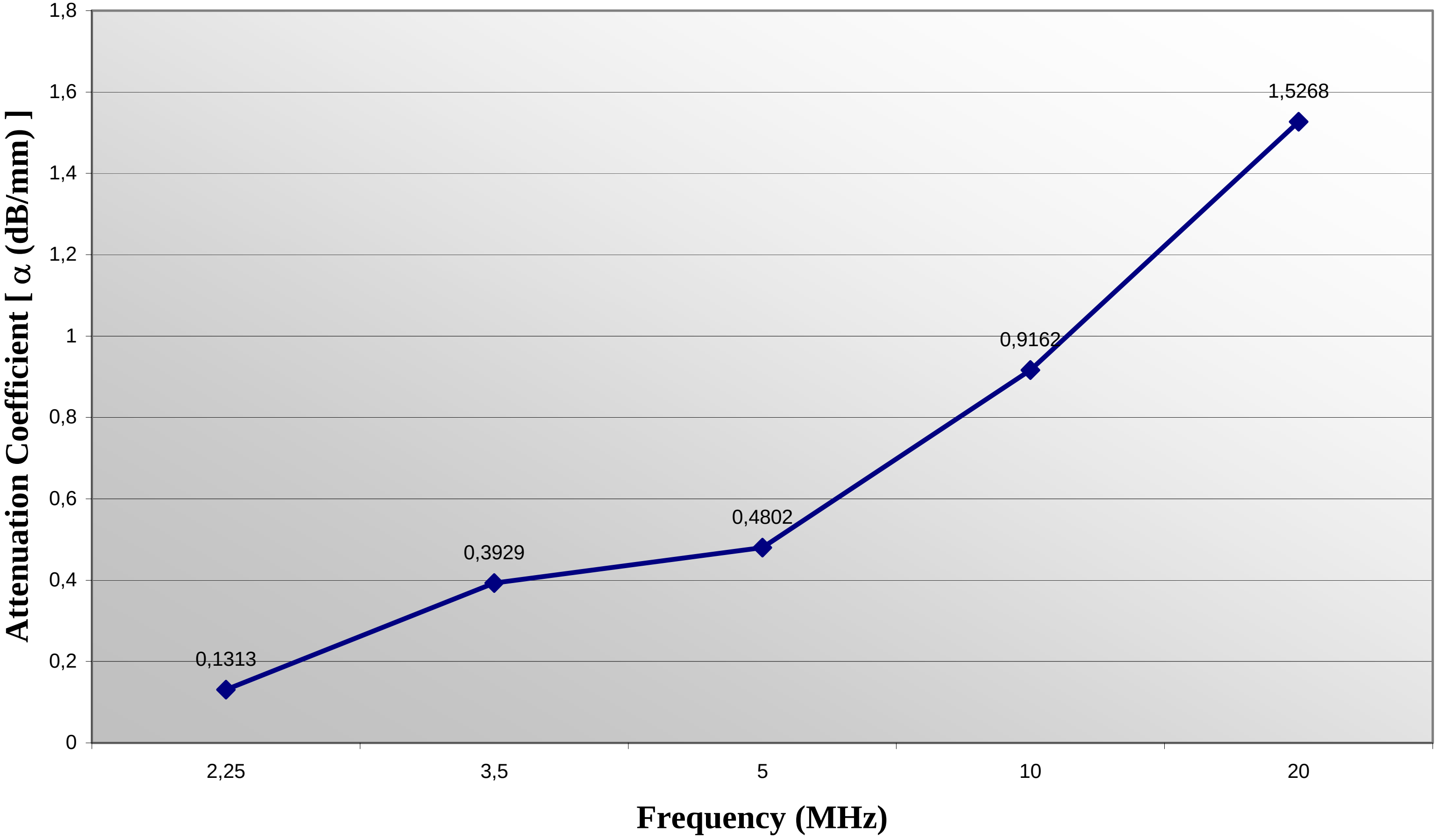

Figure 4.28 Attenuation Coefficient of Poly(HEMA-co-GMA) VT=6ml, 150μl GMA

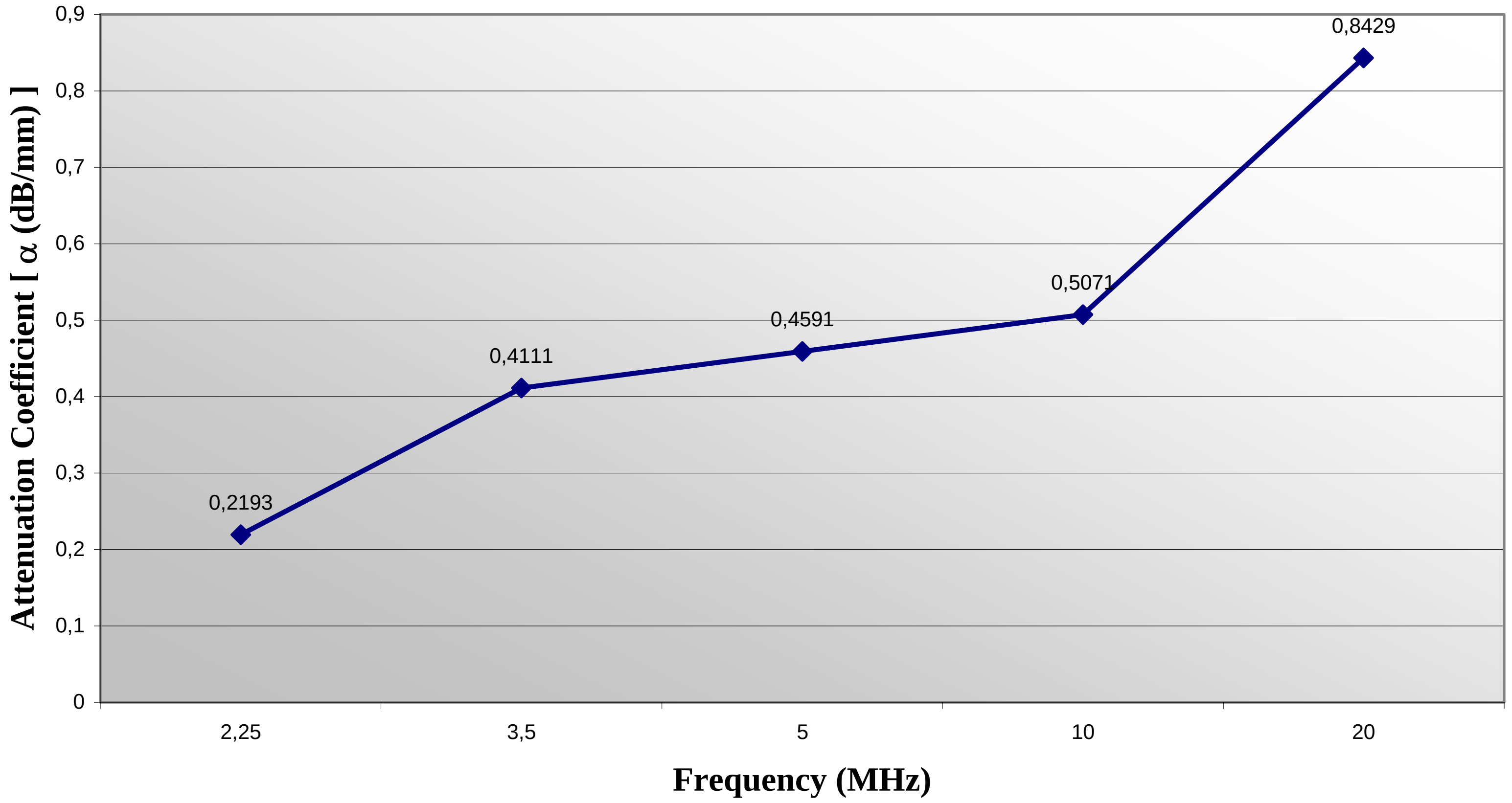

Figure 4.29 Attenuation Coefficient of Poly(HEMA-co-GMA)   VT=8ml, 50μl GMA

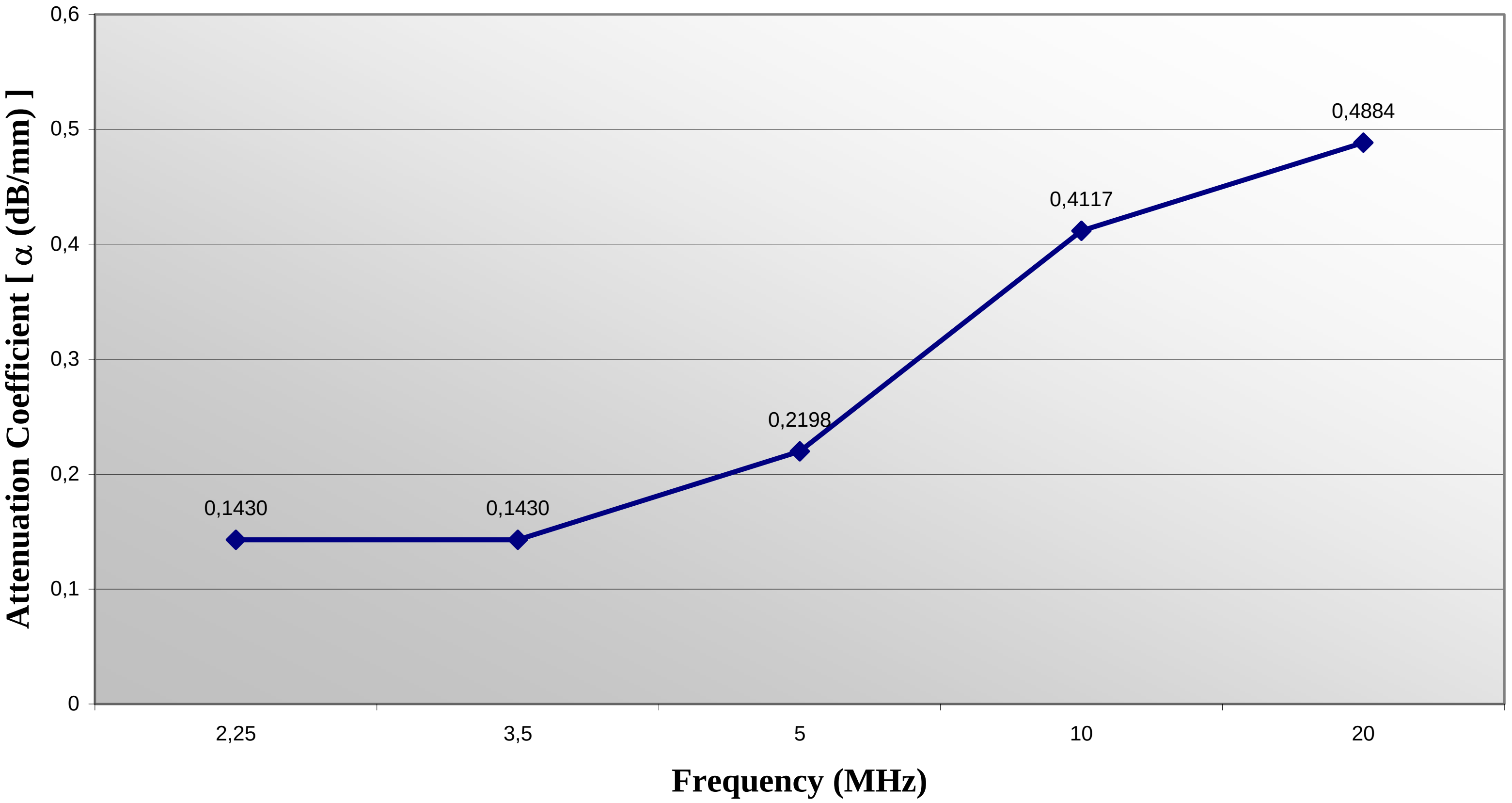

Figure 4.30 Attenuation Coefficient of Poly(HEMA-co-GMA) VT=8ml, 100µl GMA

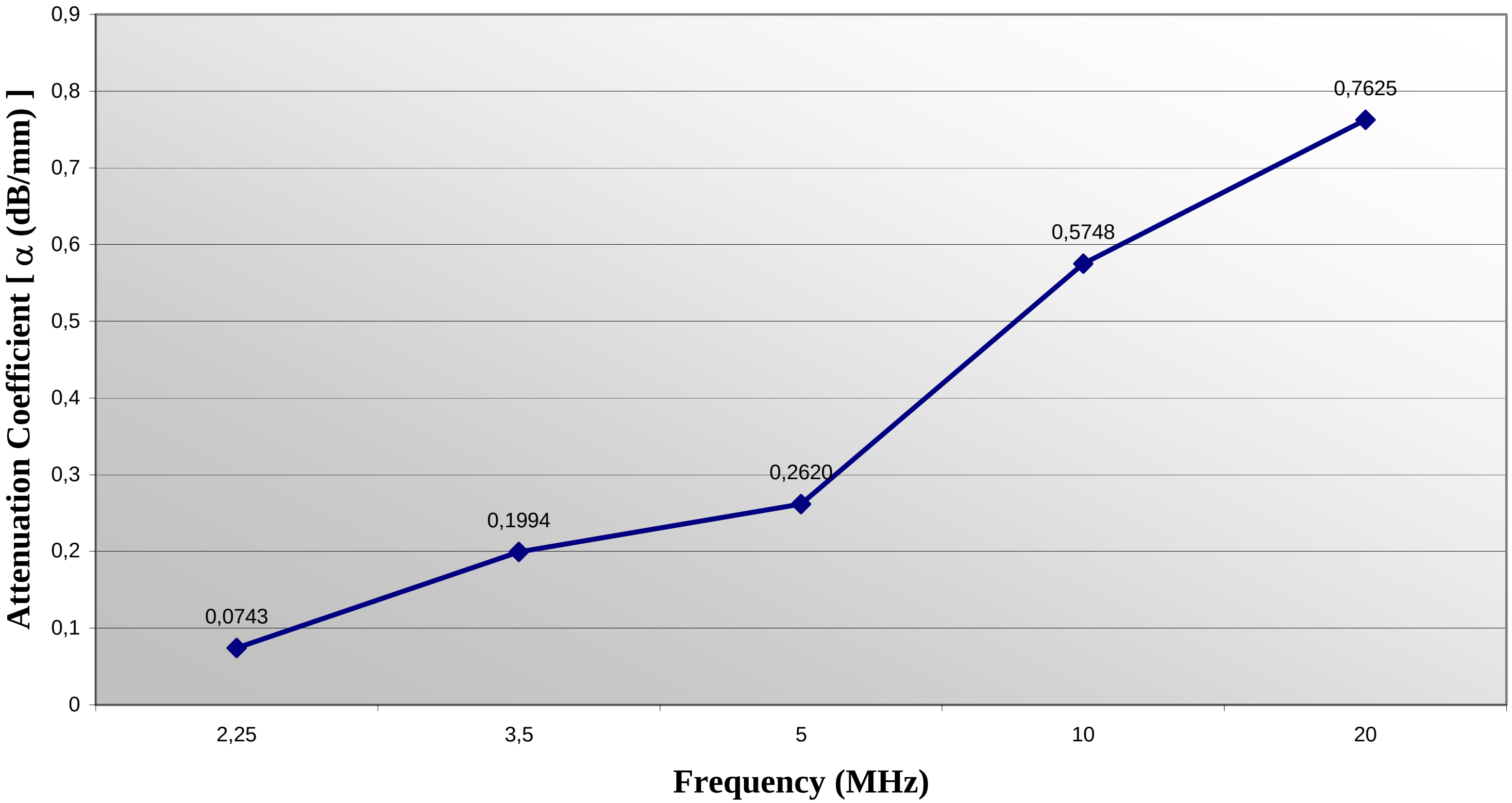

Figure 4.31 Attenuation Coefficient of Poly(HEMA-co-GMA) VT=8ml, 150µl GMA

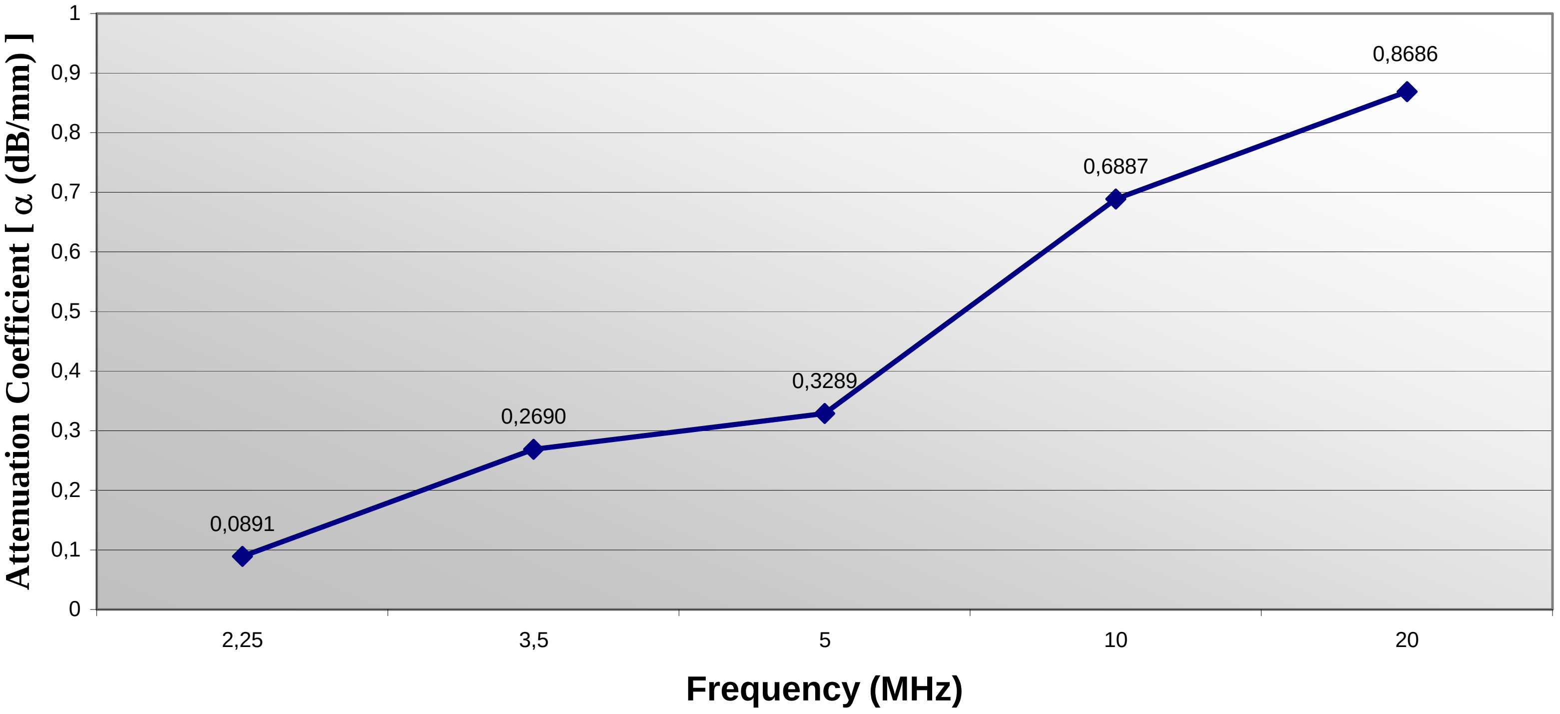

Figure 4.32 Attenuation Coefficient of Poly(HEMA-NN′) VT=6ml (3ml HEMA, 3ml NN′)

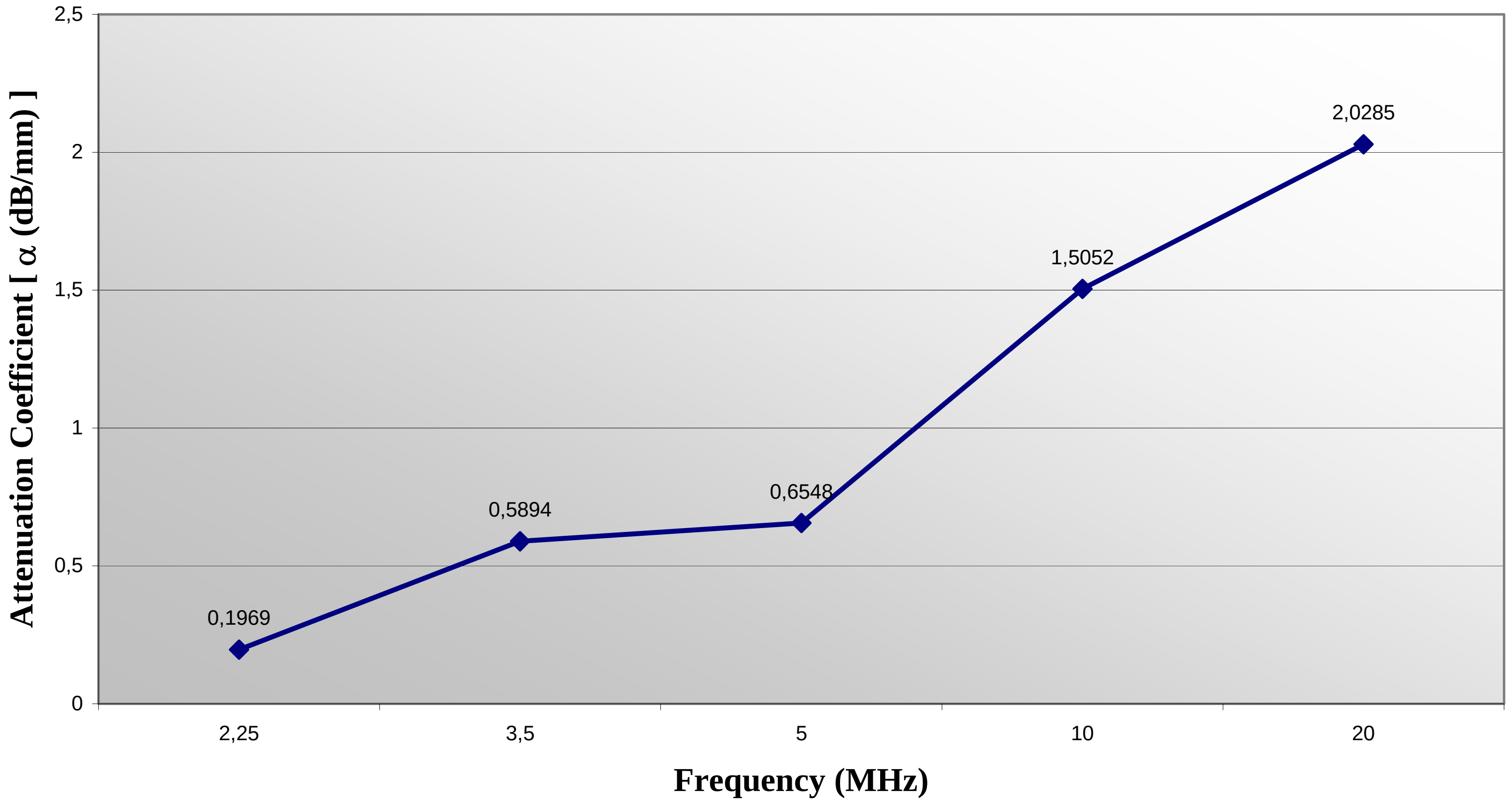

Figure 4.33 Attenuation Coefficient of Poly(HEMA-NN′-dH2O) VT=6ml (3ml HEMA,1ml NN′,2ml dH2O)

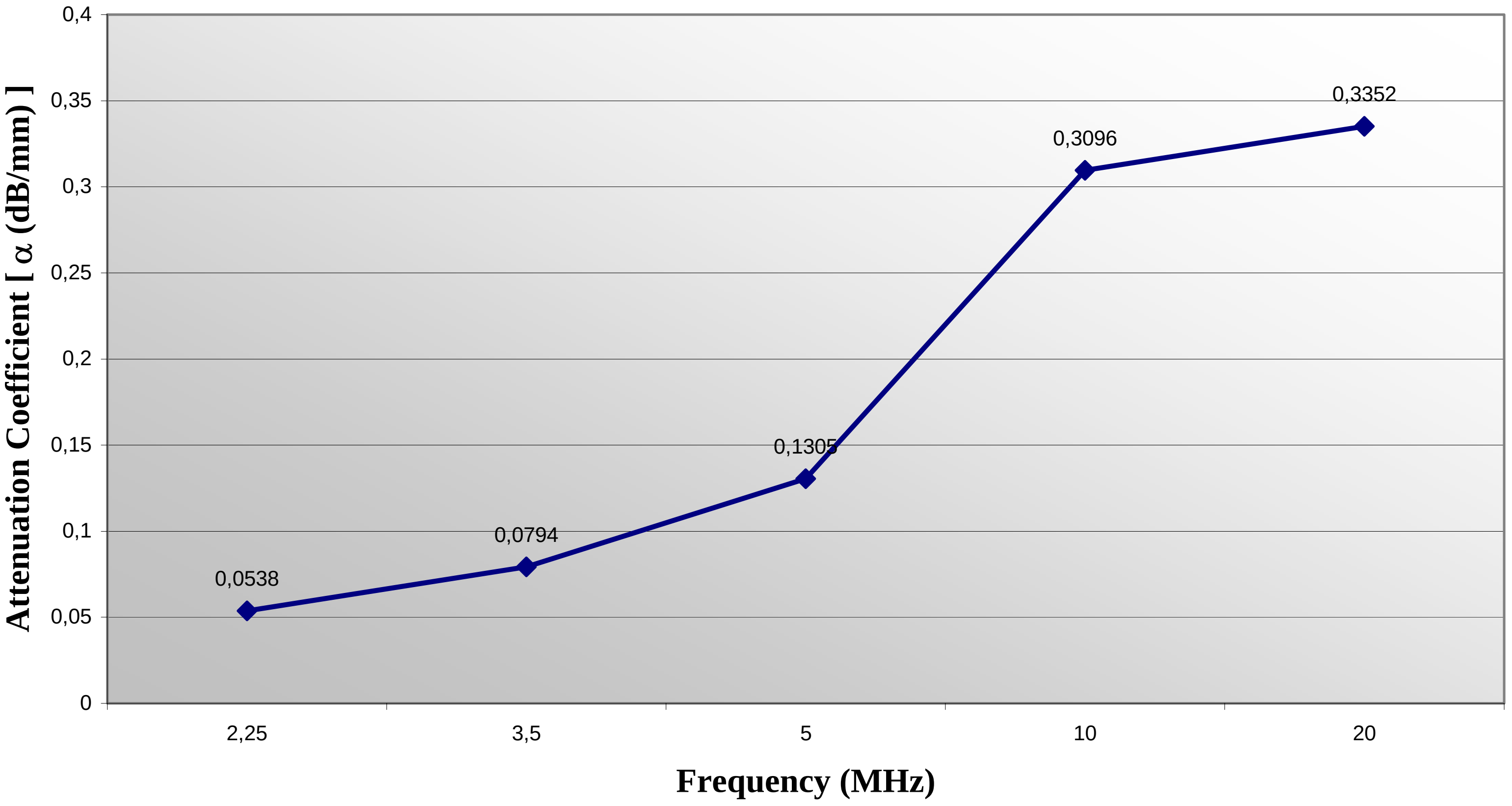

Figure 4.34 Attenuation Coefficient of Poly(HEMA-NN′-dH2O) VT=6ml (3ml HEMA,2ml NN′,1ml dH2O)

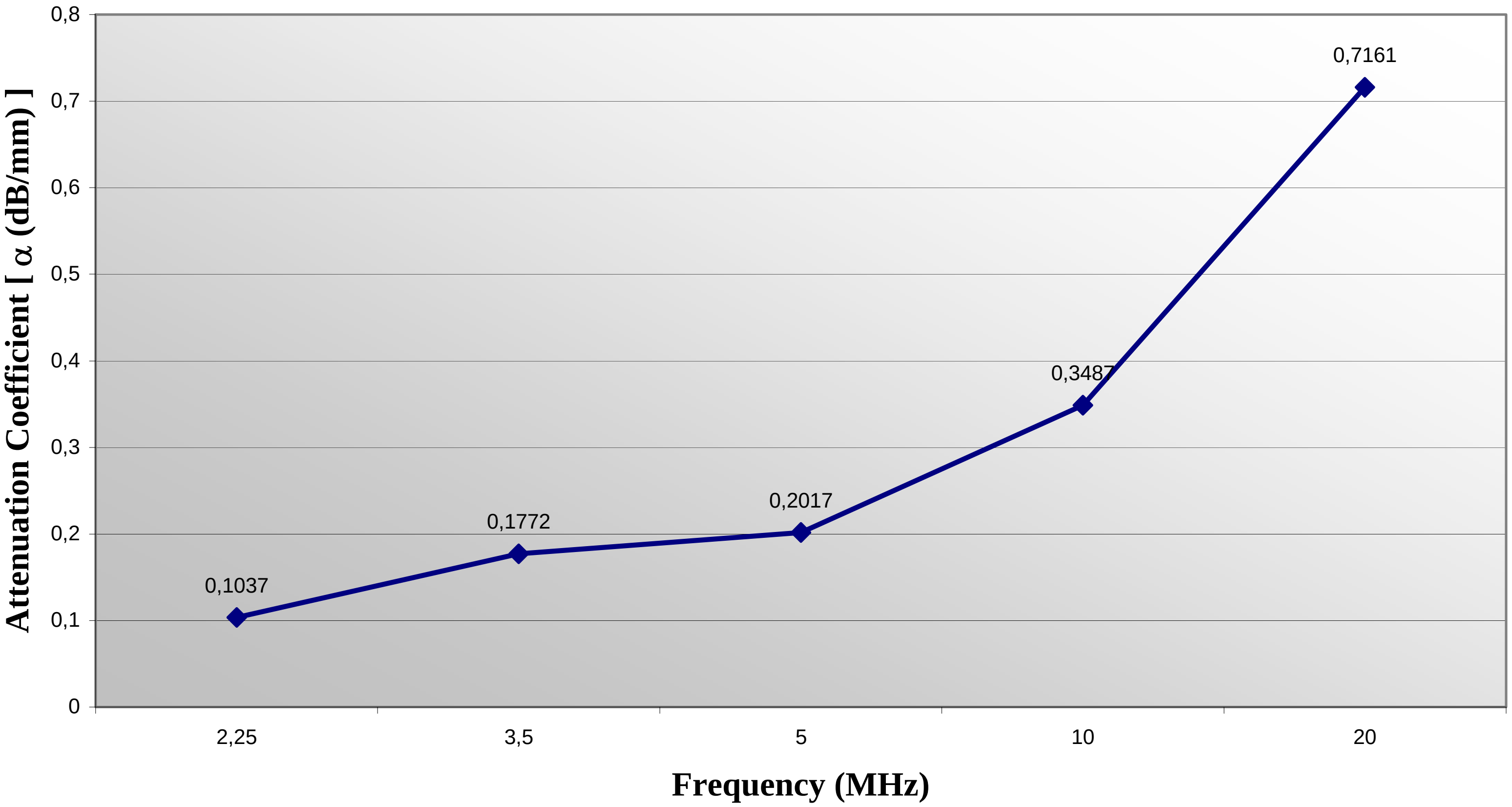

Figure 4.35 Attenuation Coefficient of Poly(HEMA-co-GMA)$_1$ VT=12ml, 50µl GMA

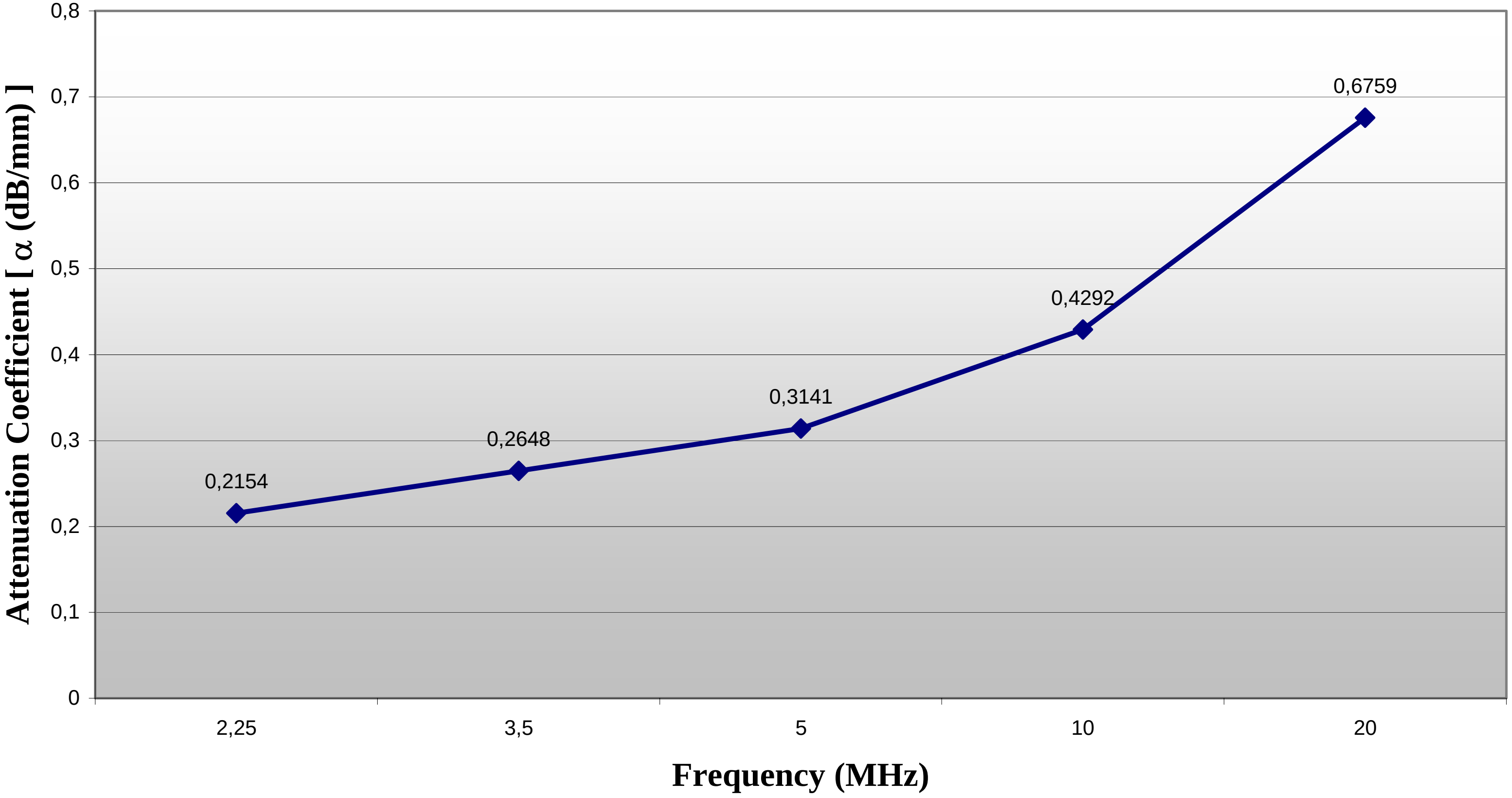

Figure 4.36 Attenuation Coefficient of Poly(HEMA-co-GMA)$_2$ VT=12ml, 100µl GMA

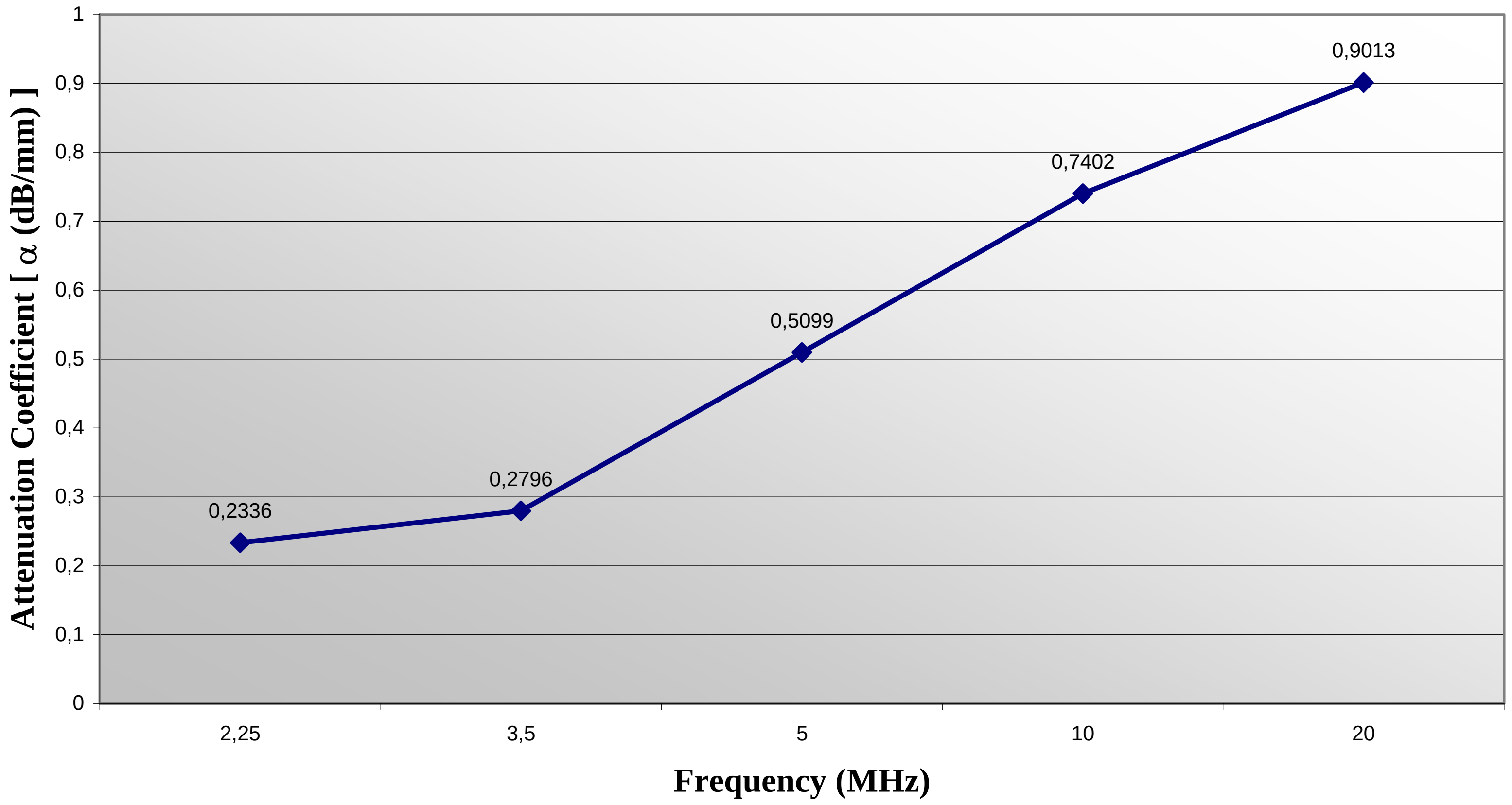

Figure 4.37 Attenuation Coefficient of Poly(HEMA-co-GMA)$_3$ VT=12ml, 150µl GMA

Table 4.43 lists the attenuation coefficient in terms of “dB/mm” at various frequencies. All the attenuation measurements of hydrophilic polymers introduced in this study offered low attenuation compared with typical plastics and rubber [Appendix]. With the increase in frequency, attenuation of polymers increased as expected.

The most significant and lowest attenuation was observed in Poly(HEMA-NN′-dH2O) which is a 6ml mixture consist of (3ml HEMA,2ml NN′,1ml dH2O) with an attenuation coefficient of 0,3352 dB/mm at 20MHz. The highest attenuation was observed in Poly(HEMA-NN′-dH2O) which is a 6ml mixture consist of (3ml HEMA, 1ml NN′, 2ml dH2O) with an attenuation coefficient of 2,0285 dB/mm at 20MHz.

Different from earlier studies, for the attenuation measurements 10MHz and 20MHz ultrasonic transducers were used. Hydrophilic polymers described in this study showed that they could easily adapt themselves in applications by offering low attenuation at high frequencies.

If attenuation coefficient values with respect to frequency is observed from figures 4.20 through 4.36, it can be concluded that 10 MHZ is the critical frequency for the hydrophilic polymers observed in this study. At 10 MHz there is a rapid increase in the attenuation coefficient of polymers. But this increment is low in comparison to other plastics and rubbers.

4.4 Coupling Efficiency Measurements

Tables 4.44 through 4.47 show coupling efficiencies of hydrophilic polymers at various frequencies. It must be noted that echo amplitude data, shown in the tables, is given in terms of the gain (dB) required to increase the signal to 80% screen height on the digital oscilloscope. Therefore, low gain corresponds to high amplitude echo and vice versa.

Table 4.44 Coupling Efficiency at 2.25MHz frequency

Frequency	**2.25 MHz**				
Sample	**Unload**	**50g**	**200g**	**500g**	**1000g**
Poly(HEMA)$_1$	75,5	75	74	73	72,5
Poly(HEMA)$_2$	73,5	72,5	71	69,5	69
Poly(HEMA)$_3$	75	73,5	71	69	67,5
Poly(HEMA)$_{6ml}$	77	75	72,5	71,5	71
Poly(HEMA)$_{9ml}$	76	75	73,5	72,5	72
Poly(HEMA)$_{12ml}$	74	73	72	71,5	71
Poly(HEMA-co-GMA) VT=6ml, 50µl GMA	75,5	73,5	71	70	69
Poly(HEMA-co-GMA) VT=6ml, 100µl GMA	76,5	75	72,5	70,5	69,5
Poly(HEMA-co-GMA) VT=6ml, 150µl GMA	76,5	75,5	74	72,5	71
Poly(HEMA-co-GMA) VT=8ml, 50µl GMA	76	75	74	73	72,5
Poly(HEMA-co-GMA) VT=8ml, 100µl GMA	76	75,5	74,5	73,5	73
Poly(HEMA-co-GMA) VT=8ml, 150µl GMA	76,5	76	75	74,5	74
Poly(HEMA-NN′), VT=6ml (3ml HEMA, 3ml NN′)	75,5	75	73	72	71,5

Table 4.44 Continued

Frequency	**2.25 MHz**				
Sample	**Unload**	**50g**	**200g**	**500g**	**1000g**
Poly(HEMA-NN′-dH2O), VT=6ml (3ml HEMA,1ml NN′,2ml dH2O)	77,5	75,5	74,5	73,5	73
Poly(HEMA-NN′-dH2O), VT=6ml (3ml HEMA,2ml NN′,1ml dH2O)	78	77	75,5	74,5	74
Poly(HEMA-co-GMA)$_1$ VT=12ml, 50μl GMA	75	74	73	72	71,5
Poly(HEMA-co-GMA)$_2$ VT=12ml, 100μl GMA	75	74,5	73,5	73	72,5
Poly(HEMA-co-GMA)$_3$ VT=12ml, 150μl GMA	76,5	76	75	74	73,5

If almost same thicknesses were compared again, for example

- Poly(HEMA-co-GMA), V_T=8ml, 150μl GMA, **t=460μm**, % 55,45 swelling ratio(SR)
- Poly(HEMA-NN′-dH2O), V_T=6ml (3ml HEMA, 1ml NN′,2ml dH2O), **t=440μm**, % 63,85 SR
- Poly(HEMA)$_1$, **t=450μm**, % 64,98 SR

As seen from figure 4.38; the higher the contact pressure, the higher the level of coupling. Similarly, echo amplitude increased with increasing contact pressure. In other words, ultrasound was transferred more effectively.

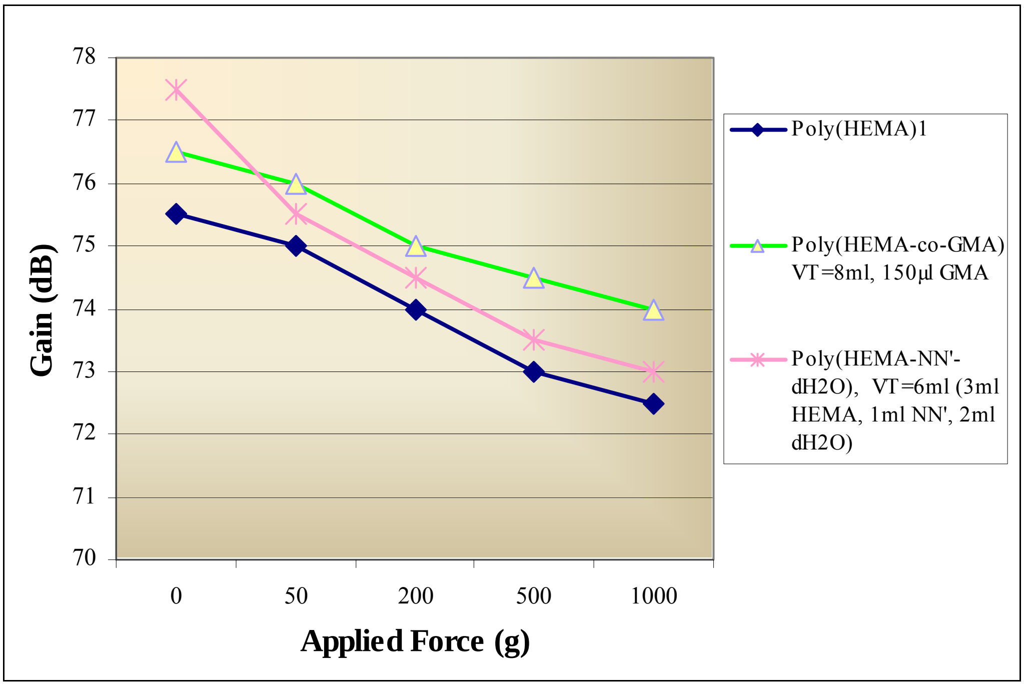

Figure 4.38 Coupling Efficiency at 2.25 MHz

Similar trends could also be observed in:

- Poly(HEMA-co-GMA), V_T=6ml, 50µl GMA, **t=580µm,** % 62,1 SR
- Poly(HEMA)$_2$, **t=570µm,** % 62,57 SR
- Poly(HEMA)$_3$, **t=550µm,** % 126,8 SR

Figure 4.39 shows this trend. Results achieved from the different hydrophilic polymers followed consistent trends: the higher the water content, the higher the amplitude of the steel backwall echo.

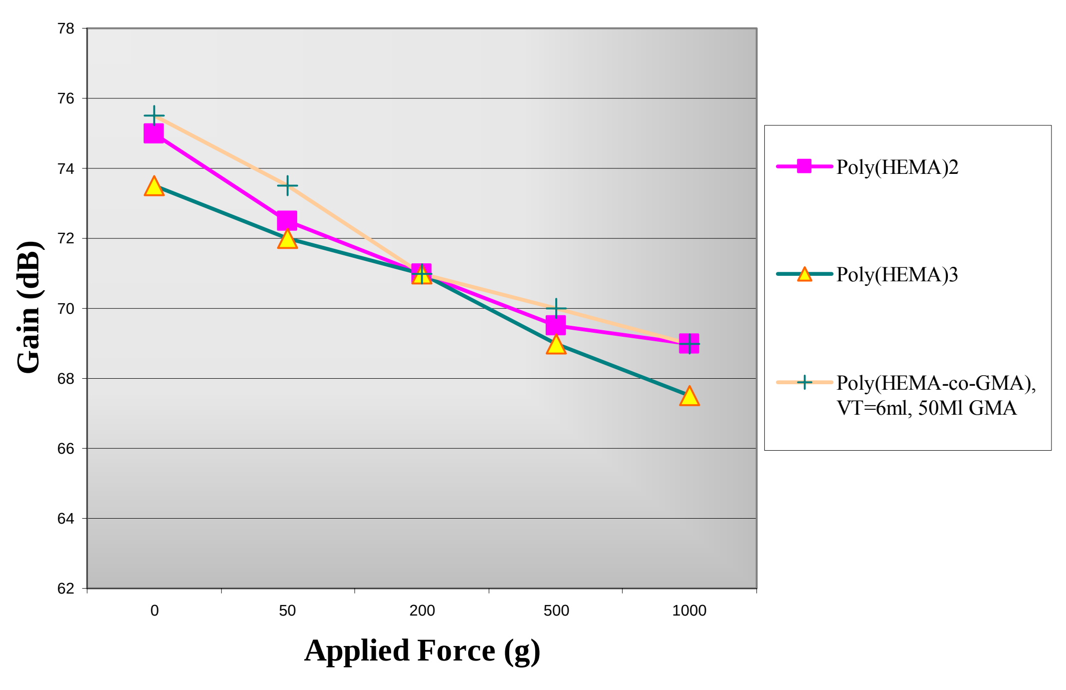

Figure 4.39 Coupling Efficiency at 2.25 MHz

Table 4.45 Coupling Efficiency at 3.5MHz frequency

Frequency	**3.5 MHz**				
Sample	**Unload**	**50g**	**200g**	**500g**	**1000g**
Poly(HEMA)$_1$	66,5	65,5	64	63	62,5
Poly(HEMA)$_2$	67,5	66,5	65	63	62,5
Poly(HEMA)$_3$	65	64,5	63	62	61,5
Poly(HEMA)$_{6ml}$	68	66,5	65	63,5	62,5
Poly(HEMA)$_{9ml}$	68	67	65,5	64	63
Poly(HEMA)$_{12ml}$	67,5	66,5	64	62,5	62
Poly(HEMA-co-GMA) VT=6ml, 50µl GMA	69	67,5	66	65	64,5
Poly(HEMA-co-GMA) VT=6ml, 100µl GMA	69	68,5	66,5	65,5	65

Table 4.45 Continued

Frequency	**3.5 MHz**				
Sample	**Unload**	**50g**	**200g**	**500g**	**1000g**
Poly(HEMA-co-GMA) VT=6ml, 150µl GMA	70	69,5	68	67	66
Poly(HEMA-co-GMA) VT=8ml, 50µl GMA	66	65	63,5	62,5	62
Poly(HEMA-co-GMA) VT=8ml, 100µl GMA	67,5	67	65	64	63
Poly(HEMA-co-GMA) VT=8ml, 150µl GMA	70,5	69	67,5	66	65
Poly(HEMA-NN′), VT=6ml (3ml HEMA, 3ml NN′)	65,5	65	64	63	62,5
Poly(HEMA-NN′-dH2O), VT=6ml (3ml HEMA,1ml NN′,2ml dH2O)	68	66,5	65,5	64	63
Poly(HEMA-NN′-dH2O), VT=6ml (3ml HEMA,2ml NN′,1ml dH2O)	73	70,5	67,5	66	65
Poly(HEMA-co-GMA)$_1$ VT=12ml, 50µl GMA	69,5	68	65,5	64,5	64
Poly(HEMA-co-GMA)$_2$ VT=12ml, 100µl GMA	69,5	69	68	67	66,5
Poly(HEMA-co-GMA)$_3$ VT=12ml, 150µl GMA	71	70,5	69,5	68	67,5

Table 4.46 Coupling Efficiency at 5MHz frequency

Frequency	**5 MHz**				
Sample	**Unload**	**50g**	**200g**	**500g**	**1000g**
Poly(HEMA)$_1$	60,5	58	57	56	55,5
Poly(HEMA)$_2$	59	57	56	54,5	53
Poly(HEMA)$_3$	57	56	54,5	52,5	51,5

Table 4.46 Continued

Frequency	**5 MHz**				
Sample	**Unload**	**50g**	**200g**	**500g**	**1000g**
Poly(HEMA)$_{6ml}$	63	61	59,5	57,5	56
Poly(HEMA)$_{9ml}$	58,5	57,5	55,5	54	53,5
Poly(HEMA)$_{12ml}$	58,5	57	55,5	53,5	52,5
Poly(HEMA-co-GMA) VT=6ml, 50µl GMA	62,5	62	60,5	58	56
Poly(HEMA-co-GMA) VT=6ml, 100µl GMA	63	62,5	61	58,5	56
Poly(HEMA-co-GMA) VT=6ml, 150µl GMA	63	62,5	61,5	59,5	57
Poly(HEMA-co-GMA) VT=8ml, 50µl GMA	58,5	57,5	56,5	55,5	55
Poly(HEMA-co-GMA) VT=8ml, 100µl GMA	59	58,5	57	56	55,5
Poly(HEMA-co-GMA) VT=8ml, 150µl GMA	63	61	59,5	58,5	58
Poly(HEMA-NN′), VT=6ml (3ml HEMA, 3ml NN′)	60,5	59,5	58,5	56,5	55,5
Poly(HEMA-NN′-dH2O), VT=6ml (3ml HEMA,1ml NN′,2ml dH2O)	61	59	57,5	56,5	56
Poly(HEMA-NN′-dH2O), VT=6ml (3ml HEMA,2ml NN′,1ml dH2O)	61	60,5	59,5	57,5	56,5
Poly(HEMA-co-GMA)$_1$ VT=12ml, 50µl GMA	63	62,5	61,5	60	59,5
Poly(HEMA-co-GMA)$_2$ VT=12ml, 100µl GMA	63	62,5	62	61	60,5
Poly(HEMA-co-GMA)$_3$ VT=12ml, 150µl GMA	65	64,5	62,5	61,5	61

Table 4.47 Coupling Efficiency at 10MHz frequency

Frequency	**10 MHz**				
Sample	**Unload**	**50g**	**200g**	**500g**	**1000g**
Poly(HEMA)$_1$	55,5	53	52	51	50,5
Poly(HEMA)$_2$	54,5	53,5	52,5	50	49
Poly(HEMA)$_3$	53,5	51,5	50	48	47
Poly(HEMA)$_{6ml}$	57	55,5	54	53	52
Poly(HEMA)$_{9ml}$	54,5	52	50,5	49,5	48,5
Poly(HEMA)$_{12ml}$	55,5	54	53	51	50
Poly(HEMA-co-GMA) VT=6ml, 50µl GMA	57	56,5	54	53	51
Poly(HEMA-co-GMA) VT=6ml, 100µl GMA	57,5	56	55	54	53,5
Poly(HEMA-co-GMA) VT=6ml, 150µl GMA	58	57,5	56	55	54
Poly(HEMA-co-GMA) VT=8ml, 50µl GMA	53,5	52,5	51	50	49,5
Poly(HEMA-co-GMA) VT=8ml, 100µl GMA	54	53,5	53	52	51
Poly(HEMA-co-GMA) VT=8ml, 150µl GMA	58	56	54,5	53,5	53
Poly(HEMA-NN′), VT=6ml (3ml HEMA, 3ml NN′)	56,5	54	52	51	50,5
Poly(HEMA-NN′-dH2O), VT=6ml (3ml HEMA,1ml NN′,2ml dH2O)	56,5	55	52,5	51,5	51
Poly(HEMA-NN′-dH2O), VT=6ml (3ml HEMA,2ml NN′,1ml dH2O)	58,5	57	54	52	51
Poly(HEMA-co-GMA)$_1$ VT=12ml, 50µl GMA	59,5	59	58	56	55,5
Poly(HEMA-co-GMA)$_2$ VT=12ml, 100µl GMA	60	59,5	58	56	55,5
Poly(HEMA-co-GMA)$_3$ VT=12ml, 150µl GMA	61	60,5	59	57,5	57

As seen from the coupling efficiency results, level of coupling is frequency independent; the higher the contact pressure, the higher the level of coupling. Frequency has an effect only on the required gain. From the results achieved from different hydrophilic polymers, it can be concluded that echo amplitude increased with increasing contact pressure.

From the scatter data shown in figures 4.40 through 4.43, it can be resulted that Poly(HEMA)$_3$ has a great coupling efficiency among others, it required low gain, in other words gave high echo amplitude.

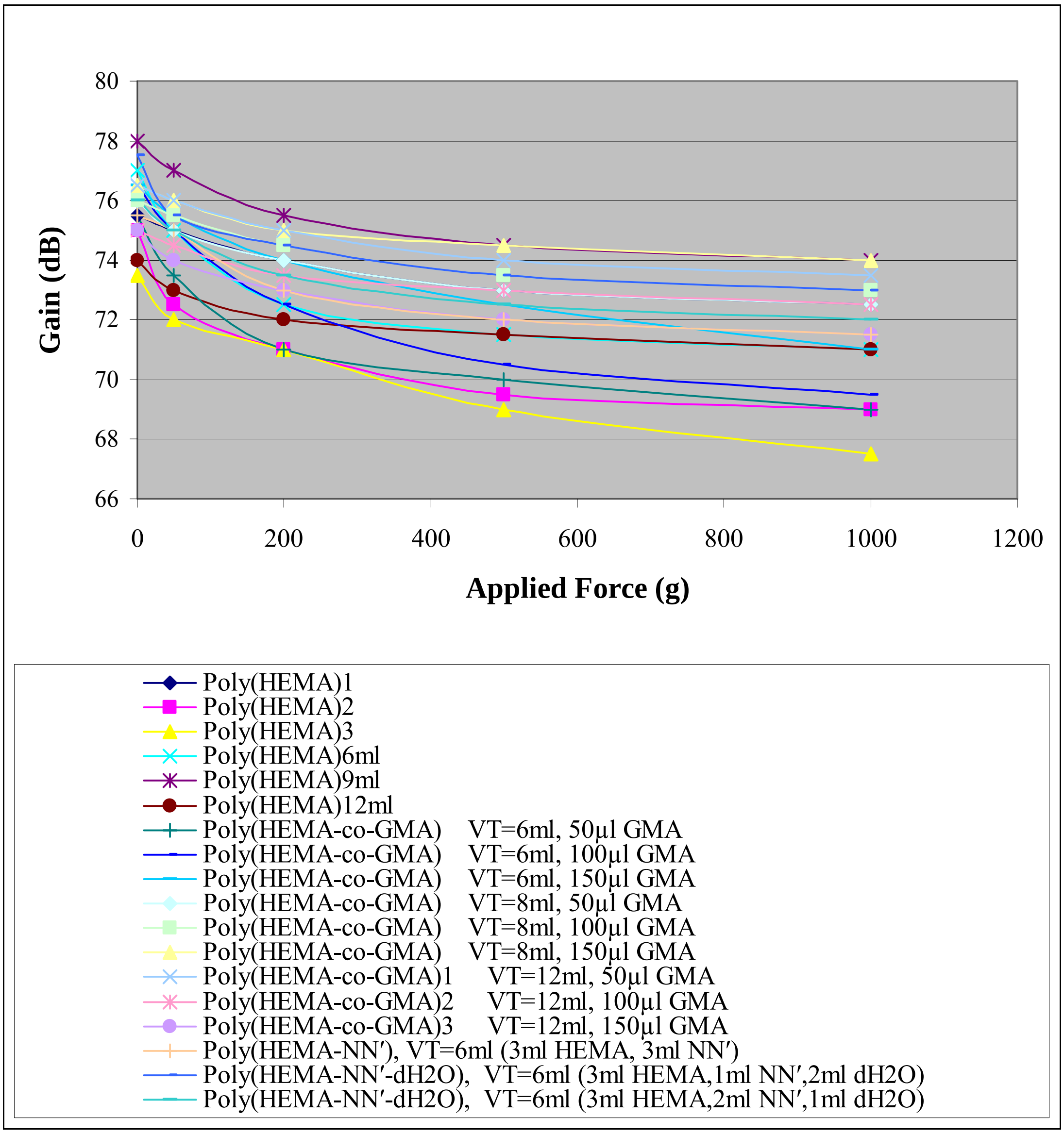

Figure 4.40 Amplitude of steel backwall echo through different hydrophilic polymers at 2.25 MHz

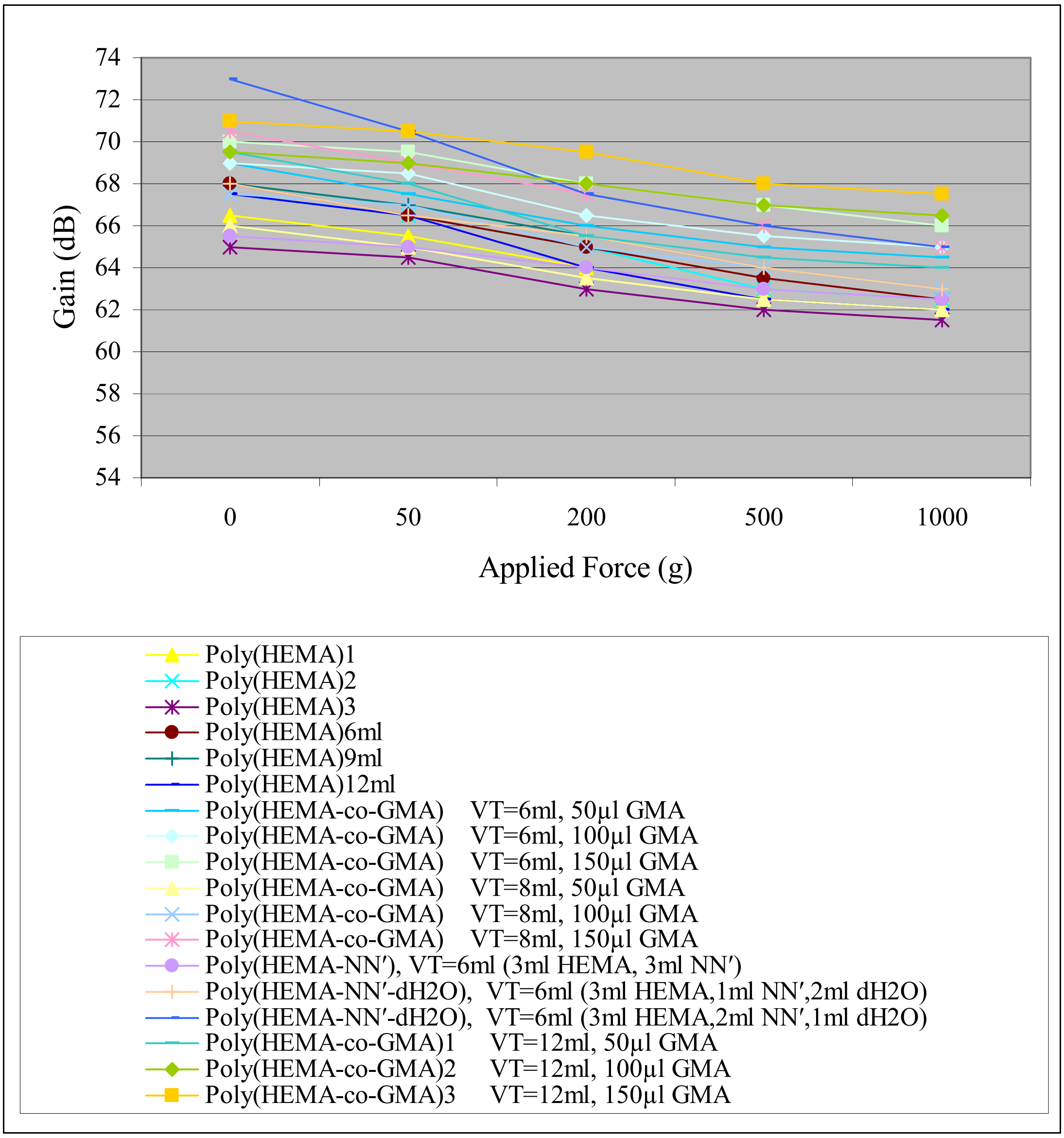

Figure 4.41 Amplitude of steel backwall echo through different hydrophilic polymers at 3.5 MHz

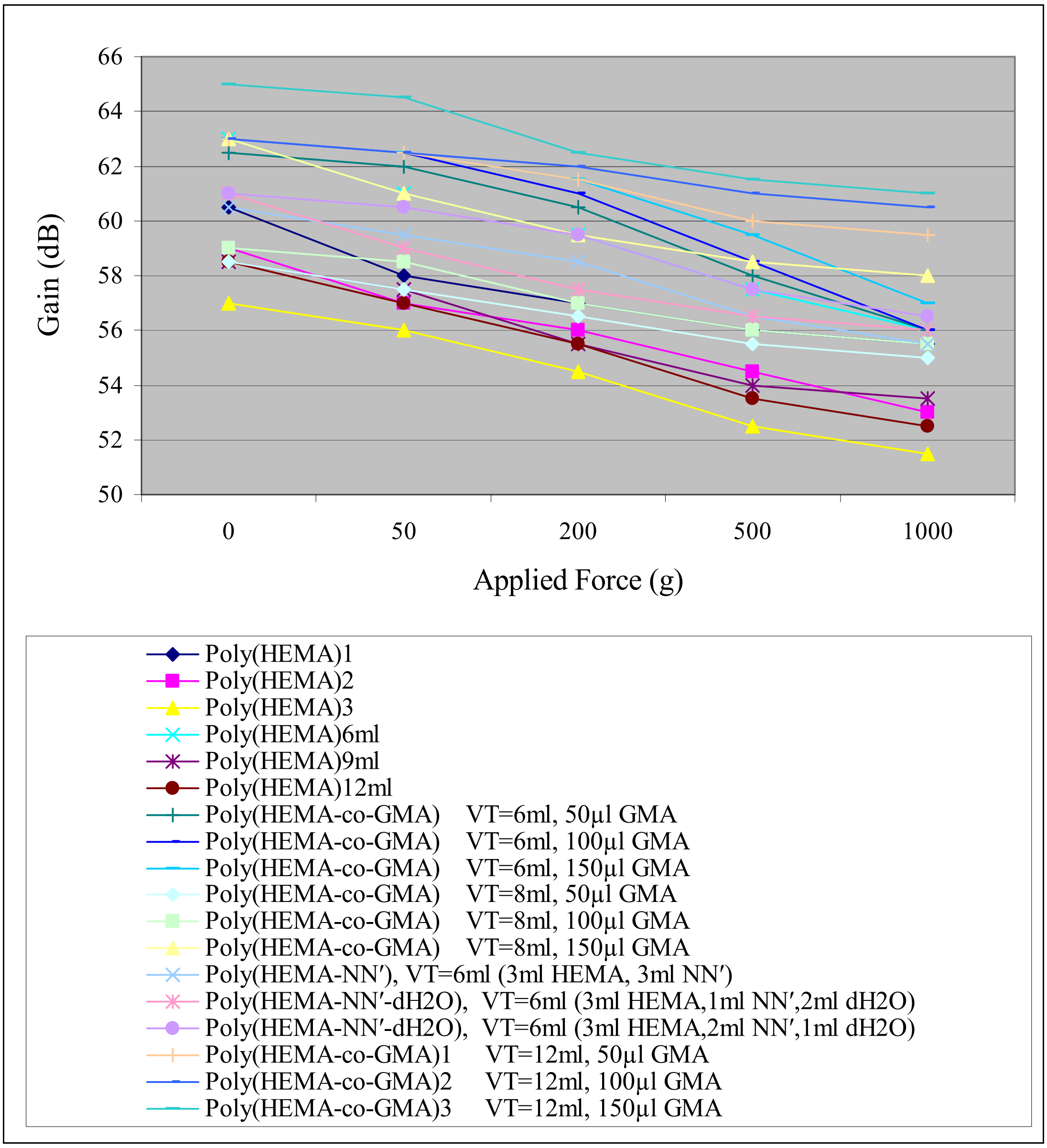

Figure 4.42 Amplitude of steel backwall echo through different hydrophilic polymers at 5 MHz

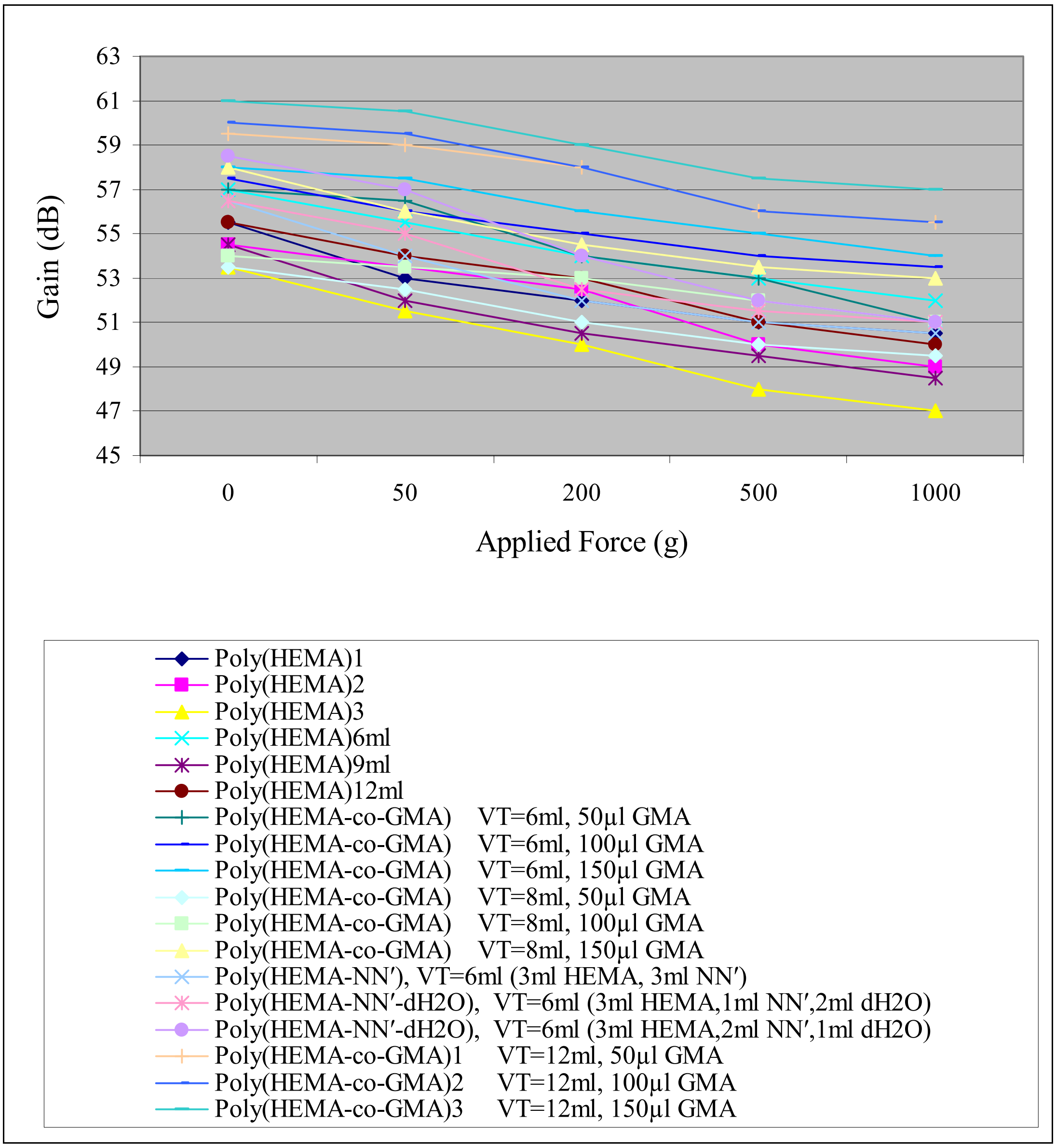

Figure 4.43 Amplitude of steel backwall echo through different hydrophilic polymers at 10 MHz

CHAPTER V

CONCLUSION

The aim of the thesis was to introduce hydrophilic polymers as new solid coupling materials to the field of ultrasonic non-destructive testing. These hydrophilic polymers were examined by their swelling ratio abilities, velocity and attenuation measurements and also coupling efficiencies.

Swellable poly(HEMA) membranes were prepared by UV-initiated photo-polymerization of HEMA, GMA, crosslinkers and benzoyl peroxide (i.e., the initiator). Polymer velocities and attenuation values were found using immersion and pulse-echo techniques. Velocity results showed that the higher the water content of the polymer, the closer the values are to those of pure water. It is also noteworthy that the acoustic impedance of all of the polymers demonstrated acoustic impedances very close to that of water.

With the increase in frequency, attenuation of polymers increased as expected but all the attenuation measurements of hydrophilic polymers introduced in this study offered low attenuation compared with typical plastics and rubber.

Different from earlier studies, for the attenuation measurements 10MHz and 20MHz ultrasonic transducers were used. The study showed that 10 MHZ was the critical frequency for the hydrophilic polymers. At 10 MHz there is a rapid increase in the attenuation coefficient of polymers. But this increment was low in comparison to other plastics and rubbers.

The most significant and lowest attenuation was observed in Poly(HEMA-NN′-dH2O) which is a 6ml mixture consist of (3ml HEMA,2ml NN′,1ml dH2O) with an attenuation coefficient of 0,3352 dB/mm at 20MHz. The highest attenuation was observed in Poly(HEMA-NN′-dH2O) which is a 6ml mixture consist of (3ml HEMA, 1ml NN′, 2ml dH2O) with an attenuation coefficient of 2,0285 dB/mm at 20MHz.

From coupling efficiency results achieved from different hydrophilic polymers, level of coupling and echo amplitude increased with increasing contact pressure. Also higher water content culminated in higher amplitude of backwall echo.

Hydrophilic polymers described in this study showed that they could easily adapt themselves in applications by offering low attenuation at high frequencies and they had the ability to couple effectively.

For future work, these polymers can be used as a part of automatic scanning system. This research can also be used as a guideline for an alternative choice of couplant while testing water sensitive materials in safety critical structures or where the test piece is avoided from contamination. Because of their coupling efficiency they may also be used for rough surfaces.

REFERENCES

(1) Krautkramer, J. and Krautkramer, H., “Ultrasonic Testing of Materials”, Springer-Verlag (Berlin), 3rd edition, 1983.

(2) Halmshaw, R., “Non-Destructive Testing”, Second Edition, Edward Arnold, London, 1991.

(3) Drinkwater, B. and Cawley, P., “An ultrasonic wheel probe alternative to liquid coupling”, Insight, Vol 36, No 6, pp. 430-433, June 1994.

(4) Billson, D.R. and Hutchins, D.A., “Development of novel piezoelectric ultrasonic transducers for couplant-free non-destructive testing”, British Journal of NDT, Vol 35, No 12, pp. 705-709, December 1993.

(5) Drinkwater, B. and Cawley, P., “The practical application of solid coupled ultrasonic transducers”, Materials Evaluation, pp. 401-406, March 1997

(6) Dickson, K.J., “Dry coupling ultrasonic method of inspection on composite and metallic honeycomb panels on aircraft structures”, Pro. 10th World Conference on NDT, pp 216-221, 1982.

(7) Bourne, S.J., Newborough, M. and Highgate, D.J., “High frequency ultrasonic wheel probe using hydrophilic polymers as novel solid couplant”, Insight, Vol 43, No 1, pp. 26-28, January 2001.

(8) Bourne, S.J., Buckley, J.M. and Kelly, P.M., “Application of Air-Scan Technology to Ballistic Impact Protective Systems”, Personal Armour Systems Symposium, Sonatest Plc, UK, Colchester 5-8th September 2000

(9) Hull, Barry and John, Vernon, “Non Destructive Testing”, ELBS Edition, Hampshire, 1989

(10) Boyd, Alan S., “Ultrasonic Testing Inspection for Butt Welds in Highway & Railway Bridges”, U.S. Department of Transportation

(11) Diederichs, R. and Ginzel, E. “Non destructive Testing Encyclopedia” December, 1999.

(12) Lach, M., Platte, M. and Ries, A., “Piezoelectric materials for ultrasonic probes”, NDT.net Online Journal, Vol.1 No.9, September 1996.

(13) Birks, A.S., Green, R.E. and McIntire, P., “Nondestructive Testing Handbook”, American Society for Nondestructive Testing, 1991.

(14) Kim, Young H. and Song, Sung-Jin, “A study on the couplant effects in contact ultrasonic testing”, 10th Asia-Pacific Conference on Non-Destructive Testing, 17-21 September 2001, Brisbane, Australia.

(15) Ginzel, Ed, “Ultrasonic Inspection 2 Training for Nondestructive Testing-Variables Affecting Test Results”, NDT.net Online Journal, Vol.4 No.6, June 1999.

(16) Kumar, A, “The Correction Factor Due to Couplant in Ultrasonic Thickness Measurement”, Insight, Vol 38, No 5, pp. 336-337, May 1996

(17) Askeland, Donald R., “The Science and Engineering of Materials”, Third Edition, PWS Publishing Company, 1994

(18) Maffezzoli, A. et al. “Ultrasonic Characterization of Water Sorption in Poly(2-hydroxyethyl methacrylate) hydrogels” Journal of Applied Polymer Science, Vol 67, pp. 823-831, 1998

(19) Bourne, S., Newborough, M. and Highgate, D, “Novel Solid Contact Ultrasonic Couplants Based On Hydrophilic Polymers”, 15th World Conference on NDT, 2000

(20) Molyneux, P. “Water-Soluble Synthetic Polymers: Properties and Behavior”, Volume 1, pp. 1-15, CRC Press, Inc. 1983.

(21) “NDT Handbook”, American Society for Non-Destructive Testing, Ultrasonic Testing, Second Edition, Volume Seven, pp. 225-226, 371.

APPENDIX

ACOUSTIC PROPERTIES OF MATERIALS

Acoustic Properties of Some Plastics

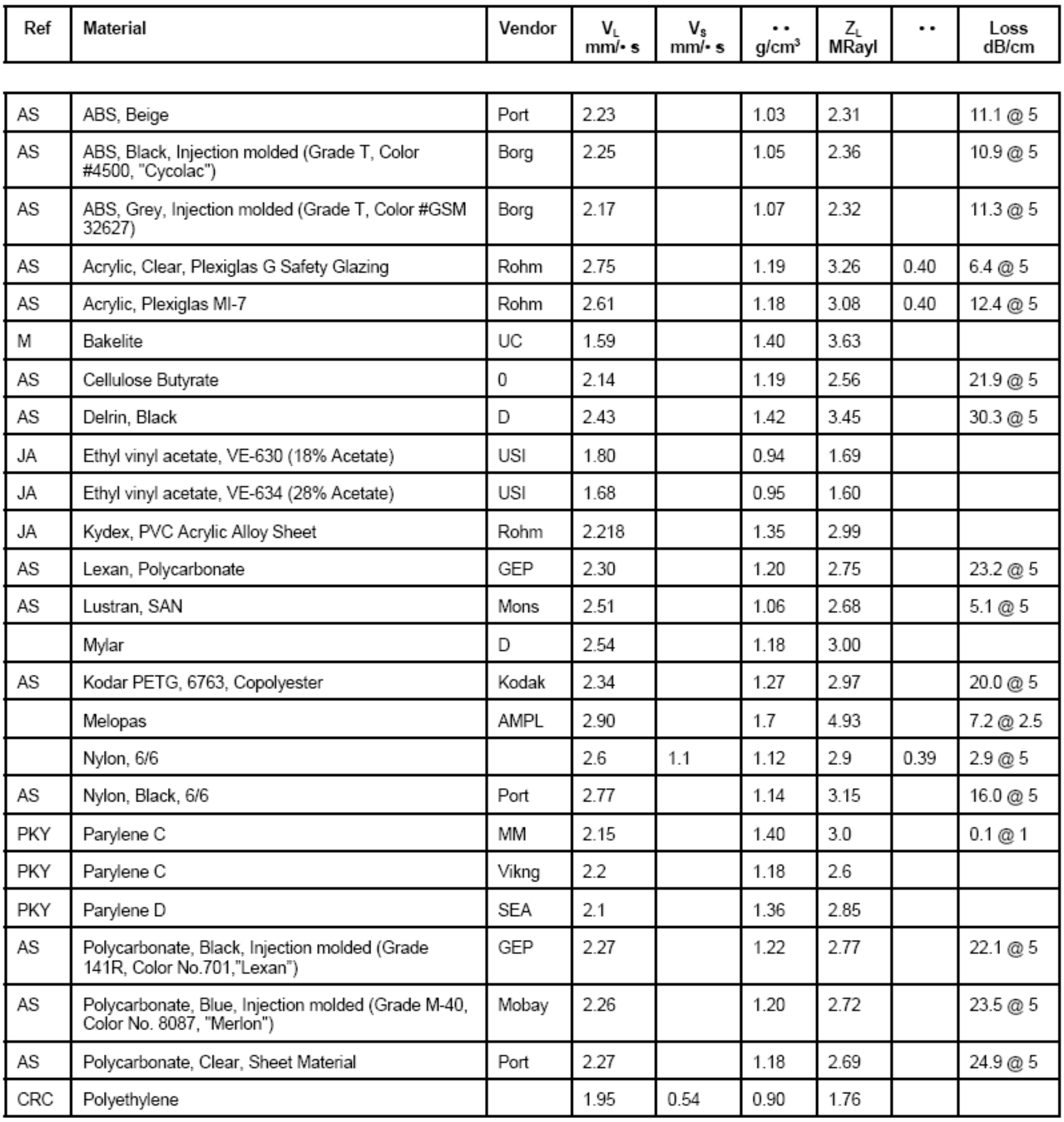

Ref	Material	Vendor	V_L mm/• s	V_s mm/• s	• • g/cm^3	Z_L MRayl	• •	Loss dB/cm
AS	ABS, Beige	Port	2.23		1.03	2.31		11.1 @ 5
AS	ABS, Black, Injection molded (Grade T, Color #4500, "Cycolac")	Borg	2.25		1.05	2.36		10.9 @ 5
AS	ABS, Grey, Injection molded (Grade T, Color #GSM 32627)	Borg	2.17		1.07	2.32		11.3 @ 5
AS	Acrylic, Clear, Plexiglas G Safety Glazing	Rohm	2.75		1.19	3.26	0.40	6.4 @ 5
AS	Acrylic, Plexiglas MI-7	Rohm	2.61		1.18	3.08	0.40	12.4 @ 5
M	Bakelite	UC	1.59		1.40	3.63		
AS	Cellulose Butyrate	0	2.14		1.19	2.56		21.9 @ 5
AS	Delrin, Black	D	2.43		1.42	3.45		30.3 @ 5
JA	Ethyl vinyl acetate, VE-630 (18% Acetate)	USI	1.80		0.94	1.69		
JA	Ethyl vinyl acetate, VE-634 (28% Acetate)	USI	1.68		0.95	1.60		
JA	Kydex, PVC Acrylic Alloy Sheet	Rohm	2.218		1.35	2.99		
AS	Lexan, Polycarbonate	GEP	2.30		1.20	2.75		23.2 @ 5
AS	Lustran, SAN	Mons	2.51		1.06	2.68		5.1 @ 5
	Mylar	D	2.54		1.18	3.00		
AS	Kodar PETG, 6763, Copolyester	Kodak	2.34		1.27	2.97		20.0 @ 5
	Melopas	AMPL	2.90		1.7	4.93		7.2 @ 2.5
	Nylon, 6/6		2.6	1.1	1.12	2.9	0.39	2.9 @ 5
AS	Nylon, Black, 6/6	Port	2.77		1.14	3.15		16.0 @ 5
PKY	Parylene C	MM	2.15		1.40	3.0		0.1 @ 1
PKY	Parylene C	Vikng	2.2		1.18	2.6		
PKY	Parylene D	SEA	2.1		1.36	2.85		
AS	Polycarbonate, Black, Injection molded (Grade 141R, Color No.701,"Lexan")	GEP	2.27		1.22	2.77		22.1 @ 5
AS	Polycarbonate, Blue, Injection molded (Grade M-40, Color No. 8087, "Merlon")	Mobay	2.26		1.20	2.72		23.5 @ 5
AS	Polycarbonate, Clear, Sheet Material	Port	2.27		1.18	2.69		24.9 @ 5
CRC	Polyethylene		1.95	0.54	0.90	1.76		

Ref	Material	Vendor	V_L mm/• s	V_s mm/• s	• • g/cm^3	Z_L MRayl	• •	Loss dB/cm
	Polypropylene, Profax 6432, Hercules	USI	2.74		0.88	2.40		5.1 @ 5
AS	Polypropylene, White, Sheet Material	Port	2.66		0.89	2.36		18.2 @ 5
	Polystyrene, "Fostarene 50"	Amer	2.45		1.04	2.55		
AS	Polystyrene, "Lustrex", Injection molded (Resin #HF55-2020-347)	Mons	2.32		1.04	2.42		3.6 @ 5
	Polystyrene, Styron 666	E	2.40	1.15	1.05	2.52	0.35	1.8 @ 5
	Polyvinyl butyral, Butacite, (used to laminate safety glass together)	D	2.35		1.11	2.60	0.37	
	PSO, Polysulfone	UC	2.24		1.24	2.78		4.25 @ 2
AS	PVC, Grey, Rod Stock (normal impact grade)	Port	2.38		1.38	3.27		11.2 @ 5
AS	Styrene Butadiene, KR 05 NW	Phil	1.92		1.02	1.95		24.3 @ 5
AS	TPX-DX845, Dimethyl pentene polymer	WP	2.22		0.83	1.84		3.8 @ 1.3, 4.4 @ 4
AS	Valox, Black, (glass filled polybutalene teraphlate "PTB")	GE	2.53		1.52	3.83		15.7 @ 5
AS	Vinyl, Rigid		2.23		1.33	2.96		12.8 @ 5

Acoustic Properties of Some Rubbers

Ref	Material	Vendor	V_L mm/• s	• • g/cm^3	Z_L MRayl	Loss dB/cm
	Adiprene LW-520	Uni	1.68	1.16	1.94	
	Butyl rubber		1.80	1.11	2.0	
AS	Dow Silastic Rubber GP45, 45 Durometer	MPC	1.02	1.14	1.16	23.4 @ 4
AS	Dow Silastic Rubber GP70, 70 Durometer	MPC	1.04	1.25	1.30	33.7 @ 4
AS	Ecogel 1265, 100PHA OF B, outgass, 80C	EC	1.96	1.10	2.16	33.4 @ 2
AS	Ecogel 1265, 100PHA OF B, 100PHA Alumina, R4	EC,B	1.70	1.40	2.38	>24.0 @ 1.3
AS	Ecogel 1265, 100PHA OF B, 1940PHA T1167, R4	EC,C	1.32	9.19	12.16	14 @ 0.4
	Ecothane CPC-39	EC	1.53	1.06	1.63	
	Ecothane CPC-41	EC	1.52	1.01	1.54	
	Neoprene		1.6	1.31	2.1	
AS	Pellathane, Thermoplastic Urethane Rubber (55D durometer)	Upj	2.18	1.20	2.62	32.0 @ 5
AS	Polyurethane, GC1090	Gall	1.76	1.11	1.96	46.1 @ 4
BB	Polyurethane, RP-6400	REN	1.50	1.04	1.56	
BB	Polyurethane, RP-6401	REN	1.63	1.07	1.74	
LP	Polyurethane, RP-6401	REN	1.71	1.07	1.83	100 @ 5
BB	Polyurethane, RP-6402	REN	1.77	1.08	1.91	
BB	Polyurethane, RP-6403	REN	1.87	1.10	2.05	

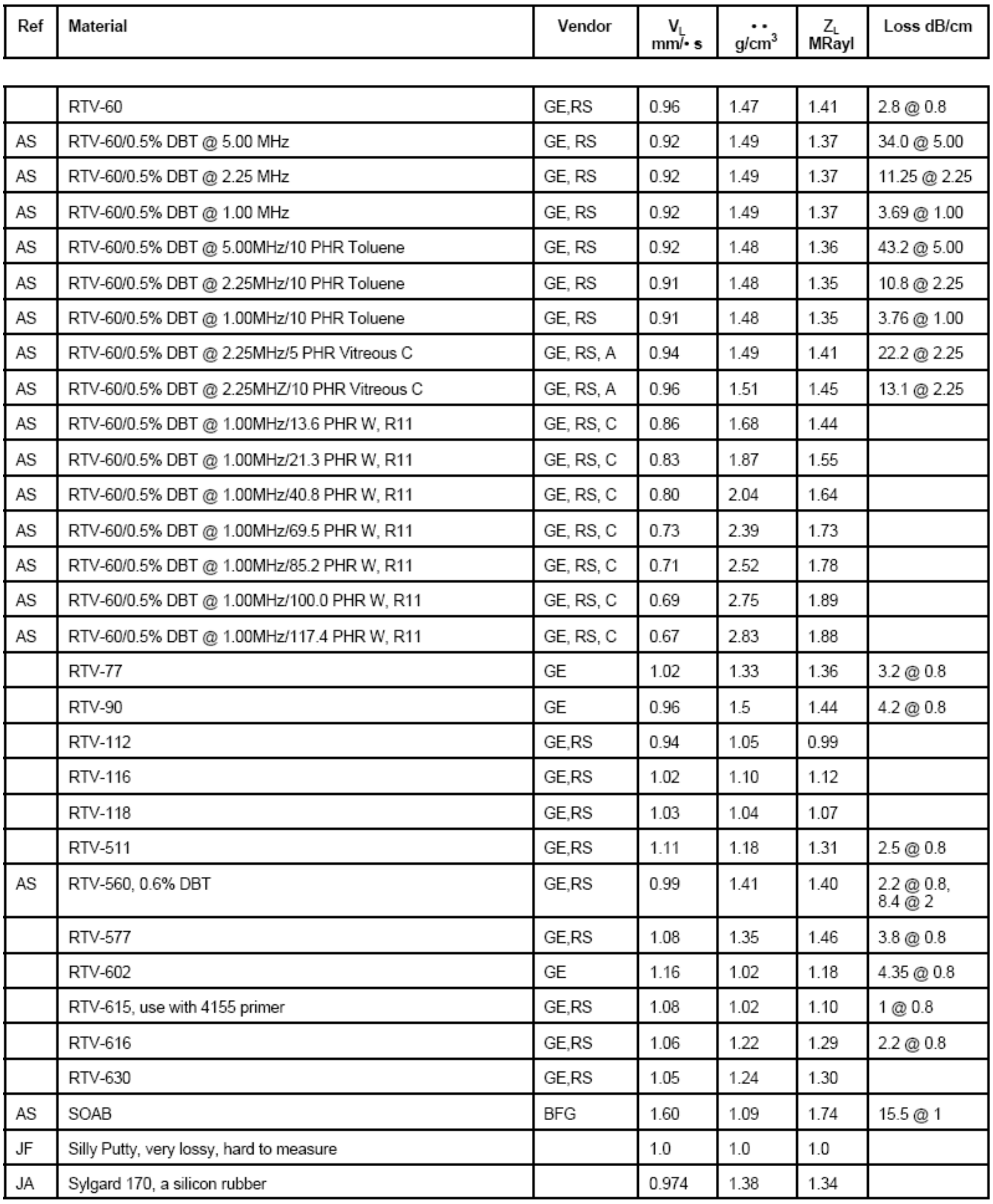

Ref	Material	Vendor	V_L mm/• s	• • g/cm^3	Z_L MRayl	Loss dB/cm
	RTV-60	GE,RS	0.96	1.47	1.41	2.8 @ 0.8
AS	RTV-60/0.5% DBT @ 5.00 MHz	GE, RS	0.92	1.49	1.37	34.0 @ 5.00
AS	RTV-60/0.5% DBT @ 2.25 MHz	GE, RS	0.92	1.49	1.37	11.25 @ 2.25
AS	RTV-60/0.5% DBT @ 1.00 MHz	GE, RS	0.92	1.49	1.37	3.69 @ 1.00
AS	RTV-60/0.5% DBT @ 5.00MHz/10 PHR Toluene	GE, RS	0.92	1.48	1.36	43.2 @ 5.00
AS	RTV-60/0.5% DBT @ 2.25MHz/10 PHR Toluene	GE, RS	0.91	1.48	1.35	10.8 @ 2.25
AS	RTV-60/0.5% DBT @ 1.00MHz/10 PHR Toluene	GE, RS	0.91	1.48	1.35	3.76 @ 1.00
AS	RTV-60/0.5% DBT @ 2.25MHz/5 PHR Vitreous C	GE, RS, A	0.94	1.49	1.41	22.2 @ 2.25
AS	RTV-60/0.5% DBT @ 2.25MHZ/10 PHR Vitreous C	GE, RS, A	0.96	1.51	1.45	13.1 @ 2.25
AS	RTV-60/0.5% DBT @ 1.00MHz/13.6 PHR W, R11	GE, RS, C	0.86	1.68	1.44	
AS	RTV-60/0.5% DBT @ 1.00MHz/21.3 PHR W, R11	GE, RS, C	0.83	1.87	1.55	
AS	RTV-60/0.5% DBT @ 1.00MHz/40.8 PHR W, R11	GE, RS, C	0.80	2.04	1.64	
AS	RTV-60/0.5% DBT @ 1.00MHz/69.5 PHR W, R11	GE, RS, C	0.73	2.39	1.73	
AS	RTV-60/0.5% DBT @ 1.00MHz/85.2 PHR W, R11	GE, RS, C	0.71	2.52	1.78	
AS	RTV-60/0.5% DBT @ 1.00MHz/100.0 PHR W, R11	GE, RS, C	0.69	2.75	1.89	
AS	RTV-60/0.5% DBT @ 1.00MHz/117.4 PHR W, R11	GE, RS, C	0.67	2.83	1.88	
	RTV-77	GE	1.02	1.33	1.36	3.2 @ 0.8
	RTV-90	GE	0.96	1.5	1.44	4.2 @ 0.8
	RTV-112	GE,RS	0.94	1.05	0.99	
	RTV-116	GE,RS	1.02	1.10	1.12	
	RTV-118	GE,RS	1.03	1.04	1.07	
	RTV-511	GE,RS	1.11	1.18	1.31	2.5 @ 0.8
AS	RTV-560, 0.6% DBT	GE,RS	0.99	1.41	1.40	2.2 @ 0.8, 8.4 @ 2
	RTV-577	GE,RS	1.08	1.35	1.46	3.8 @ 0.8
	RTV-602	GE	1.16	1.02	1.18	4.35 @ 0.8
	RTV-615, use with 4155 primer	GE,RS	1.08	1.02	1.10	1 @ 0.8
	RTV-616	GE,RS	1.06	1.22	1.29	2.2 @ 0.8
	RTV-630	GE,RS	1.05	1.24	1.30	
AS	SOAB	BFG	1.60	1.09	1.74	15.5 @ 1
JF	Silly Putty, very lossy, hard to measure		1.0	1.0	1.0	
JA	Sylgard 170, a silicon rubber		0.974	1.38	1.34	

Reference: Onda Corporation Web Site (www.ondacorp.com)

Attenuation in water

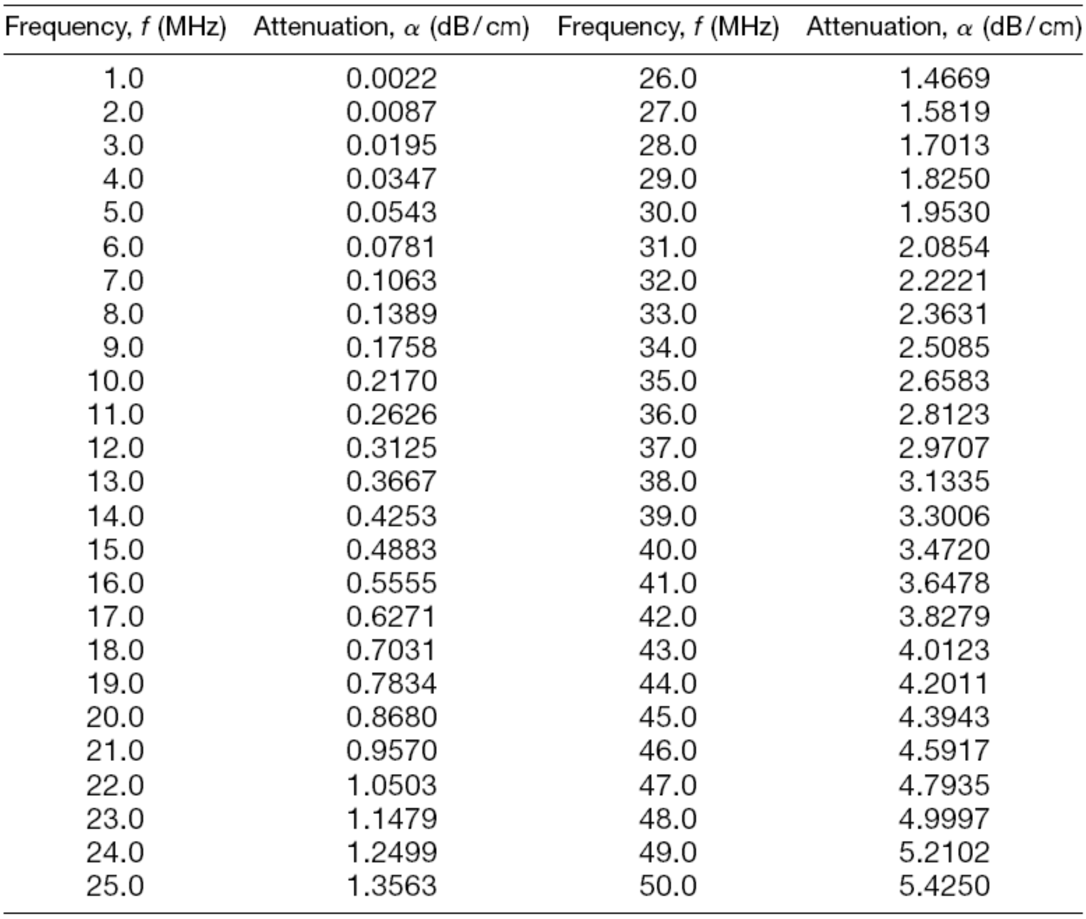

Frequency, f (MHz)	Attenuation, α (dB/cm)	Frequency, f (MHz)	Attenuation, α (dB/cm)
1.0	0.0022	26.0	1.4669
2.0	0.0087	27.0	1.5819
3.0	0.0195	28.0	1.7013
4.0	0.0347	29.0	1.8250
5.0	0.0543	30.0	1.9530
6.0	0.0781	31.0	2.0854
7.0	0.1063	32.0	2.2221
8.0	0.1389	33.0	2.3631
9.0	0.1758	34.0	2.5085
10.0	0.2170	35.0	2.6583
11.0	0.2626	36.0	2.8123
12.0	0.3125	37.0	2.9707
13.0	0.3667	38.0	3.1335
14.0	0.4253	39.0	3.3006
15.0	0.4883	40.0	3.4720
16.0	0.5555	41.0	3.6478
17.0	0.6271	42.0	3.8279
18.0	0.7031	43.0	4.0123
19.0	0.7834	44.0	4.2011
20.0	0.8680	45.0	4.3943
21.0	0.9570	46.0	4.5917
22.0	1.0503	47.0	4.7935
23.0	1.1479	48.0	4.9997
24.0	1.2499	49.0	5.2102
25.0	1.3563	50.0	5.4250

Reference: Krautkramer, J. and Krautkramer, H., “Ultrasonic Testing of Materials”, Springer-Verlag (Berlin)